IN 47

1935-?

128 P

NASA Technical Memorandum   109012

Windshear Database for Forward-Looking Systems Certification

G. F. Switzer
Research Triangle Institute
Research Triangle Park, North Carolina

F. H. Proctor and D. A. Hinton
Langley Research Center
Hampton, Virginia

J. V. Aanstoos
Research Triangle Institute
Research Triangle Park, North Carolina

November 1993

NASA

National Aeronautics and
Space Administration

Langley Research Center
Hampton, Virginia 23681-0001

Table of Contents

List of Tables

Abstract

This document contains a description of a comprehensive database that is to be used for certification testing of airborne forward-look windshear detection systems. The database was developed by NASA Langley Research Center, at the request of the Federal Aviation Administration (FAA), to support the industry initiative to certify and produce forward-look windshear detection equipment. The database contains high-resolution, three-dimensional fields for meteorological variables that may be sensed by forward-looking systems. The database is made up of seven case studies, which have been generated by the Terminal Area Simulation System, a state-of-the-art numerical system for the realistic modeling of windshear phenomena. The selected cases represent a wide spectrum of windshear events. General descriptions and figures from each of the case studies are included, as well as equations for F-Factor, radar-reflectivity factor, and rainfall rate. The document also describes scenarios and paths through the data sets, jointly developed by NASA and the FAA, to meet FAA certification testing objectives. Instructions for reading and verifying the data from tape are included.

Conversion Table

Conversion factors for metric (SI) to customary U.S. units

To Convert	Multiply by	To Get
cubic meter (m^3)	35.31	cubic feet (cu ft)
gram (g)	0.035274	ounces (oz)
kilometer (km)	0.62137	statute miles
kilometer (km)	0.5396	nautical miles
meter (m)	3.2808	feet (ft)
meters per second (m/s)	196.8	feet per minute (ft/min)
meters per second (m/s)	1.9426	knots
meters per second (m/s)	2.237	miles per hour (mph)
millibar (mb)	9.869232×10^{-4}	atmospheres (atm)
millibar (mb)	0.02953	inches of mercury
millimeters per hour (mm/hr)	0.03937	inches per hour (in/hr)
pascal (Pa)	0.01	millibar (mb)
pascal (Pa)	1	newton per sq meter ($N\ m^{-2}$)

Glossary

bow echo: Rapidly-moving, crescent-shaped radar echo that is convex in the direction of motion. Typically associated with strong, straight winds.

graupel: Small soft hail or snow pellets.

FBAR: An average of the wind shear hazard index (F-factor) taken over a flight path segment of a specified distance (1 km in this document).

hazardous windshear: Region of performance-decreasing winds with a 1-km averaged F-factor exceeding 0.105.

LLWAS: Low Level Wind Shear Alert System -- An array of anemometers located within the airport area; designed to detect windshear on and near airport runways.

macroburst: Region of divergent outflow from storm downdraft(s) that has a horizontal scale greater than 4 km.

microburst: Region of divergent windshear that has a horizontal wind change of at least 10 m/s within a 4-km segment.

performance-decreasing winds: Windshear that causes a loss of aircraft performance.

stable layer: A vertical thickness of air with static stability: a parcel displaced vertically within such a layer is subjected to a buoyant force opposite to its displacement.

TDWR: Terminal Doppler Weather Radar -- a ground-based Doppler radar designed to detect microburst and gust front windshear along airport approach and departure paths and provide warnings to Air Traffic Control personnel

thunderstorm gust front: The transition zone at the leading edge of strong outflow from thunderstorm downdrafts. Often referred to as "gust front."

1.0 Introduction

1.1 Purpose

This document describes the windshear database developed for the certification testing of airborne forward-looking windshear detection systems. This database was developed by NASA Langley Research Center at the request of the Federal Aviation Administration (FAA) to support the industry initiative to certify and produce practical windshear detection equipment. The database will be used with vendor-developed sensor simulation software and vendor-collected ground clutter data to demonstrate detection performance in a variety of meteorological conditions. The database is generated by the Terminal Area Simulation System (TASS) -- a sophisticated, state-of-the-art, meteorological cloud model -- which outputs fields for meteorological variables that may be sensed by a forward-look windshear system or that may affect the performance of such a system. The fields are described in detail below and include wind, temperature, radar-reflectivity factor, water vapor, rain, and hail. The database contains a number of windshear cases that encompasses a wide range of events, suitable for testing and certification of windshear detection instrumentation. Description of the specific paths to be used to test and certify windshear detection systems are contained to insure that such systems are adequately tested. These paths represent the intent of the FAA as of this writing. Subsequent FAA certification documentation may modify the path descriptions and will take precedent over the paths described here. Also included are instructions to read the database from tape and verify the database.

1.2 Overview of Documentation

The TASS model is described in Section 1.3. Chapter 2 describes the data sets in detail, covering such characteristics as: variables, grid spacing, domain size and dimensions, initial conditions, and general meteorological descriptions of each case. Descriptions of the certification paths to be used with each data set are found in Chapter 3. Chapter 4 contains descriptions of the plots of key variables and derived values which are included in this report as Appendix A. Appendix A also contains Skew-T diagrams of the input soundings used to generate the database, and appendix B contains a brief explanation of Skew-T diagrams. Chapter 5 details the instructions for reading and verifying the database tapes. Appendix C shows the aircraft hazard factor or F-factor equations used in this document. Appendix D contains the supplementary equations for radar reflectivity factor, rainfall rate, and temperature conversion. Appendix E is a listing of a sample FORTRAN code to read and verify the database, and appendix F is the output of the code in appendix E.

1.3 Description of TASS Model

TASS, also known as the NASA Windshear Model, is a multi-dimensional numerical cloud model developed at NASA Langley Research Center for the general purpose of studying convective phenomena such as microbursts, convective rain

storms, gust fronts, and hailstorms (e.g., Proctor 1987a, 1987b). TASS implements a numerical solution of a 3-dimensional time-dependent equation set for compressible nonhydrostatic fluids. Prognostic equations are incorporated for the following 11 variables: the 3 velocity components, pressure, potential temperature, water vapor, liquid cloud droplets, cloud ice crystals, rain, snow, and hail/graupel. Subgrid turbulence closure is achieved using first-order diagnostic approximation with Richardson number dependency. The surface friction layer is parameterized using Monin-Obukhov similarity theory. Lateral boundaries are open and utilize radiation boundary conditions so as to minimize wave reflection. The treatment of the water substances (water vapor, liquid cloud droplets, cloud ice crystals, rain, snow and hail/graupel) allows for condensation, evaporation, freezing, and sublimation, including subsequent latent heat exchanges. Parameterizations for the numerous cloud microphysical interactions are similar to those in Lin et al. (1983), and are listed in Table 1.1.

TASS utilizes an efficient yet highly-accurate numerical solution of the time-dependent equation set. The governing equations are approximated on a staggered three-dimensional grid, the vertical spacing of which may be either linear or stretched. The model domain may translate along with the movement of a microburst or convective storm, even at variable speeds.

Given an initial atmospheric sounding (vertical profile of ambient temperature, dewpoint, and wind velocity) and an initial triggering impulse, TASS can numerically-simulate the time-dependent life-cycle of a convective storm, including any subsequent microburst(s) that may develop (e.g., Proctor and Bowles 1992). Alternatively, the model may directly simulate the evolution of a microburst by prescribing a precipitation distribution at the model top boundary (e.g. Proctor 1988, 1989). For representative ambient conditions that are supplied as input, TASS has produced simulations of real-world events that are of reasonable comparison with observations.

The evolution of numerous windshear events have been simulated with TASS, and include both "wet" and "dry" microburst events. As defined by Fujita (1985), a "dry" microburst produces less than 0.01 inches of precipitation at the ground during the event (note however, that all microbursts are associated with precipitation, although in some cases very little or none may reach the ground); greater precipitation than this defines a "wet" microburst. Radar meteorologists prefer the terms "low-reflectivity," "moderate-reflectivity," and "high-reflectivity" microburst. These terms are defined by the associated radar-reflectivity factor being less than 35 dBZ, 35-55 dBZ, or greater than 55 dBZ, respectively (e.g., Roberts and Wilson 1989). "Low-reflectivity microburst" is synonymously used for "dry microburst" , and vice versa.

Table 1.1 Cloud Microphysical Interactions

Accretion of cloud droplets by rain

Condensation of water vapor into cloud droplets

Berry-Reinhardt formulation for autoconversion of cloud droplet water into rain

Evaporation of rain and cloud droplets

Spontaneous freezing of supercooled cloud droplets and rain

Initiation of cloud ice crystals

Ice crystal and snow growth due to riming

Vapor deposition and sublimation of hail/graupel, snow, and cloud ice crystals

Accretion by hail/graupel of cloud droplets, cloud ice crystals, rain, and snow

Contact freezing of supercooled rain resulting from collisions with cloud ice crystals or snow

Production of hail/graupel from snow riming

Melting of cloud ice crystals, snow, and hail/graupel

Shedding of unfrozen water during hail wet growth

Shedding of water from melting hail/graupel and snow

Conversion of cloud ice crystals into snow

Accretion by snow of cloud droplets, cloud ice crystals, and rain

Evaporation or vapor condensation on melting hail/graupel and snow

2.0 Database Description

In order to provide a wide range of scenarios for the testing of look-ahead sensors, the database is divided into nine subsets from seven TASS case-study simulations. The windshear types represented include microburst types ranging from: 1) small- to large-scale events, 2) low- to high-reflectivity events, 3) symmetrical to asymmetrical events, and 4) weak to hazardous windshear. The database also includes scenarios with: 1) growing and decaying events, 2) interacting microbursts, 3) windshear with intervening rain, 4) microburst penetrating a ground based stable layer, and 5) a gust front with hazardous shear. Several of the numerically-modelled events in this database represent real accident or incident windshear cases.

Table 2.1 summarizes each of the 7 cases utilized in generating the 9 certification data sets. Each data set contains data for the appropriate variables in three-dimensional space, but frozen in time. Two of these cases, Case 3 (Denver 7/11/88) and Case 5 (Denver 7/8/89), have data sets taken from two different times of the storm evolution.

2.1 Variables

Table 2.2 lists each of the meteorological variables that are available in the database. This selection of variables represents those that may be sensed by a forward-look windshear system or that may affect the performance of such a system. Each variable is represented by an array of data in three-dimensional space. In some cases, hailwater and cloud droplet water did not occur anywhere within the domain of the data set; hence, the fields for hailwater and cloud droplet water are given only for those data sets in which either were present below 2 km above ground level (AGL).

Fields of radar-reflectivity factor, RRF, are diagnosed from the model precipitation fields and are included in each data set. An additional field, RRFI, approximates the contribution of radar-reflectivity factor from insects as well as precipitation, and is included in cases 5-7. Not unexpectedly, the difference of values between the RRF and RRFI fields is very small, except in the precipitation free areas where insects solely contribute to the radar reflectivity. The maximum difference in magnitudes between the RRF and RRFI fields are usually small and are less than a few dBZ.

4

Table 2.1 Description of Windshear Certification Database

Case No.	Simulation Description	Model Simulation Time (minutes)	Stage of Evolution for Primary Microburst	Approximate Peak 1-kilometer FBAR @ 150 kts	Approximate Diameter of Outflow @ Peak ΔV (km)	Approximate Microburst Core Reflectivity (dBZ)	Intervening Rain	Temp. Lapse Rate	Symmetry
1	DFW Accident Case, Wet Microburst, Rain and Hail	11	Peak Intensity	0.20	3.5	55	No	Adiabatic	Axisymmetric
2	6/20/91 Orlando, Florida, NASA Research Flight, Wet Microburst	37	Peak Intensity	0.19	3.5	50	Yes	Adiabatic	Rough Symmetry
3	7/11/88 Denver, Colorado, Incident Case, Multiple Microburst	49	Developing	0.08	3	35	Light	Adiabatic	Varies Between Microbursts
		51	Near Peak	0.20	1.5 - 3	20 - 40	Yes		
4	7/14/82 Denver, Colorado, Stable Layer, Warm Microburst	36	Past Peak but Quasi-Steady	0.29	1.0	27	No	Stable Layer	Axisymmetric
5	7/8/89 Denver, Colorado, Very Dry Microburst	40	Near peak	0.18	3	17 - 20	No	Adiabatic	Rough Symmetry
		45	2nd Pulse	0.16	3	5			Asymmetric
6	Derived Florida Sounding, Highly Asymmetric Microburst	14	Decaying	0.16	1	50	Light	Adiabatic	Asymmetric
7	8/2/81 Adjusted Knowlton, Montana Sounding, Gust Font	27	N/A	0.14	N/A	20 (in area of largest FBAR)	No	Adiabatic	Asymmetric

Table 2.2. List of Variables Contained in Certification Database

Variable	Description	Units	Not Included in Cases
U	Eastward Component of Wind Velocity	meters per second	—
V	Northward Component of Wind Velocity	meters per second	—
W	Vertical Component of Wind Velocity	meters per second	—
TAU	Temperature	degrees Kelvin	—
RRF	Radar-Reflectivity Factor	decibels of Z (dBZ)	—
XIV	Water Vapor	grams per cubic meter	—
RAIN	Rainwater Content	grams per cubic meter	—
HAIL	Hailwater Content	grams per cubic meter	2, 4, and 5
CLD	Liquid Cloud-Droplet Water	grams per cubic meter	1-6
RRFI	Radar Reflectivity Including Insects	dBZ	1-4

2.2 Generation of Certification Database

The certification data sets are processed from several archived raw data files for selected cases and simulation times. The data sets were generated from TASS case simulations conducted over the past several years, and contain a number of fields with data points located on a spatially-staggered mesh. Also, the domain and grid sizes in the raw data sets vary between cases. To make them suitable for inclusion in the windshear certification database, the data is interpolated to a common grid spacing, details of which are discussed below. The data contained in the database is reduced by windowing (extracting) only the lower 2 km of the simulation, and by excluding any unnecessary fields. The specifications for the original TASS data sets are listed in Table 2.3.

2.2.1 Grid Spacing of Original and Final Data Sets

In order to achieve a user-friendly database for certification purposes, the data is translated to a 3-dimensional grid of uniform spacing. The cell resolution chosen to retain the salient details of each event is 100 by 100 meters horizontally and 50 meters vertically. Exceptions are for cases 1 and 4 which are interpolated with a resolution of 50 meters in all three directions. These two cases require smaller grid sizes in order to maintain the identity of the small-scale features.

As noted in Table 2.3 the vertical extent of each raw data set is significantly higher than what is needed to simulate the scenarios associated with landing approach and takeoff. The database is limited to 2 km AGL in order to reduce size, but yet retain ample data for adequate certification testing. The vertical limitation of the database is more than sufficient to resolve the surface outflow of all the simulated microburst events.

The horizontal-domain size of each case is the same for the original and final data. The exception is for case 7 where the gust front domain is clipped by 6 km to reduce database size. The details of the interpolated database are given in Table 2.4.

2.2.2 Interpolation

The interpolation strategy is chosen to preserve the 1-km averaged F-Factor, or FBAR (explained in appendix C). The interpolation strategy results in losses of 2 to 10 percent of FBAR. There are two different interpolation processes depending on whether the original data set is 2-D axisymmetric or 3-D.

For the 3-D case simulations, interpolation from the TASS model spacing to a uniform grid spacing was accomplished using calls to routines in the IMSL Math/Library (1989). The data translation consisted of a 2-step process, in which a 2-D horizontal interpolation was followed by a 1-D vertical interpolation. The 2-D interpolation was accomplished by the subroutine "QD2VL" which is quadratic in 2-space, and the 1-D

vertical interpolation was by way of the routine "CSINT" which is a cubic spline algorithm.

In the 2-D axisymmetric simulations (cases 1 and 4) the data is symmetric with regard to the vertical axis of an isolated microburst, and was transformed from a cylindrical to a cartesian coordinate system. In a two step procedure, data was first interpolated based on weighted averages in the 2-D axisymmetric plane. Data was then mapped into a 3-D cartesian grid by rotating the interpolated radial-vertical plane around the axis of the microburst. Data at grid points outside of the cylindrical sweep of the radial-vertical plane were set equal to that along the edge of the sweep.

Table 2.3 Description of Original (raw) TASS Data Set[1].

Case No.	Simulation Description	2-D axisymmetric or 3-D?	Horizontal Grid Spacing (meters)	Vertical Grid Spacing (meters)	Number of Grid Points X, Y, Z or R, Z	Height of Top Boundary (km)	Simulates Parent Storm?	For more details of case simulation, see
1	DFW Accident Case	2-D axisymmetric	20	20	201 x 201	4	NO	Proctor (1988), pp 3150-3154
2	06/20/91 Orlando, Florida, Wet Microburst	3-D	150	stretched from 70 to 440	101 x 101 x 71	18	YES	Proctor (1992)
3	7/11/88 Denver, Colorado, Multiple Microburst	3-D	200	stretched from 80 to 475	91 x 61 x 35	10	YES	Proctor and Bowles (1992)
4	07/14/82 Denver, Colorado, Warm Microburst	2-D axisymmetric	25	25	201 x 201	5	NO	Proctor (1989), pp 2155-2157
5	7/8/89 Denver, Colorado, Very Dry Microburst	3-D	160	stretched from 70 to 365	101 x 101 x 71	13	YES	Proctor (1993)
6	Derived Florida Sounding, Highly Asymmetric Microburst	3-D	100	stretched from 50 to 285	101 x 101 x 33	5	NO	--
7	8/2/81 Montana Gust Font	3-D	100	stretched from 50 to 210	201 x 51 x 31	4	NO	--

[1]Original data set not included with interpolated data set.

Table 2.4 Domain Information for Interpolated Windshear Database

Data Set Name	Origin (m) X_o, Y_o		Grid Cell Size (m) $\Delta X \times \Delta Y \times \Delta Z$	Domain Size (km) $X \times Y \times Z$	Number of Grid Points $IX \times IY \times IZ$
Case 1 11 min	-4000	-4000	50 x 50 x 50	8 x 8 x 2	161 x 161 x 41
Case 2 37 min	-8834	-8880	100 x 100 x 50	15 x 15 x 2	151 x 151 x 41
Case 3 49 min	1190	-10500	100 x 100 x 50	18 x 12 x 2	181 x 121 x 41
Case 3 51 min	2232	-10570	100 x 100 x 50	18 x 12 x 2	181 x 121 x 41
Case 4 36 min	-5000	-5000	50 x 50 x 50	10 x 10 x 2	201 x 201 x 41
Case 5 40 min	-4210	2275	100 x 100 x 50	16 x 16 x 2	161 x 161 x 41
Case 5 45 min	-3738	3639	100 x 100 x 50	16 x 16 x 2	161 x 161 x 41
Case 6 14 min	8071	-3500	100 x 100 x 50	10 x 10 x 2	101 x 101 x 41
Case 7 27 min	18510	-1500	100 x 100 x 50	14 x 5 x 2	141 x 51 x 41

2.3 General Meteorological Description of Each Case

Below is a condensed summary for each case. Soundings for each of the cases, along with figures produced from the interpolated database, are included in appendix A. Further descriptions for each of the simulations, including comparison and validation with observed data, may be found in the references listed in Table 2.3. [Cases 6 and 7 were generated recently (primarily for this database) and no documentation currently exists other than below.]

2.3.1 Case 1: DFW Microburst

The 2 August 1985, Dallas-Ft. Worth (DFW) microburst was a high-reflectivity microburst that resulted in the crash of a commercial jetliner. This event is simulated with the 2-D axisymmetric TASS model by assuming an environmental sounding interpolated from observed data.

The simulated microburst is associated with high reflectivity due to rain and hail, moderate rainfall rates, pronounced temperature drop, and hazardous wind shear with strong outflow winds. The data set is taken near the time of peak intensity, at 11 minutes simulation time. Although the numerical simulation is 2-D, there is reasonable comparison with observed data taken from aircraft flight data recorders. Other details of this simulation, including comparisons with the airplane flight profiles, are in Proctor (1988).

2.3.2 Case 2: Orlando Microburst

The 20 June 1991, Orlando microburst, was encountered by a NASA aircraft instrumented with in-situ and forward-look windshear sensors, and was also measured within the Terminal Doppler Weather Radar (TDWR) test bed. The parent storm and ensuing microbursts are simulated with 3-D TASS. Comparisons of the simulation with observed data indicate a reasonable agreement.

The simulation, as verified from measurements, indicates a high-reflectivity microburst with hazardous shear and heavy rainfall rates. Although the area covered by the outflow is roughly symmetrical, complex regions of windshear hazard are embedded within the outflow. The data set is taken at a simulation time of 37 minutes, when the microburst is near peak intensity. This time corresponds to observed measurements[1] at approximately 2046 Universal Coordinated Time (UTC). The microburst contains multiple downdraft cores and regions of upflow embedded within the outflow. The strongest hazard is located near the southern end of the outflow and has a peak FBAR of about 0.19. An approach from the north would encounter intervening rain, as well as pockets of both performance increase and decrease, before

---

[1]Measurements from TDWR and NASA's aircraft penetration.

entering the area of primary hazard. The outflow near ground level is associated with a pronounced temperature change, with the maximum drop being about 6° C.

2.3.3 Case 3: Denver Multiple Microburst Event

The 11 July 1988, Denver, storm is simulated by initializing 3-D TASS with the 2000 UTC observed special sounding. This storm is of special interest, since it produced a severe low- to moderate-reflectivity microburst of unusual intensity that was inadvertently encountered by 4 commercial jetliners trying to land at Denver Stapleton. An in-depth study of this incident, including comparisons with TDWR, surface measurements, and flight data recorder (from the four aircraft) data are presented in Proctor and Bowles (1992), and Schlickenmaier (1989). Very good agreement with observed measurements was obtained.

Model results show that multiple microbursts (with FBAR of up to 0.2) formed downstream of the main precipitation shaft, which itself was characterized by a weak microburst. The microbursts (all produced by one storm) grow and interact, eventually coalescing into a large macroburst outflow. Some of the microbursts display large asymmetry. The most eastern of these microbursts is the one that was encountered by the 4 aircraft.

Data sets are given at two simulation times: 49 and 51 min. The first is near the time of initial ground contact for the downstream eastern microburst. Several minutes latter it grows into a hazardous microburst, which is captured in the second data set. At 51 minutes, the eastern microburst is near peak intensity. It is near this time that the first two encounters takes place. Low-level outflow from this microburst has peak ΔV (velocity change) of up to 40 m/s. The most westward microburst, which is associated with the storms primary rainshaft, remains weak although associated with moderate values of radar reflectivity. Temperature drops in the microburst outflows are only a few degrees C.

2.3.4 Case 4: Denver Warm Microburst

Data for this case is from a 2-D axisymmetric simulation of a narrow, low-reflectivity, microburst occurring in an environment characterized by a low-level stable layer. This simulation does not attempt to model a particular observed event, but uses an input sounding (14 July 1982) measured during the Joint Airport Weather Studies (JAWS). The temperature profile from the sounding has been modified for an isothermal temperature profile between the ground and 500 m, resulting in a ground-based stable layer.

Relative to the size and intensity of other microbursts, this event contains a strong narrow-core downdraft, shallow outflow, and very large FBAR. However, the region occupied by the hazardous shear is small in horizontal scale compared to most other events. This simulated microburst also is characterized by warm outflow (positive temperature change from ambient). The time-freeze used for this case is when the

microburst is in a quasi-steady state, at 36 minutes, some 13 minutes after peak intensity. Similar microburst that were characterized by downward-protruding, stalactite-appearing radar echoes were observed during JAWS (see Fujita and Wakimoto 1983). Numerous warm microburst were measured by ground-based instruments during JAWS (Bedard and LeFebvre 1988).

2.3.5 Case 5: Denver Dry Microburst

On 8 July 1989, a very strong microburst was detected by LLWAS, within the approach corridor just north of Denver Stapleton Airport. The microburst was encountered by a Boeing 737-200 in a "go around" configuration and was reported to have lost considerable air speed and altitude during penetration (Wilson et al. 1991; Hughes 1990). LLWAS data revealed a pulsating microburst with peak strength associated with the first pulse. Interviews indicated that the microburst was accompanied by no apparent visible clues such as rain or virga, although blowing dust was reported. A National Center for Atmospheric Research (NCAR) research Doppler radar was operating, although poorly sited for low-level wind shear detection at Stapleton. Meaningful velocity could not be measured at the lowest radar scan due to very low reflectivity factor. This case attracts special interest since it may represent a dangerous microburst that is difficult to detect with Doppler radar.

The life-cycle of the microburst-producing storm is simulated with the 3-D version of TASS. Environmental conditions are taken from a sounding observed near the time and location of the event. Results from the numerical simulation show a low-reflectivity microburst with three distinguishable pulses. Data sets are generated from the simulation at two times: i) at 40 minutes, which is near peak intensity; and ii) 5 minutes later, which is near the time of the second microburst pulse. The first and strongest pulse (at 40 minutes) is associated with a peak velocity differential (ΔV)of 37 m/s and a peak horizontal wind speed of 26 m/s. At this time, radar reflectivity in most of the microburst outflow is less than -5 dBZ, and reflectivity exceeding 10 dBZ is confined to a 1-2 km diameter area within the core of the microburst. By the time of the second pulse (45 minutes), there is even less precipitation at low levels, yet hazardous levels of wind shear are maintained. The outflow from the first pulse has expanded into a macroburst and grown more asymmetric with time. The microburst associated with the second pulse is embedded within this larger scale outflow. The temperature change between the environment and outflow remain small at all times, never more than 2.5°C.

2.3.6 Case 6: Highly-Asymmetric Florida Microburst

A translating microburst with highly-asymmetric outflow is simulated with the 3-D model, by allowing an isolated precipitation shaft to fall through a prescribed ambient wind with vertical shear. The same ambient temperature and humidity profile from Case 2 is used in this simulation. The model simulation produces a wet microburst, with a bow-shaped radar-reflectivity pattern. Strong horizontal winds are generated along the leading edge of the translating outflow. The microburst contains high values of radar reflectivity, large rainfall rates and a pronounced temperature drop. The data

of radar reflectivity, large rainfall rates and a pronounced temperature drop. The data set chosen for certification testing is at 14 minutes, within the period of decaying intensity. Hazardous windshear exists, but is located in a very small region. The diameter of the hazardous shear is about 1 km with a peak FBAR of about 0.16. Other regions of performance decreasing F-factor exist within the asymmetric outflow, but generally contain weak values. Movement of the microburst is to the east at 17.5 m/s.

2.3.7 Case 7: Montana Gust Front

Thunderstorm gust fronts are characterized by a region of performance-increasing shear and turbulence, but usually pose little hazard due to performance decreasing shear. Surges and secondary discontinuities within the outflow behind gust fronts have been observed (Goff 1976), and may be associated with hazardous windshear. The case described below is selected because it has both a strong gust front (with performance-increasing shear) and a "discontinuity" in the outflow associated with hazardous windshear.

A gust front is simulated with 3-D TASS using the 2 August 1981, Knowlton special sounding with modified[2] winds. For this case the model assumes periodic north/south boundaries, and a gust front is generated from a north-south oriented line of precipitation.

At the simulation time chosen for this data set, the gust front is well developed and is translating toward the east at about 21 m/s. The gust front is characterized by strong performance-increasing shear (negative F-factor), pronounced temperature change, very-low radar reflectivity, and upward motion. A region of hazardous windshear is located within the outflow some distance behind the gust front. It is associated with a horizontal roll-vortex that is located at the edge of the precipitation shaft.

---

[2]The observed ambient winds are rotated 270° (a wind blowing toward the south is now blowing toward the east) and the now north-south component is set to zero. This is done to allow the simulation of a gust front within a high-resolution rectangular domain.

3.0 Certification Path Scenarios

3.1 Path Descriptions

The certification test paths through the simulation database have been carefully chosen to encounter a range of windshear alert situations. Table 3.1 summarizes the scenarios to be applied, and the certification path definitions are detailed in Table 3.2. These paths are subject to change in subsequent FAA certification documents.

The following assumptions are used for these path definitions:

1. Glide slope angle = 3° (flight path angle = -0.0524 radians).

2. Runway length = 3 km.

3. Glide path intercept point = 300 meters down runway.

4. Middle marker is 900 meters from runway threshold.

5. The above conditions produce a glide path height of 63 meters at the middle marker.

6. Go-around maneuvers are begun at an altitude of 30 meters, at a position 300 meters from runway threshold.

7. Takeoff ground roll length = 2 km.

8. Flight path angle after takeoff or go-around = 0.10 radians (5.73°).

9. Radius of turn, 25 degrees bank, at 103 m/s (200 knots) = 2.32 km.

10. The curved approaches are flown at a constant altitude of 1000 feet (305 meters) above ground level (AGL).

Paths are specified by direction of takeoff or approach, X or Y coordinate of flight path, and runway threshold coordinates. The path direction is specified by either compass direction or flight direction. North, East, South, West correspond to flight direction or track 360, 90, 180, and 270, respectively. The coordinates are specified with respect to the microburst data set and are in metric units. Microbursts are static during each simulation run. Drift angle runs are accomplished by biasing the orientation of the sensor, not through the presence of any ambient crosswind.

3.2 Hazards Along Path

In addition to specifying the details of each of the certification paths, Table 3.2 includes the values of peak FBAR and peak radar reflectivity along the path, as well as comments noting path-specific hazard details.

Table 3.1 Path Scenario Definitions

Scenario	Location of icon leading edge (where FBAR = 0.10)	Airspeed (Knots)	Used with Data Sets
1. Aligned for takeoff, near microburst	2 km from brake release	0*	Case 3 at 51 minutes Case 4 at 36 minutes Case 7 at 27 minutes
2. Aligned for takeoff, far microburst	5.5 km from brake release	0*	Case 1 at 11 minutes Case 3 at 51 minutes Case 5 at 40 minutes
3. Straight approach 3 degree glide slope	near the middle marker	150	Case 1 at 11 minutes Case 2 at 37 minutes Case 3 at 49 minutes Case 3 at 51 minutes Case 4 at 36 minutes Case 5 at 40 minutes Case 5 at 45 minutes Case 6 at 14 minutes Case 7 at 27 minutes
4. Curved approach	near the localizer intercept point	200	Case 3 at 51 minutes Case 5 at 40 minutes Case 6 at 14 minutes
5. Straight approach with drift 25 degree drift angle 3 degree glide slope	near the runway threshold	120	Case 4 at 36 minutes Case 5 at 40 minutes
6. Go-around	3.3 km from initiation of missed approach	150	Case 2 at 37 minutes Case 5 at 40 minutes

* For calculation of parameters along the path the airspeed is fixed at 150 knots.

Table 3.2 Certification Path Definitions

Data Set	Scenario	Windshear Penetration Path	Approximate Peak FBAR	Approximate Peak RRF (dBZ)	Notes
Case 1 11 min	2	Takeoff toward east along Y = 0 axis Brake release at X,Y = (-6.8,0) km	0.2	57	Takeoff roll occurs outside domain of data set, with sensor looking into the data set.
	3	Approach toward east along Y = 0 axis Place runway threshold at X,Y = (0,0)	0.14	55	Approach may begin outside the boundary of the data set.
Case 2 37 min	3	Approach toward south along X = -1.8 km line Place runway threshold at X,Y = (-1.8,-1.9)	0.14	50	About 4 km of intervening rain on path prior to encountering hazard.
	6	Approach toward west along Y = -1.4 km line Place runway threshold at X,Y = (2.2,-1.4) Go-around point is X,Y = (2.5,-1.4)	0.19	50	Runway touchdown zone is in clear air with microburst and 50 dBZ precipitation at far end of runway.
	3	Approach toward east along Y = 1.1 km line Place runway threshold at X,Y = (-1.8,1.1)	0.06	50	Below-alert threshold case. FBAR of .08 exists 500 m right of path; 0.17 exists 2.5 km right of runway touchdown zone.
Case 3 49 min	3	Approach toward east along Y = -4.5 km line Place runway threshold at X,Y = (8.6,-4.5)	0.08	25	Microburst strength is below alert threshold.
	3	Approach toward north along X = 8.5 km line Place runway threshold at X,Y = (8.5,1.9)	0.13	37	Light precipitation about 2 km from event with moderate to heavy occurring about 1 km to right of max shear.
Case 3 51 min	1	Takeoff toward north along X = 16.2 km line Brake release at X,Y = (16.2,-7.6) km	0.17	24	
	2	Takeoff toward east along Y = -5.0 km line Brake release at X,Y = (8.5,-5.0) km	0.19	37	Takeoff is in very weak shear with 20 to 35 dBZ precipitation, followed by about 1 km of clear air before encountering a 0.19 FBAR shear in 25 dBZ precipitation.
	3	Place runway threshold at X,Y = (12.2,-3.0) Orient runway on true heading of 360	0.15	42	Mostly clear view of threat, with rain on each side of path.

17

Table 3.2 Certification Path Definitions (continued)

Data Set	Scenario	Windshear Penetration Path	Approximate Peak FBAR	Approximate Peak RRF (dBZ)	Notes
Case 3 51 min	3	Place runway threshold at X,Y = (12.2,-3.0) Orient runway on true heading of 045	0.18	42	Path between 2 small rain cells (30-35 dBZ) about 3 km short of runway.
	3	Place runway threshold at X,Y = (12.2,-3.0) Orient runway on true heading of 090	0.17	41	Passes through intervening cell (20-30 dBZ and FBAR = .08) for last 4 km of approach to primary threat (FBAR=.17).
	3	Place runway threshold at X,Y = (12.2,-3.0) Orient runway on true heading of 135	0.13	42	Passes along edge of adjacent precipitation cell before primary threat. Strong shear exists at far end of runway.
	3	Place runway threshold at X,Y = (12.2,-3.0) Orient runway on true heading of 270	0.17	41	3 km from runway path touches edge of strong shear to south producing weak shear and 5-10 dBZ on path.
	3	Place runway threshold at X,Y = (12.2,-3.0) Orient runway on true heading of 315	0.2	42	Penetrates 0.2 FBAR shear 3-4 km short of runway, with 25 dBZ precipitation. Primary shear has peak FBAR of 0.13 along path. Should detect both.
	4	Localizer course eastward on Y = -3.1 km line Center of turn at X,Y = (11.5,-5.42). Fly north along X = 9.18 km line to X,Y = (9.18, -5.42); then turn right to intercept localizer at X,Y = (11.5,-3.1)	0.15	43	Path encounters precipitation about 1 km prior to beginning the turn, completes turn in moderate to heavy precipitation. Turn goes through FBAR of 0.12 prior to primary threat.
Case 4 36 min	1	Takeoff toward east along Y = 0 axis Brake release at X,Y = (-2.7,0) km	0.23	27	Microburst has very small rain shaft: diameter of 5 dBZ contour is less than 1 km at 50 m altitude.
	3	Approach toward east along Y = 0 axis Place runway threshold at X,Y = (0.2,0) km	0.24	27	
	5	Approach toward east along Y = 0 axis Place runway threshold at X,Y = (-0.7,0) km	0.19	27	Worst-case drift approach at 120 Knots.

Table 3.2 Certification Path Definitions (continued)

Data Set	Scenario	Windshear Penetration Path	Approximate Peak FBAR	Approximate Peak RRF (dBZ)	Notes
Case 5 40 min	2	Takeoff toward west along Y = 10.6 km line Brake release at X,Y = (10.1,10.6) km	0.18	22	Diameter of 5 dBZ contour ~1.6 km. About 1 km to each side of primary shear is FBAR of about .12-.15, with reflectivity of less than 0 dBZ.
	3	Approach toward north along X = 3.8 km line Place runway threshold at X,Y = (3.8,10.9) km	0.16	17	
	5	Approach toward north along X = 3.8 km line Place runway threshold at X,Y = (3.8,10.0) km	0.12	18	Peak along-path FBAR occurs after landing, with little or no vertical component. During approach, sensor would likely see the higher FBAR values above the runway.
	6	Approach toward north along X = 3.8 km line Place runway threshold at X,Y = (3.8,6.8) km Go-around point at X,Y = (3.8,6.5) km	0.17	23	Go-around maneuver.
	4	Localizer course westward on Y = 10.6 km Center of turn at X,Y = (4.4,8.28) Fly north along X = 6.72 km line to X,Y = (6.72,8.28); then turn left to intercept localizer at X,Y = (4.4,10.6) km	0.16	21	Curved approach at 200 knots.
	4	Localizer course westward on Y = 10.6 km Center of turn at X,Y = (4.4,12.92) Fly south along X = 6.72 km line to X,Y = (6.72,12.92); then turn right to intercept localizer at X,Y = (4.4,10.6) km	0.16	21	Curved approach at 200 knots.
Case 5 45 min	3	Approach toward north along X = 4.67 km line Place runway threshold at X,Y = (4.67,12.2) km	0.15	7	2nd microburst pulse, extremely dry. Zero dBZ contour diameter <1 km. Core penetration at 100 m altitude.
Case 6 14 min	4	Localizer course southward on X = 14.33 km Center of turn at X,Y = (12.01,1.08) Fly east along Y = 3.4 km line to X,Y = (12.01,3.4); then turn right to intercept localizer at X,Y = (14.33,1.08)	0.11	52	Higher FBAR (0.15) region exists 200 m to left of localizer. Localizer is offset slightly from microburst core to bring core into 25 degree minimum field of view early in turn.

Table 3.2 Certification Path Definitions (concluded)

Data Set	Scenario	Windshear Penetration Path	Approximate Peak FBAR	Approximate Peak RRF (dBZ)	Notes
Case 6 14 min	3	Localizer on X = 14.6 km line. Runway threshold at X,Y = (14.6,4.9). Orient runway on true heading of 360	0.15	52	Clear view of windshear during approach. Microburst core near X,Y = (14.2,0.5)
	3	Localizer on Y = (X - 13.9) km line. Runway threshold at X,Y = (17.2,3.3). Orient runway on true heading of 045	0.18	50	Microburst core near X,Y = (14.2,0.5)
	3	Localizer on Y = 0.5 km line. Runway threshold at X,Y = (15.1,0.5). Orient runway on true heading of 090	0.10	52	FBAR of .12 exists near path. Intervening rain at 2.5 km prior to peak. Microburst core near X,Y = (14.2,0.5)
	3	Localizer on X = 14.5 km line. Runway threshold at X,Y = (14.5,-3.5). Orient runway on true heading of 180	0.15	52	2 km of intervening rain prior to peak. Microburst core near X,Y = (14.2,0.5)
	3	Localizer on Y = (X - 13.9) km line. Runway threshold at X,Y = (11.6,-2.3). Orient runway on true heading of 225	0.19	50	Clear view of windshear during approach. Microburst core near X,Y = (14.2,0.5)
	3	Localizer on Y = 0.5 km line. Runway threshold at X,Y = (13.3,0.5). Orient runway on true heading of 270	0.13	52	Clear view of windshear during approach. Microburst core near X,Y = (14.2,0.5)
	3	Localizer on Y = -(X - 14.67) km line. Runway threshold at X,Y = (12.87,1.80). Orient runway on true heading of 315	0.13	52	Clear view of windshear during approach. Microburst core near X,Y = (14.2,0.5)
Case 7 27 min	1	Takeoff toward west along Y = 1.0 km line. Brake release at X,Y = (25.5,1.0)	0.12	50	Peak FBAR occurs about X = 22.3 km. Reflectivity in shear about 20 dBZ.
	3	Approach toward west along Y = 1.0 km line. Place runway threshold at X,Y = (21.5,1.0) km	0.13	26	

4.0 Plot Descriptions

Appendix A.1 contains vertical atmospheric sounding plots for each of the case studies. [Ambient wind profiles are not used in the axisymmetric cases (cases 1 and 4), and therefore are not included in Figs. A.1.1 and A.1.4.] An explanation of how to read the soundings is in appendix B.

Appendix A.2 contains contour plots of North-South and East-West FBAR plotted at two elevations, 50 m and 300 m. The plots at 50 m show the F-factor field at the lowest elevation above the ground, while the plots at 300 m display the fields near the altitude at which detection sensors must activate. Many of the certification paths encounter the peak shear near these altitudes. Contour plots for East-West FBAR are shown for each case, and North-South FBAR for cases 2, 3, 5 and 6. The North-South FBAR in cases 1 and 4 is not shown, but does not differ from the structure and magnitude of the East-West FBAR because of axial symmetry. Definitions of East-West and North-South FBAR are contained in appendix C.

Appendix A.3 contains contour plots of radar reflectivity factor plotted at 150 meters elevation for all cases. The radar reflectivity field is shown only at the one altitude; however, variations between the ground and 300 m are usually small.

Two-dimensional wind-vector fields are displayed for all cases in appendix A.4. Fields are given for both a horizontal and vertical cross section, with the horizontal slice taken at 50 meters elevation. The location of the vertical cross section varies between case to reflect the most hazardous plane of the flight scenarios.

Appendix A.5 contains the plots of parameters along specific flight path scenarios. The parameters consist of FBAR, radar reflectivity, along-path wind speed, and altitude. For the curved-approach scenarios the altitude is omitted since it is constant at 304.8 meters (1000 ft).

5.0 Instructions for Reading Tape and Verifying Certification Database

The database is in alpha-numeric format on an 8mm Exabyte data cartridge (2.5 gigabyte capacity), and created by the UNIX utility **tar**. Each data set is a separate **tar** volume on the tape.

The suggested **tar** extraction command is:

tar xv "tape device"

This will extract the files in their original name. The tape device must be a non-rewinding tape drive[4]. Repeat the above command until all desired volumes are extracted. In the last **tar** volume and in appendix E is a sample FORTRAN program "datachk.f" to check the consistency of the database. Appendix F has the output from this program for each data set. Table 5.1 gives the file names, size and description of each of the **tar** volumes on the magnetic tape.

Table 5.1 Contents of 8mm Magnetic Tape

File Name	Size (bytes)	tar volume #	Description
c1_11.faa.for	86,084,361	1	Case #1 at 11 minutes simulation time
c2_37.faa.for	66,257,496	2	Case #2 at 37 minutes simulation time
c3_49.faa.for	72,733,937	3	Case #3 at 49 minutes simulation time
c3_51.faa.for	72,733,937	4	Case #3 at 51 minutes simulation time
c4_36.faa.for	117,400,896	5	Case #4 at 36 minutes simulation time
c5_40.faa.for	86,084,361	6	Case #5 at 40 minutes simulation time
c5_45.faa.for	86,084,361	7	Case #5 at 45 minutes simulation time
c6_14.faa.for	38,113,011	8	Case #6 at 14 minutes simulation time
c7_27.faa.for	29,852,511	9	Case #7 at 27 minutes simulation time
datachk.f	11,250	10	FORTRAN code to read and verify the database

Access to the variables within each data set is accomplished by modifying the datachk.f program. The necessary information to read the database is as follows:

The files are read by first reading the title header as follows (FORTRAN code):

```
        read(1,1000) title
1000    format(a80)
```

---

[4]A non-rewinding tape drive is not physically different from a rewinding one. The difference is in how the tape handler responds after a tape read. A rewinding tape always rewinds the tape after each read, whereas the tape position is unaltered after a read on a non-rewinding tape. The user is to refer to the specific environmental variable to access the tape drive as a non-rewinding device.

and then each variable by using:

```
        read(1,2000) var,ix,iy,iz,time,xstart,ystart,dxy,dz,
    1      (((q(i,j,k),i=1,ix),j=1,iy),k=1,iz)
  2000   format(a4,/,3i4,/,5e12.4,/,(8e10.4))
```

The codes (4-character name in **var**) for the variables are explained in Table 2.2 and are as follows:

```
"U   "   "V   "   "W   "   "TAU "   "XIV "
"RRF "   "RAIN"   "HAIL"   "RRFI"   "CLD "
```

The variables **ix,iy**, and **iz** are the size of the 3-D data set and correspond to x, y, and z directions, respectively. The variable **time** is simulation time in seconds, and **xstart** and **ystart** are the locations of the minimum x and y values for the grid. The variable **dxy** is the horizontal spacing, and **dz** is the vertical spacing. Figure 5.1 shows the relationship among computational and physical dimensions. For a given i, j, and k location the physical position is:

$$X(i) = xstart + (i-1)^*dxy$$
$$Y(j) = ystart + (j-1)^*dxy$$
$$Z(k) = (k-1)^*dz$$
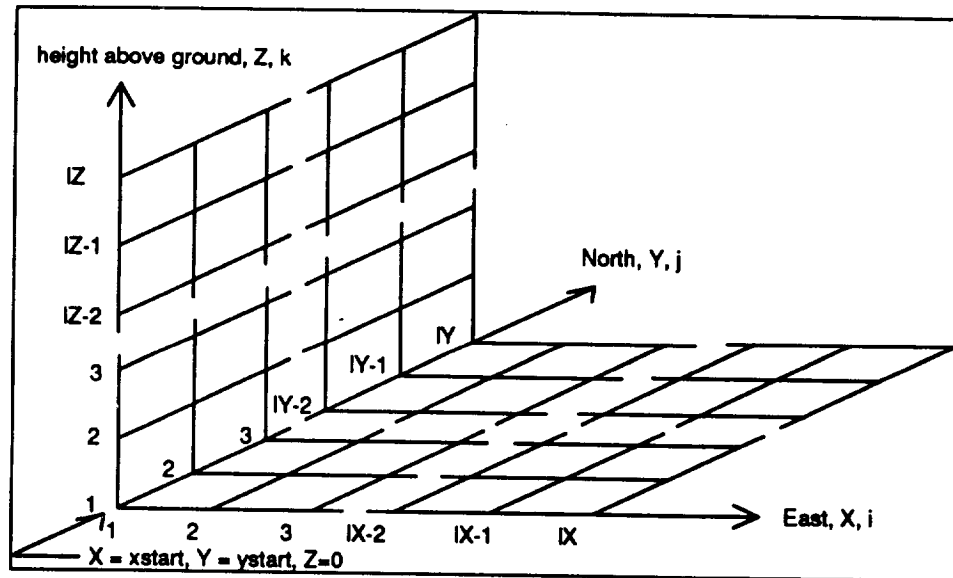
Figure 5.1 Relationship Among Computational and Physical Dimensions (note that North is into the page).

6.0 Concluding Remarks

The NASA Langley Research Center, at the request of the FAA, has developed a database of hazardous windshear phenomena to support the certification of airborne forward-look windshear detection and alerting systems. The database contains high-resolution, three-dimensional fields for meteorological variables that may be sensed in windshear environments by forward-looking systems. Six microburst case studies and one gust front are provided. Also defined are the scenarios required to test forward-look systems using the database and various takeoff and landing flight paths. The database and scenarios represent a wide range of ambient meteorological conditions, microburst reflectivity, size, intensity, intervening precipitation, and symmetry. The scenarios provide cases for windshear detection during takeoff roll, initial climb, straight-in approach, curved approaches, go-around maneuvers, and landings with significant wind drift angles. This document has described the database formulation, the ambient conditions and resultant windshear for each case study, the scenarios and certification testing paths through the data sets, and instructions for reading the database from magnetic tape.

References

Bacon, D. B., T. J. Dunn, M. R. Sands, and R. A. Sarma, 1991: Single burst nuclear cloud database, Volume I -- cloud rise and stabilization modeling. DNA-TR-90-36-V1, 151 pp.

Bedard, A. J., Jr., and T. J. LeFebvre, 1986: Surface measurements of gust fronts and microbursts during the JAWS project: Statistical results and implications for wind shear detection, prediction, and modeling. NOAA Tech. Memo. ERL WPL-135, Wave Propagation Laboratory, Boulder, CO, 112 pp. [Available from the National Technical Information Service, Springfield, VA, 22161.]

Bowles, R. L., 1990: Reducing windshear risk through airborne systems technology. The 17th Congress of the ICAS, Stockholm, Sweden, 27 pp.

Federer, B., and Waldvogel, 1975: Hail and raindrop size distributions from a Swiss multicell storm. J. Appl. Meteor., 14, 91-97.

Fujita, T. T., 1985: The Downburst, Microburst, and Macroburst. University of Chicago Press, , 122 pp.

Fujita , T. T., and R. M. Wakimoto, 1983: JAWS microbursts revealed by triple-Doppler radar, aircraft, and PAM data. Preprints, 13th Conf. on Severe Local Storms, Tulsa, Amer. Meteor. Soc., 97-100.

Goff, R. C., 1976: Vertical structure of thunderstorm outflows. Mon. Wea. Rev., 104, 1429-1440.

Gunn, R. and G. D. Kinzer, 1949: The terminal velocity of fall for water drops in stagnant air. J. Meteor., 6, 243-248.

Hodson, M. C., 1986: Raindrop size distribution. J. Climate Appl. Meteor., 25, 1070-1074.

Huffman, P., and P. Haines, 1984: Visibility in heavy precipitation and its use in diagnosing high rainfall rates. AIAA Paper 84--0541.

Hughes, D., 1990: LLWAS credited with helping 737 survive major microburst. Aviation Week & Space Technology, 133, July-16, pgs. 91 & 93.

IMSL Math/Library 1989, Users Manual, IMSL Math/Library collection of FORTRAN Subroutines and Functions, Version 1.1. IMSL, Houston, TX.

Kessler, E., 1969: On the distribution and continuity of water substance in atmospheric circulations. Metor. Monogr., No. 32, Amer. Meteor. Soc., 84 pp.

Lin, Y-L., R. D. Farley, and H. D. Orville, 1983: Bulk parameterization of the snow field in a cloud model. J. Climate Appl. Meteor., 22, 1065-1092.

List, R., N. R. Donaldson, and R. E. Stewart, 1987: Temporal evolution of drop spectra to collisional equilibrium in steady and pulsating rain. J. Atmos. Sci., 362-372.

Marshal, J. S., and W. M. Palmer, 1948: The distribution of raindrops with size. J. Meteor., 5, 165-166.

Proctor, F. H., 1987: The Terminal Area Simulation System, Volume I: Theoretical formulation. NASA Contractor Rep. 4046, NASA, Washington, DC, 176 pp. [Available from the National Technical Information Service, Springfield, VA, 22161.]

Proctor, F. H., 1987: The Terminal Area Simulation System, Volume II: Verification Experiments. NASA Contractor Rep 4047, NASA, Washington, DC, 112 pp. [Available from the National Technical Information Service, Springfield, VA, 22161.]

Proctor, F. H., 1988: Numerical simulations of an isolated microburst. Part I: Dynamics and structure. J. Atmos. Sci., 45, 3137-3160.

Proctor, F. H., 1989: Numerical simulations of an isolated microburst. Part II: Sensitivity experiments. J. Atmos. Sci., 46, 2143-2165.

Proctor, F. H., 1992: Three-dimensional numerical simulation of the 20 June 1991, Orlando Microburst. Fourth Combined Manufacturers' and Technologists' Airborne Wind Shear Review Meeting, Williamsburg, VA, 214-242.

Proctor, F. H., 1993: Case study of a low-reflectivity pulsating microburst: Numerical simulation of the Denver, 8 July 1989, Storm. To appear in Preprints, 17th Conference on Severe Local Storms, St. Louis, Amer. Meteor. Soc.

Proctor, F. H. and R. L. Bowles, 1992: Three-dimensional simulation of the Denver 11 July 1988 microburst-producing storm. Meteorol. and Atmos. Phys., 47., 107-124.

Roberts, R. D., and J. W. Wilson, 1989: A proposed microburst nowcasting procedure using single-Doppler radar. J. Appl. Meteor., 28, 285-303.

Schlickenmaier, H. W. (editor), 1989: Windshear Case Study: Denver, Colorado, July 11, 1988. Final Report, DOT/FAA/DS-89/19, Federal Aviation Administration, 552 pp. [Available from the National Technical Information Service, Springfield, VA, 22161.]

Sekhon, R. S., and R. C. Srivastava, 1971: Doppler radar observations of drop-size distributions in a thunderstorm. J. Atmos. Sci., 28, 983-994.

Wilson, F. W., Jr., R. C. Goff, and R. H. Gramzow, 1991: An intense microburst at Denver's Stapleton International Airport. Preprints, Fourth Intl. Conf. on the Aviation Weather System, Paris, Amer. Meteor. Soc.

Appendix A

Database Plots

Appendix A.1

Input Sounding Plotted on Skew T-log p Diagrams
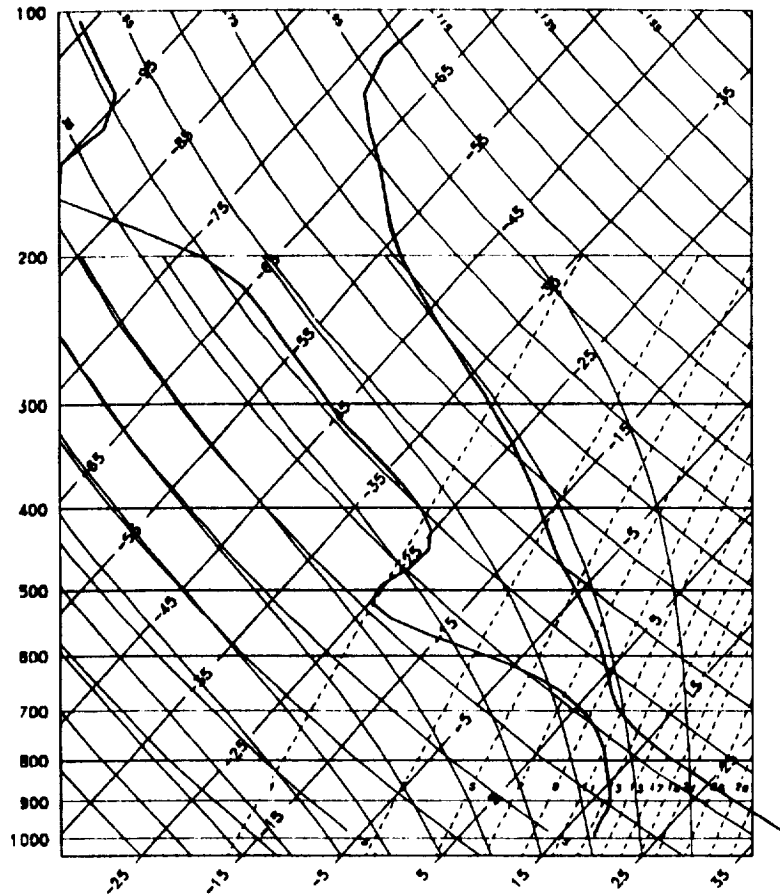
Figure A.1.1 Skew-T diagram of atmospheric sounding for case #1; sounding interpolated from data observed at Dallas, Ft. Worth, 3 August 1985, 0000 UTC. [See appendix B for explanation of Skew-T diagram.]
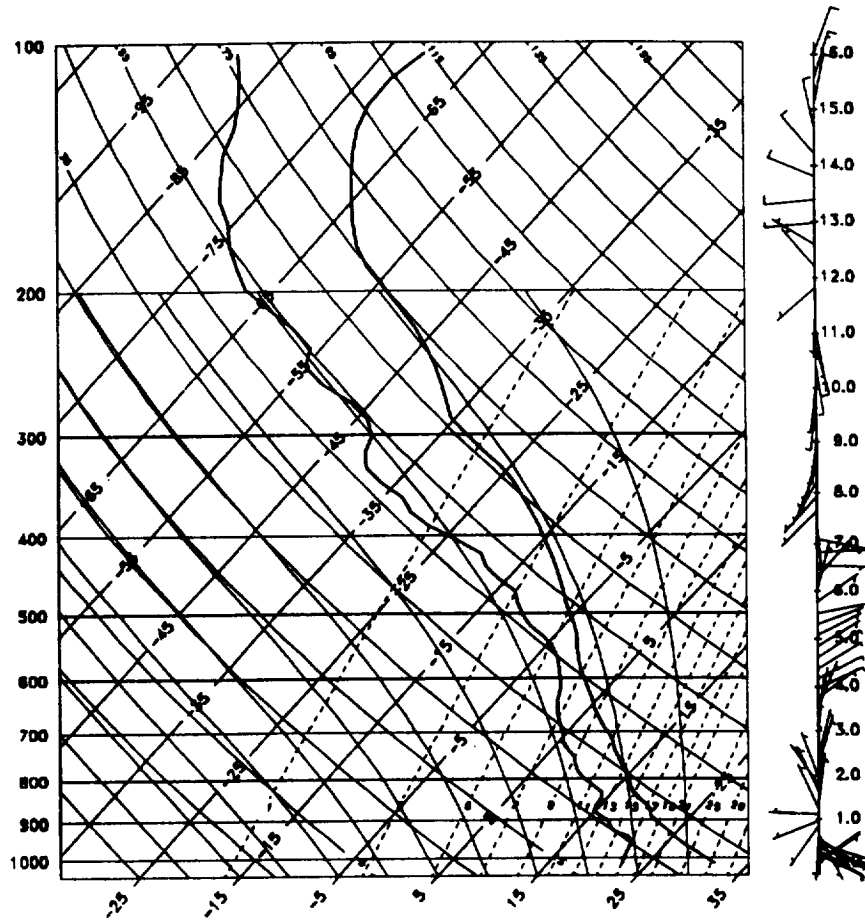
Figure A.1.2 Same as Fig. A.1.1, but for case #2. Modified from special sounding observed at Orlando, Florida based, 20 June 1991, 2035 UTC. Wind barbs are pointed along the compass direction of the wind. Each full wind barb equals 5 m/s (10 knots).
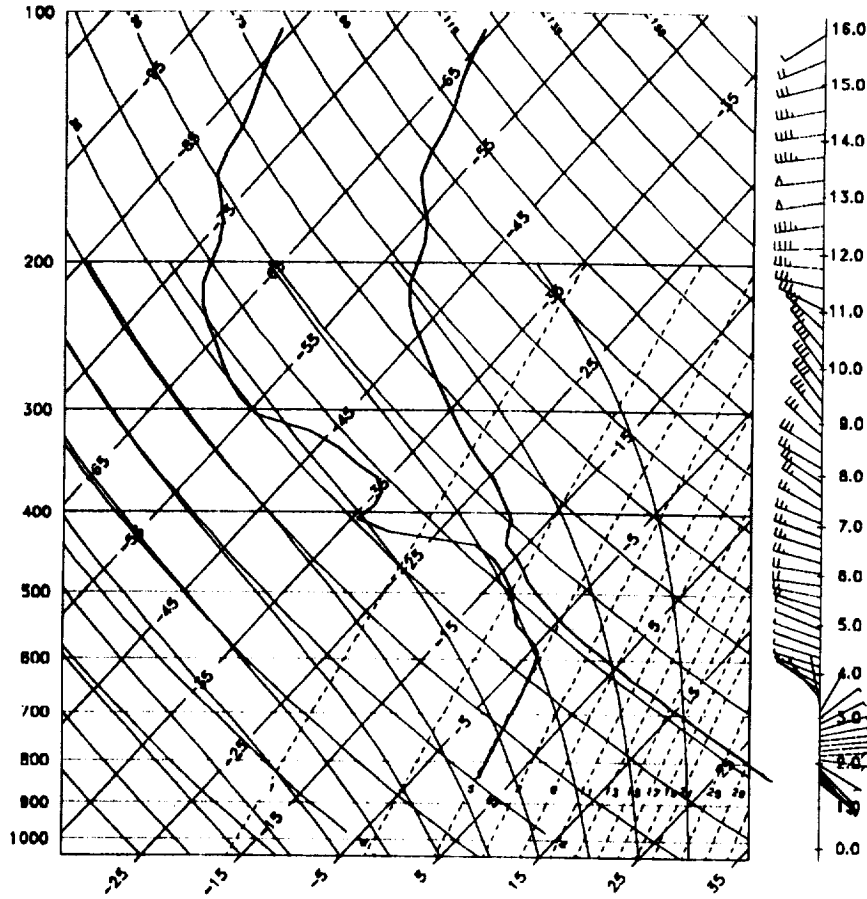
Figure A.1.3 Same as Fig. A.1.2, but for case #3. Special sounding observed at Denver, Colorado, 11 July 1988, 2000 UTC, modified for latest surface observations.
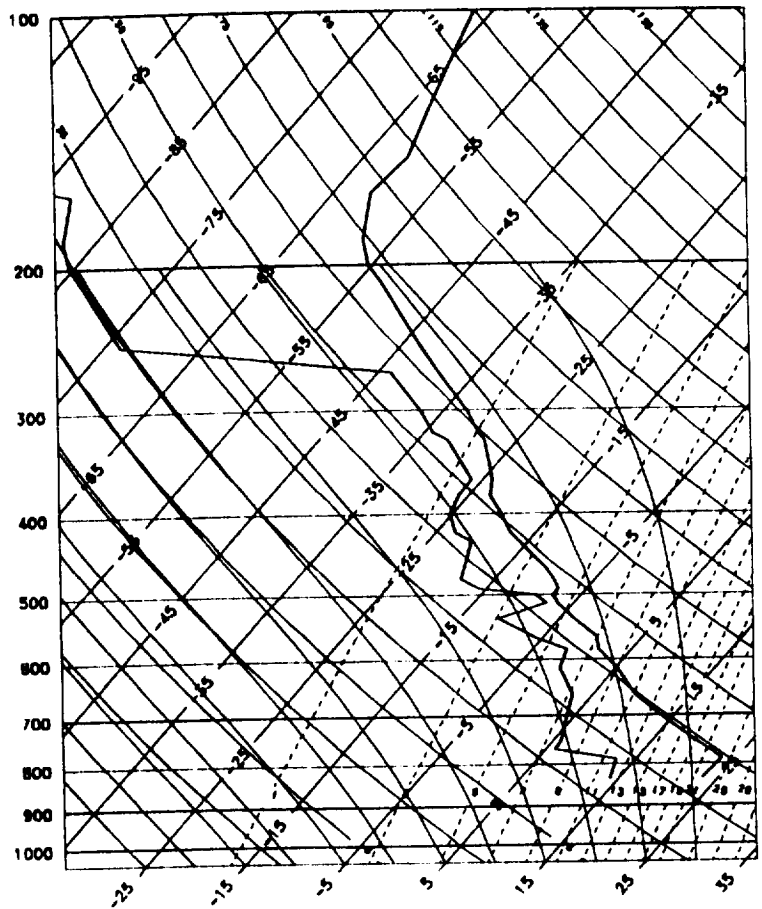
Figure A.1.4 Same as Fig. A.1.1, but for case #4. From observed sounding at Denver, Colorado, 14 July 1982 2000 UTC, but modified for a 500 m deep surface-base isothermal layer.
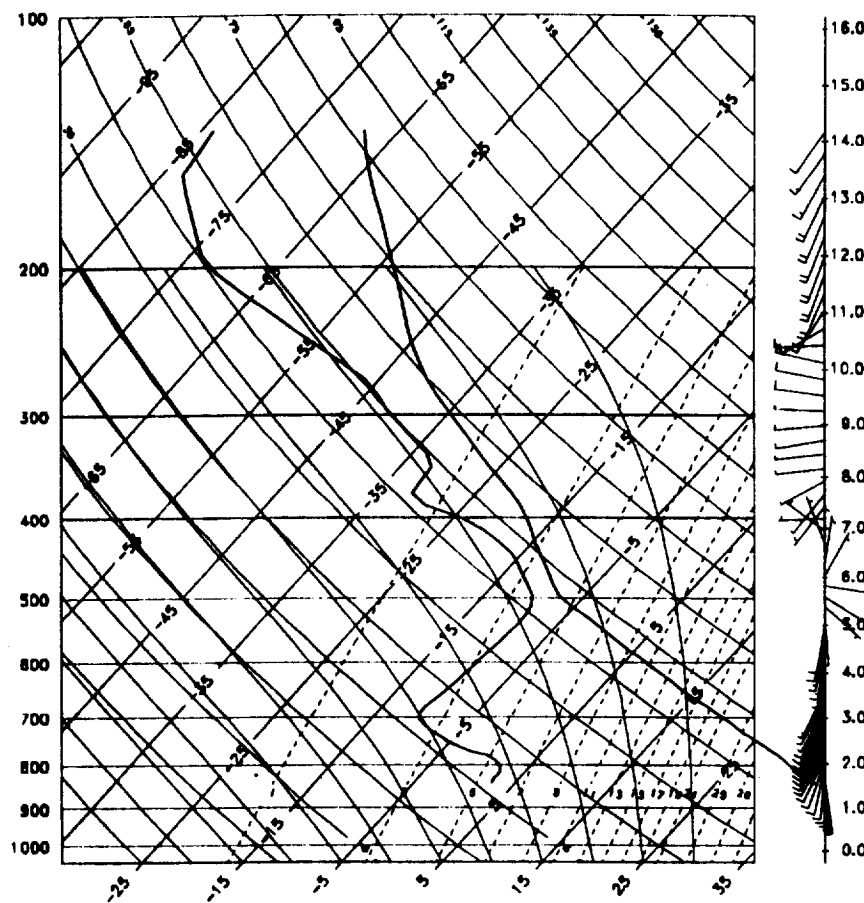
Figure A.1.5 Same as Fig. A.1.2, but for case #5. Sounding observed at Denver, Colorado, 9 July 1989, 0000 UTC.
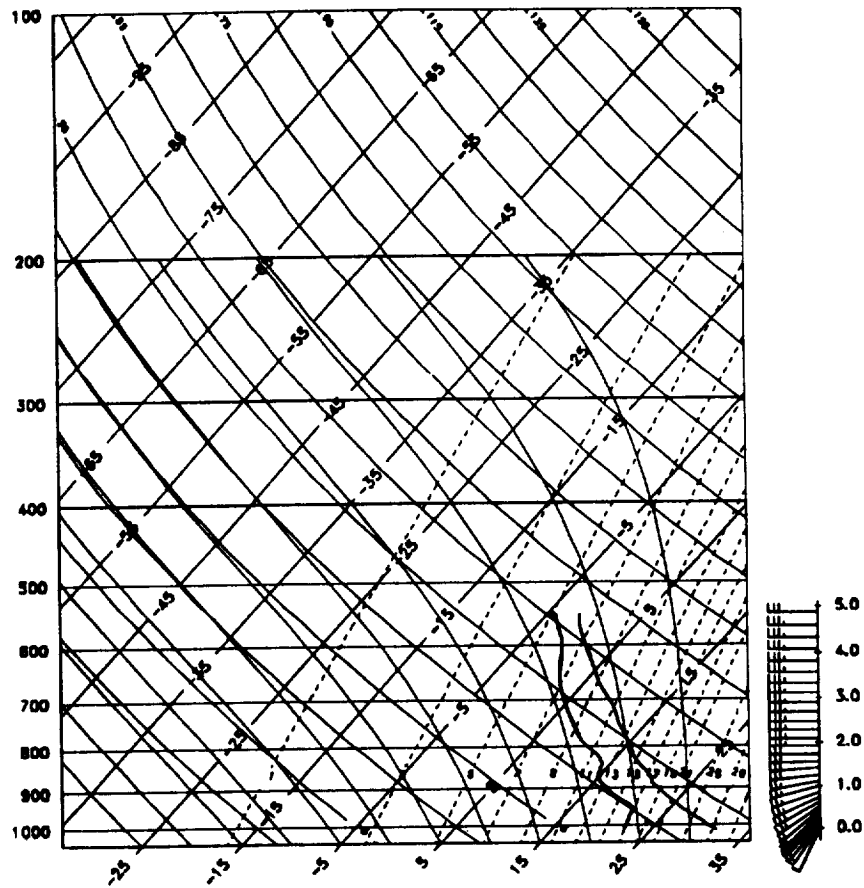
Figure A.1.6 Same sounding as Fig. A.1.2, but observed winds replaced by hypothetical winds. Environmental winds modified in order to create asymmetric microburst in case #6.
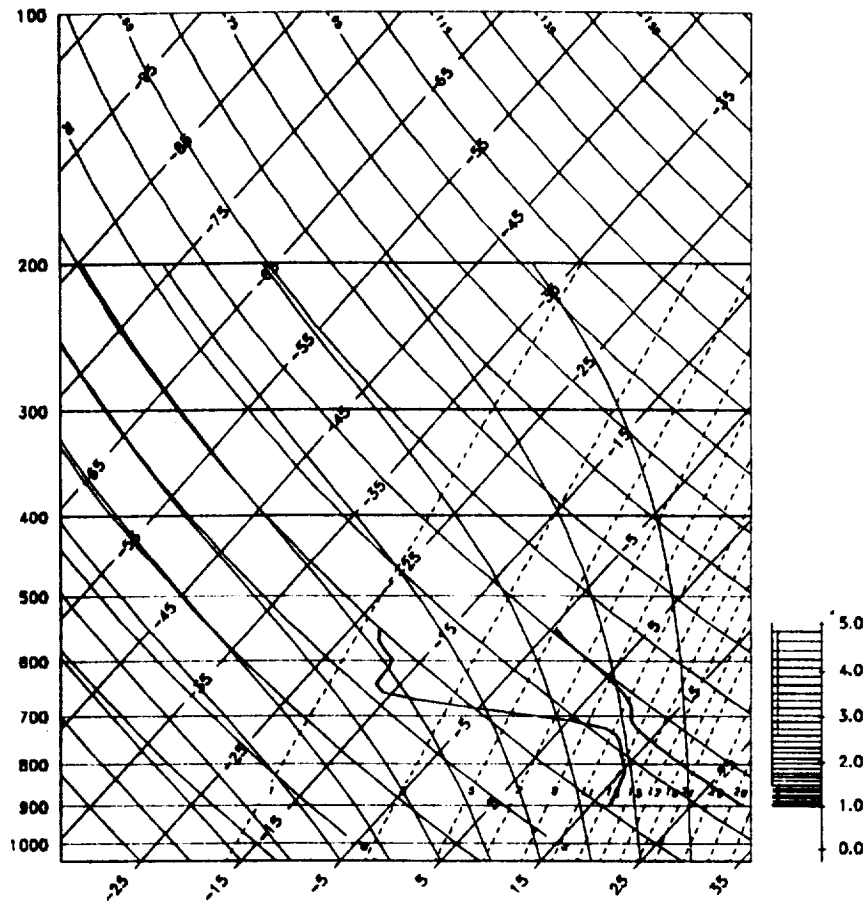
Figure A.1.7 Same as Fig. A.1.2, but for case #7. Modified from special sounding observed at Knowlton, Montana, 3 August 1981, 0000 UTC. Only the northern component of the observed ambient wind is used and is shifted 90°.

Appendix A.2

North-South and East-West $\bar{F}_{Km}$ Contour Plots

Case #1-11, DFW Accident Case, Wet Microburst
E-W 1 Km Averaged F Factor at Z= 300.0 meters
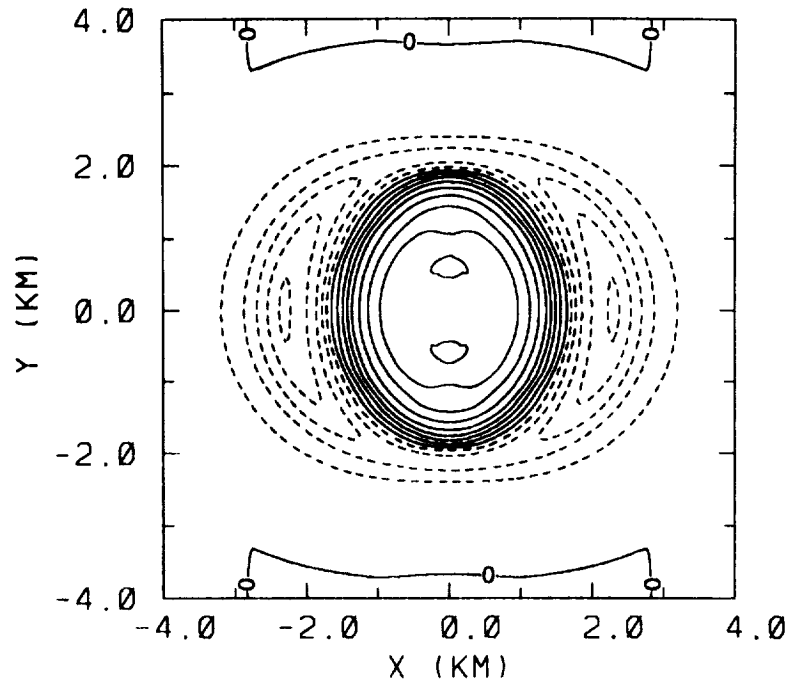
Figure A.2.1 Data Set #1-11: East-West $\bar{F}_{Km}$ at 300 meters elevation. The contour interval is 0.025. Contours with a negative value are dashed. Maximum value is about 0.20.

Case #1-11, DFW Accident Case, Wet Microburst
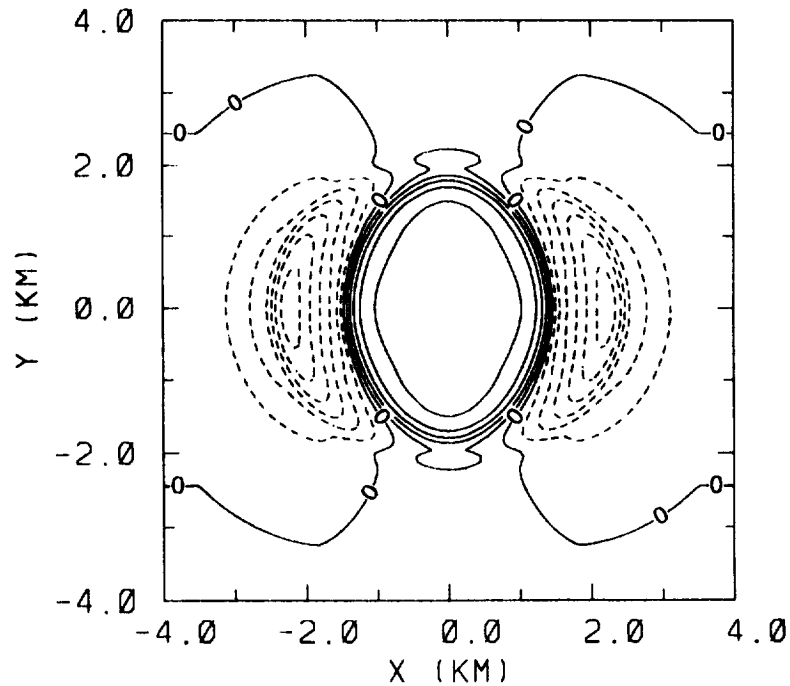E-W 1 Km Averaged F Factor at Z= 50.0 meters

Figure A.2.2 Data Set #1-11: East-West $\bar{F}_{Km}$ at 50 meters elevation. Contours as in Figure A.2.1 with maximum value of about 0.15.

Case #2-37:   06/20/91 Orlando - NASA Event #143
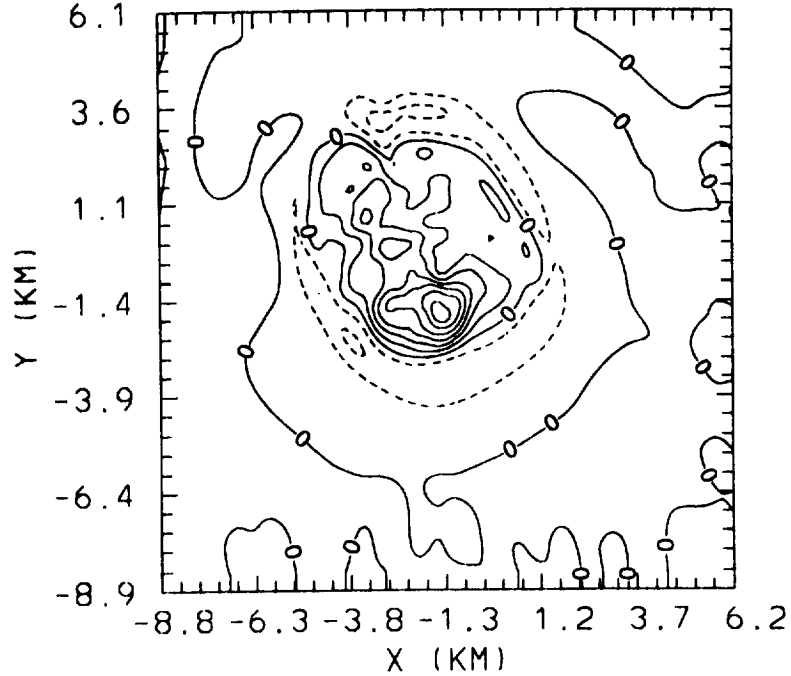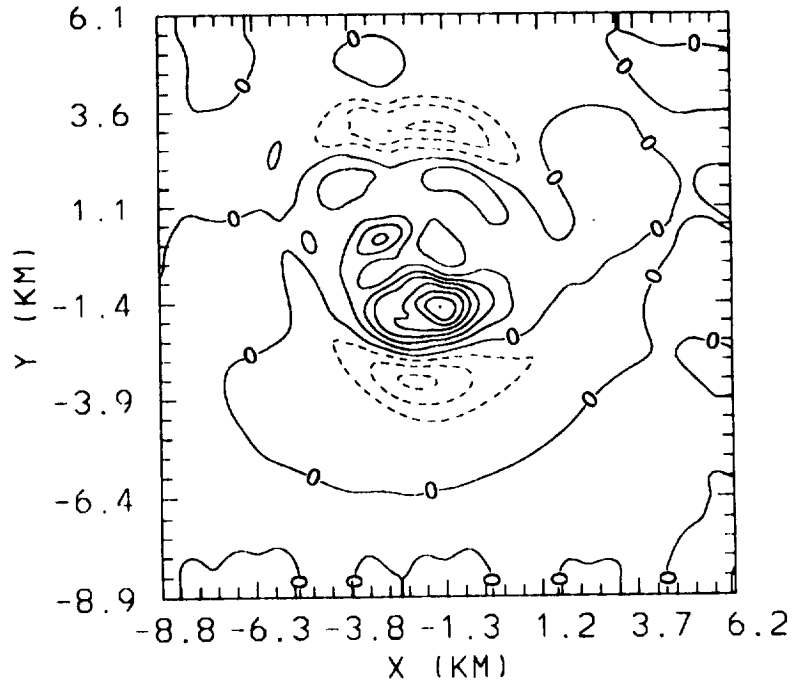N-S 1 Km Averaged F Factor at Z= 300.0 meters

Figure A.2.3 Data Set #2-37: North-South $\bar{F}_{Km}$ at 300 meters elevation. Contours as in Figure A.2.1 with maximum value of about 0.17.

Case #2-37:   06/20/91 Orlando - NASA Event #143
N-S 1 Km Averaged F Factor at Z= 50.0 meters

Figure A.2.4 Data Set #2-37: North-South $\bar{F}_{Km}$ at 50 meters elevation. Contours as in Figure A.2.1 with maximum value of about 0.17.

A-11

Case #2-37,   06/20/91 Orlando - NASA Event #143
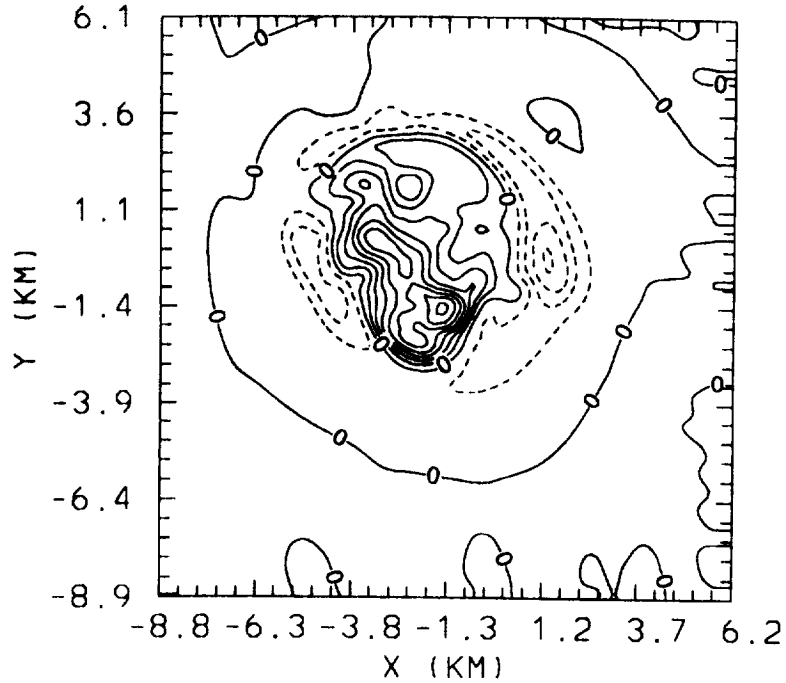E-W 1 Km Averaged F Factor at Z= 300.0 meters

Figure A.2.5 Data Set #2-37: East-West $\bar{F}_{Km}$ at 300 meters elevation. Contours as in Figure A.2.1 with maximum value of about 0.18.

Case #2-37,   06/20/91 Orlando - NASA Event #143
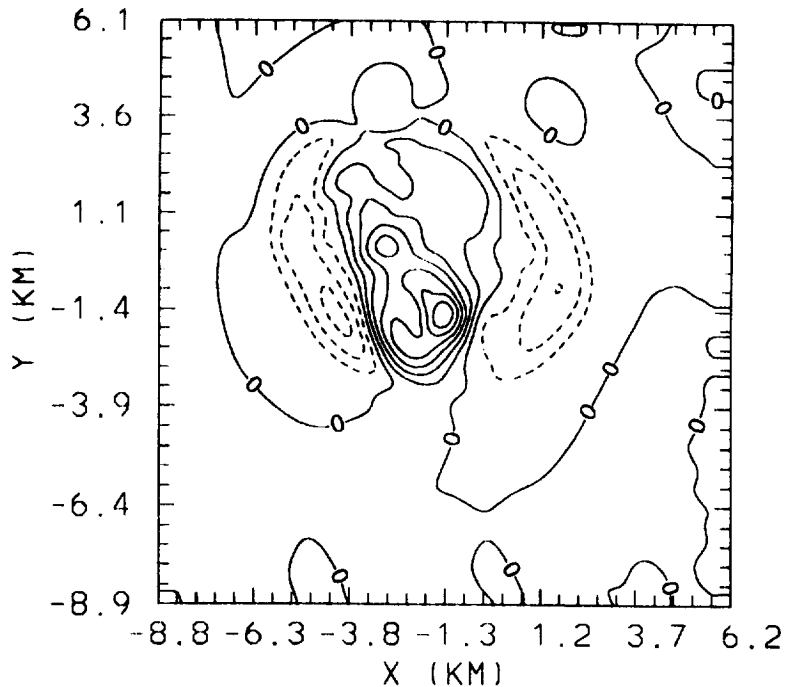E-W 1 Km Averaged F Factor at Z= 50.0 meters

Figure A.2.6 Data Set #2-37: East-West $\bar{F}_{Km}$ at 50 meters elevation. Contours as in Figure A.2.1 with maximum value of about 0.17.

Case #3-49, 07/11/88 Denver - Multiple Microburst
N-S 1 Km Averaged F Factor at Z= 300.0 meters

Figure A.2.7 Data Set #3-49: North-South $\bar{F}_{Km}$ at 300 meters elevation. Contours as in Figure A.2.1 with maximum value of about 0.19.

Case #3-49, 07/11/88 Denver - Multiple Microburst
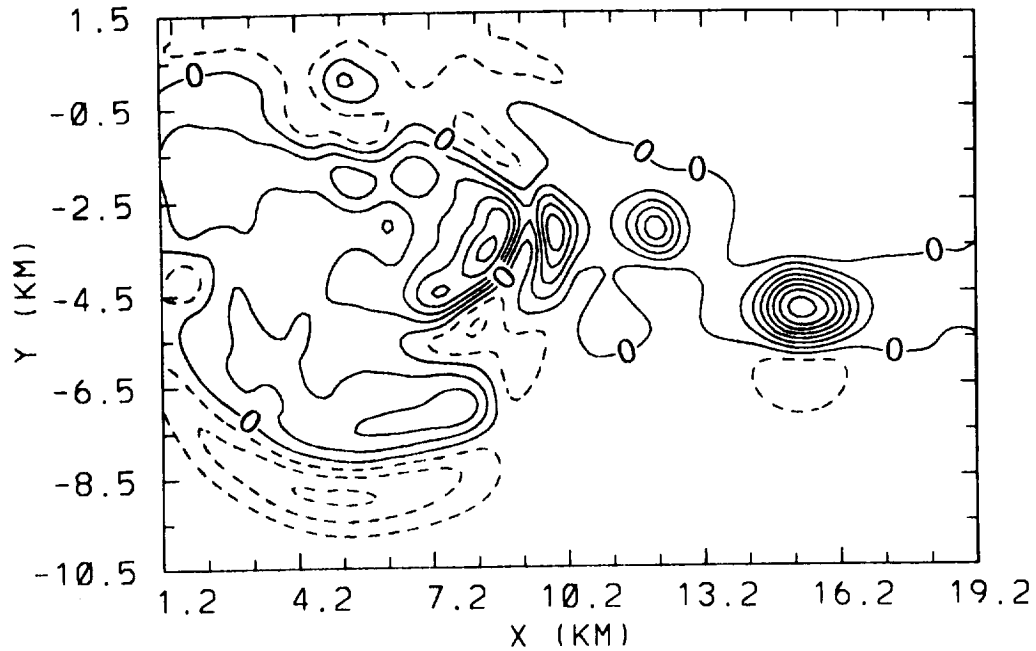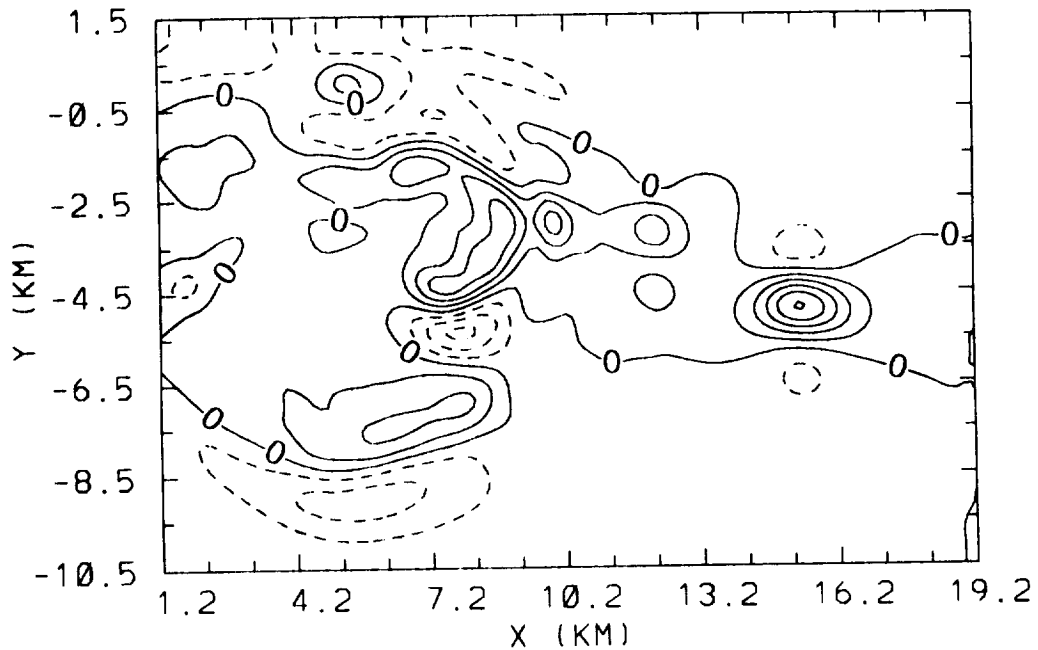N-S 1 Km Averaged F Factor at Z= 50.0 meters

Figure A.2.8 Data Set #3-49: North-South $\bar{F}_{Km}$ at 50 meters elevation. Contours as in Figure A.2.1 with maximum value of about 0.13.

Case #3-49: 07/11/88 Denver - Multiple Microburst
E-W 1 Km Averaged F Factor at Z= 300.0 meters

Figure A.2.9 Data Set #3-49: East-West $\bar{F}_{Km}$ at 300 meters elevation. Contours as in Figure A.2.1 with maximum value of about 0.17.

Case #3-49: 07/11/88 Denver - Multiple Microburst
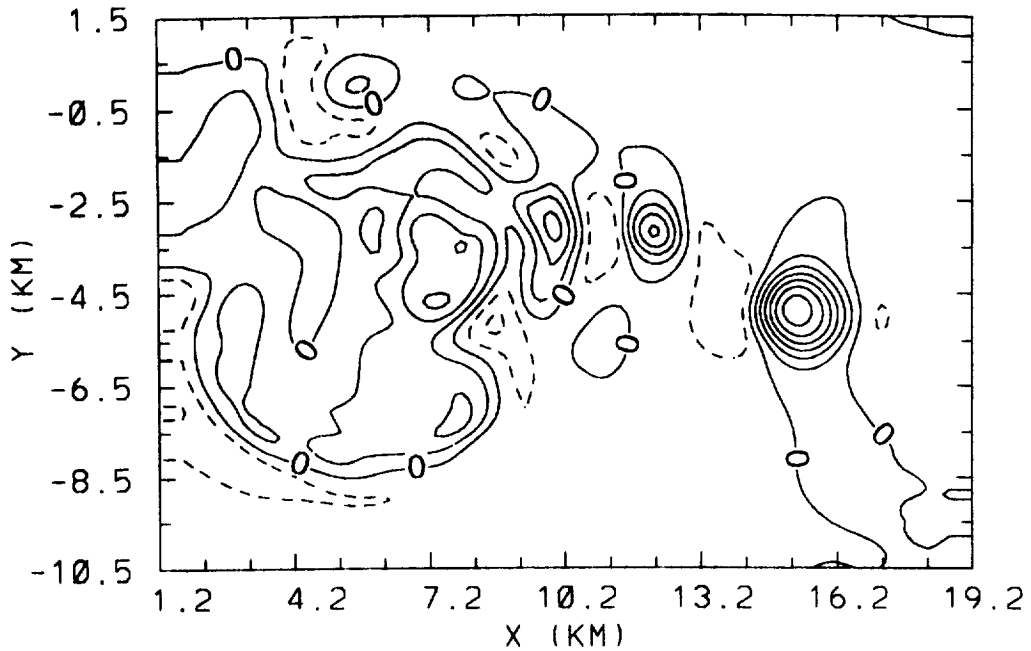E-W 1 Km Averaged F Factor at Z= 50.0 meters

Figure A.2.10 Data Set #3-49: East-West $\bar{F}_{Km}$ at 50 meters elevation. Contours as in Figure A.2.1 with maximum value of about 0.11.

Case #3-51, 07/11/88 Denver - Multiple Microburst
N-S 1 Km Averaged F Factor at Z= 300.0 meters

Figure A.2.11 Data Set #3-51: North-South $\bar{F}_{Km}$ at 300 meters elevation. Contours as in Figure A.2.1 with maximum value of about 0.24.

Case #3-51, 07/11/88 Denver - Multiple Microburst
N-S 1 Km Averaged F Factor at Z= 50.0 meters

Figure A.2.12 Data Set #3-51: North-South $\bar{F}_{Km}$ at 50 meters elevation. Contours as in Figure A.2.1 with maximum value of about 0.20.

Case #3-51: 07/11/88 Denver - Multiple Microburst
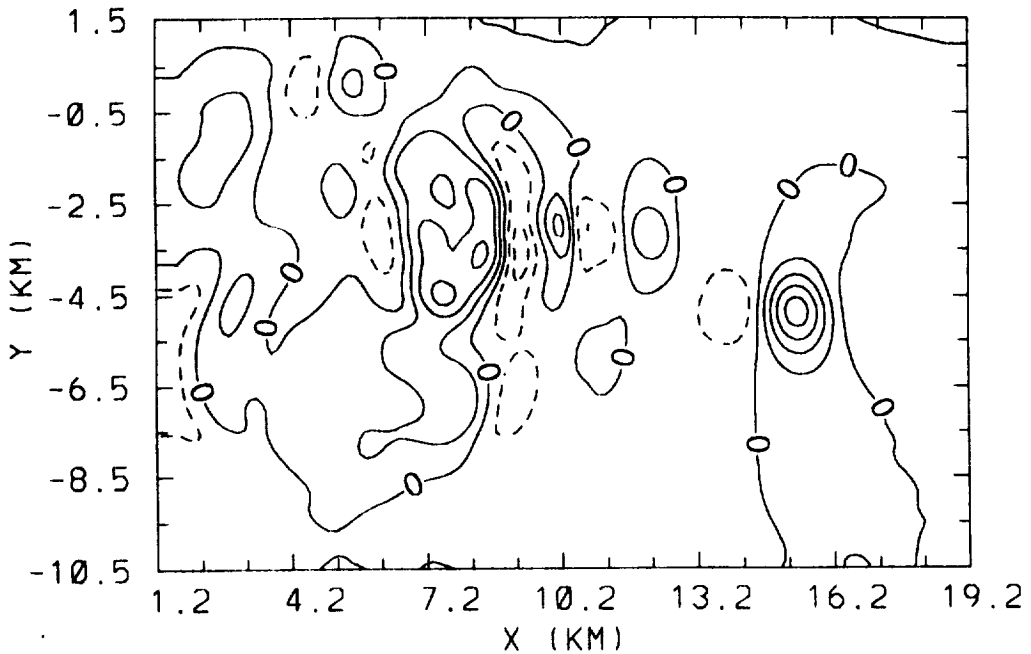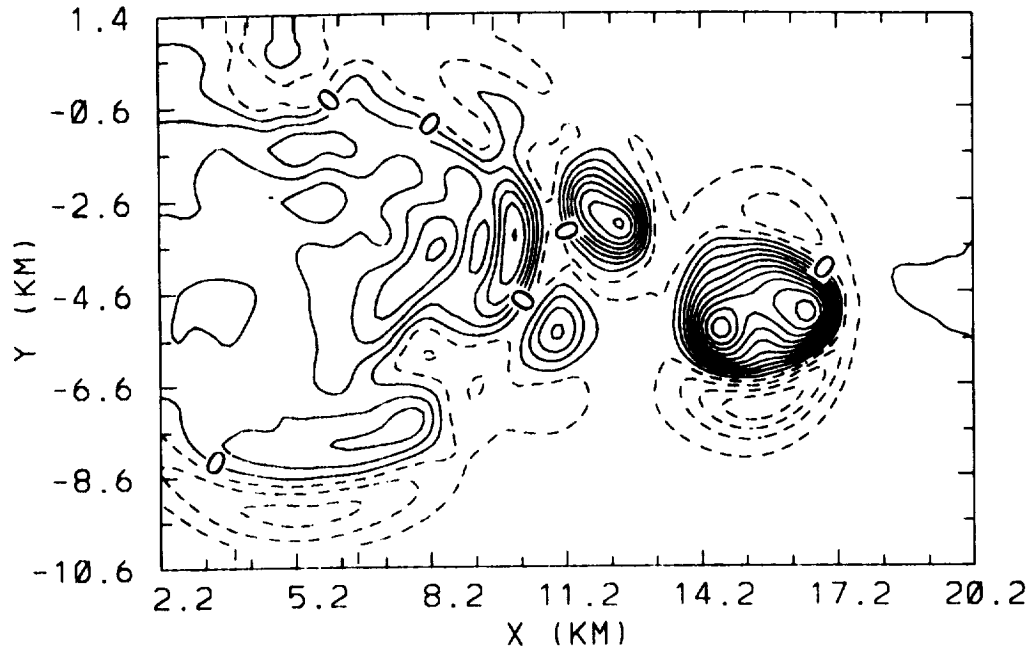E-W 1 Km Averaged F Factor at Z= 300.0 meters

Figure A.2.13 Data Set #3-51: East-West $\bar{F}_{Km}$ at 300 meters elevation. Contours as in Figure A.2.1 with maximum value of about 0.18.

Case #3-51: 07/11/88 Denver - Multiple Microburst
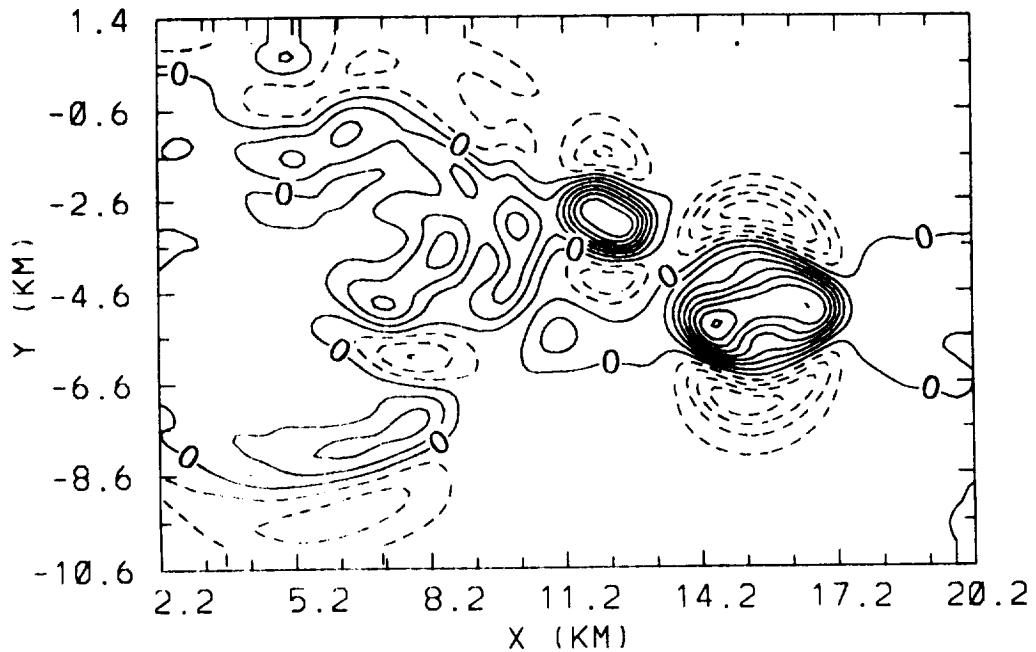E-W 1 Km Averaged F Factor at Z= 50.0 meters

Figure A.2.14 Data Set #3-51: East-West $\bar{F}_{Km}$ at 50 meters elevation. Contours as in Figure A.2.1 with maximum value of about 0.20.

A-16

Case #4-36, 07/14/82 Denver - Temperature Inversion
E-W 1 Km Averaged F Factor at Z= 300.0 meters

Figure A.2.15 Data Set #4-36: East-West $\bar{F}_{Km}$ at 300 meters elevation. Contours as in Figure A.2.1 with maximum value of about 0.18.

Case #4-36, 07/14/82 Denver - Temperature Inversion
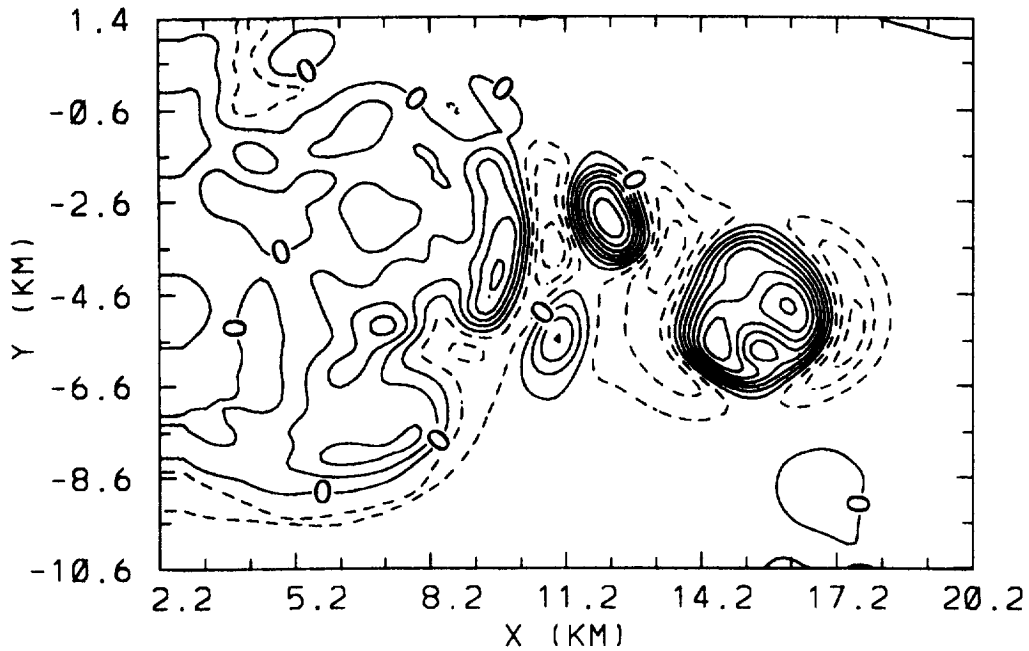E-W 1 Km Averaged F Factor at Z= 50.0 meters

Figure A.2.16 Data Set #4-36: East-West $\bar{F}_{Km}$ at 50 meters elevation. Contours as in Figure A.2.1 with maximum value of about 0.29.

Case #5-40, DRY - Microburst NASA Derived
N-S 1 Km Averaged F Factor at Z= 300.0 meters

Figure A.2.17 Data Set #5-40: North-South $\bar{F}_{Km}$ at 300 meters elevation. Contours as in Figure A.2.1 with maximum value of about 0.21.

Case #5-40, DRY - Microburst NASA Derived
N-S 1 Km Averaged F Factor at Z= 50.0 meters

Figure A.2.18 Data Set #5-40: North-South $\bar{F}_{Km}$ at 50 meters elevation. Contours as in Figure A.2.1 with maximum value of about 0.18.

Case #5-40, DRY - Microburst NASA Derived
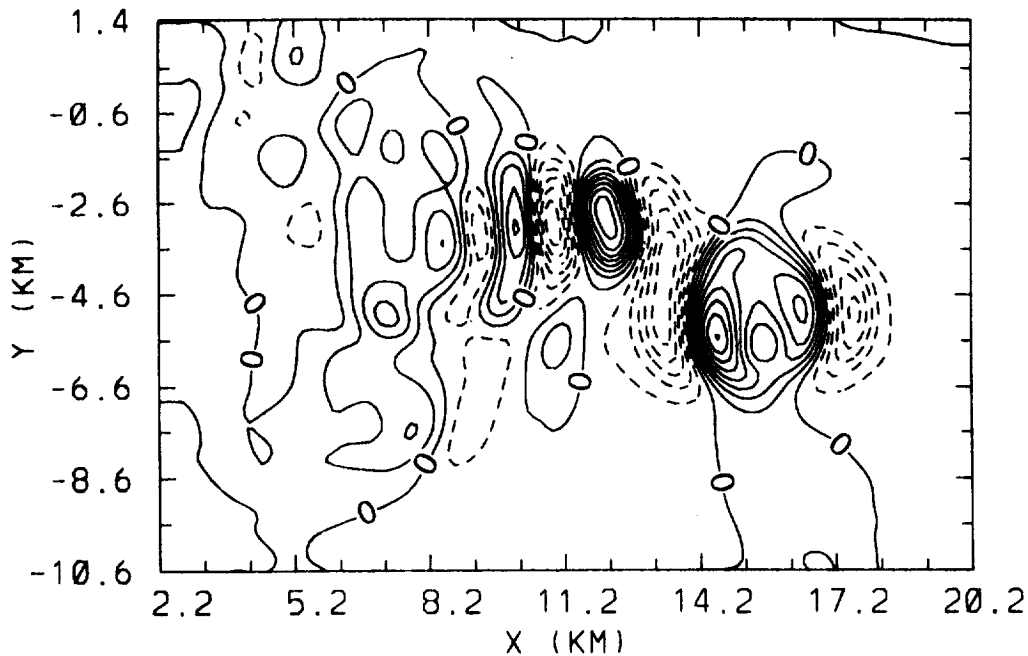E-W 1 Km Averaged F Factor at Z= 300.0 meters

Figure A.2.19 Data Set #5-40: East-West $\bar{F}_{Km}$ at 300 meters elevation. Contours as in Figure A.2.1 with maximum value of about 0.18.

Case #5-40, DRY - Microburst NASA Derived
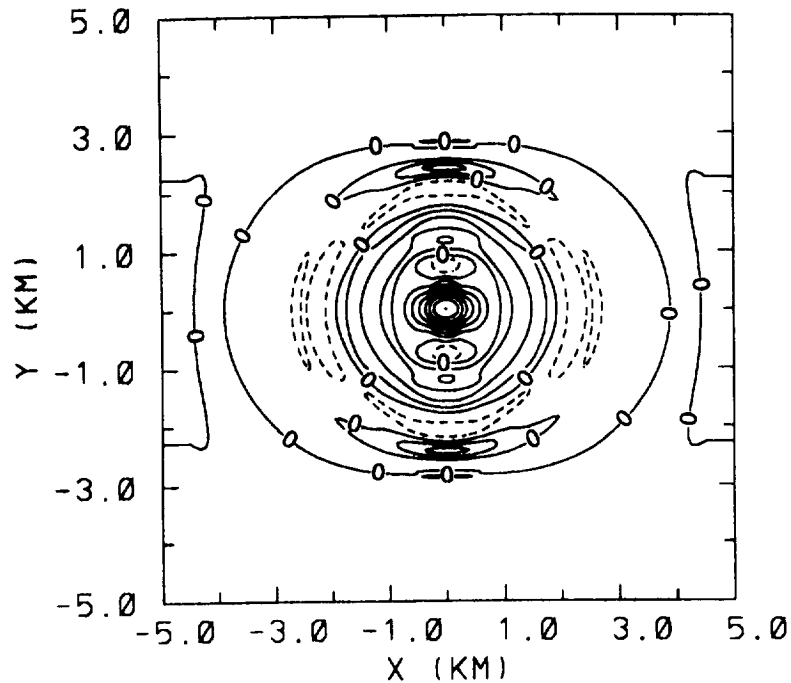E-W 1 Km Averaged F Factor at Z= 50.0 meters

Figure A.2.20 Data Set #5-40: East-West $\bar{F}_{Km}$ at 50 meters elevation. Contours as in Figure A.2.1 with maximum value of about 0.18.

Case #5-45, DRY - Microburst NASA Derived
N-S 1 Km Averaged F Factor at Z= 300.0 meters

Figure A.2.21 Data Set #5-45: North-South $\bar{F}_{Km}$ at 300 meters elevation. Contours as in Figure A.2.1 with maximum value of about 0.16.

Case #5-45, DRY - Microburst NASA Derived
N-S 1 Km Averaged F Factor at Z= 50.0 meters

Figure A.2.22 Data Set #5-45: North-South $\bar{F}_{Km}$ at 50 meters elevation. Contours as in Figure A.2.1 with maximum value of about 0.15.

Case #5-45, DRY - Microburst NASA Derived
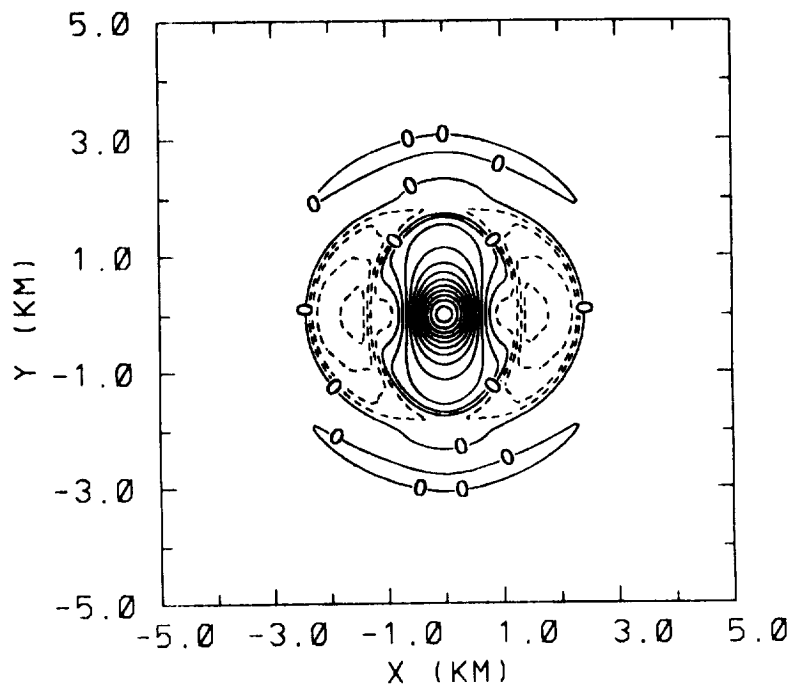E-W 1 Km Averaged F Factor at Z= 300.0 meters
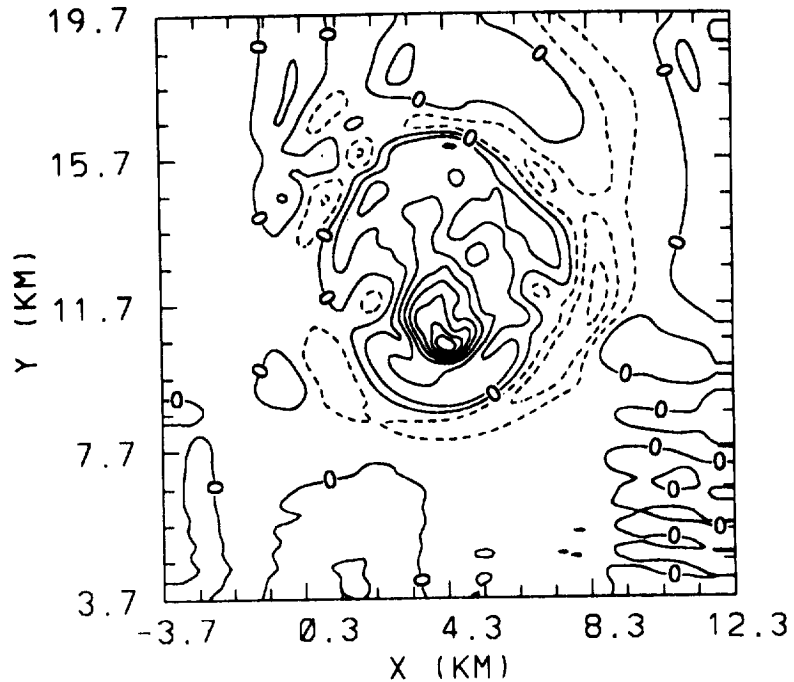
Figure A.2.23 Data Set #5-45: East-West $\bar{F}_{Km}$ at 300 meters elevation. Contours as in Figure A.2.1 with maximum value of about 0.20.

Case #5-45, DRY - Microburst NASA Derived
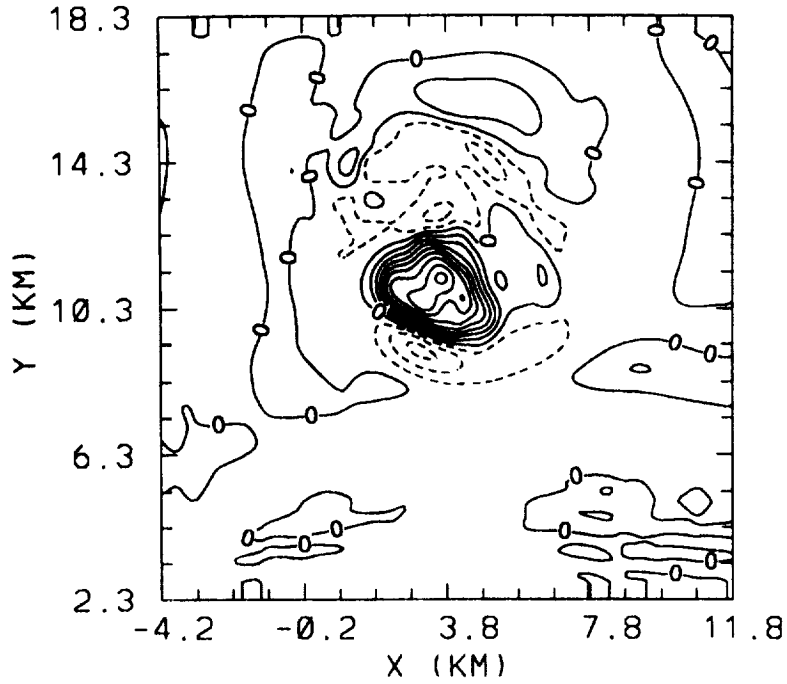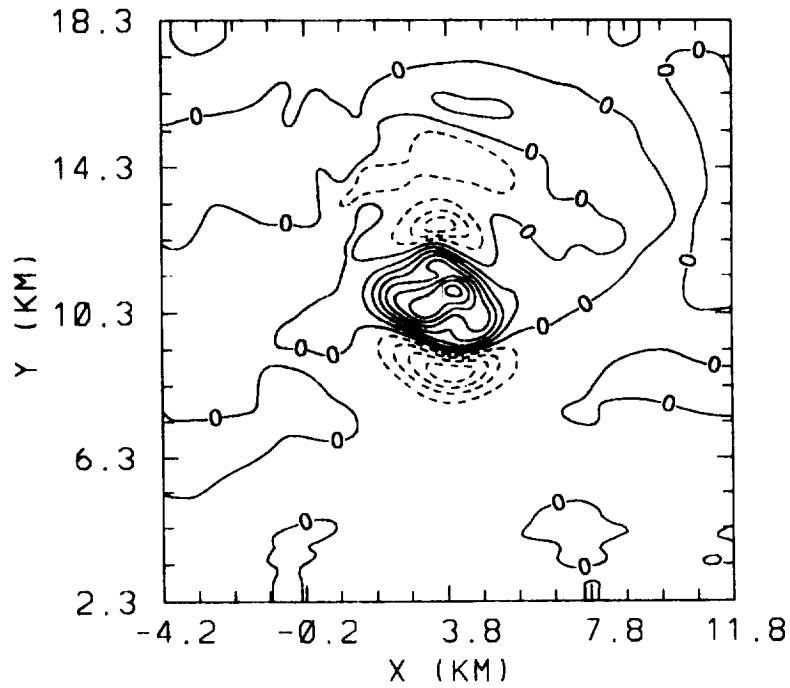E-W 1 Km Averaged F Factor at Z= 50.0 meters
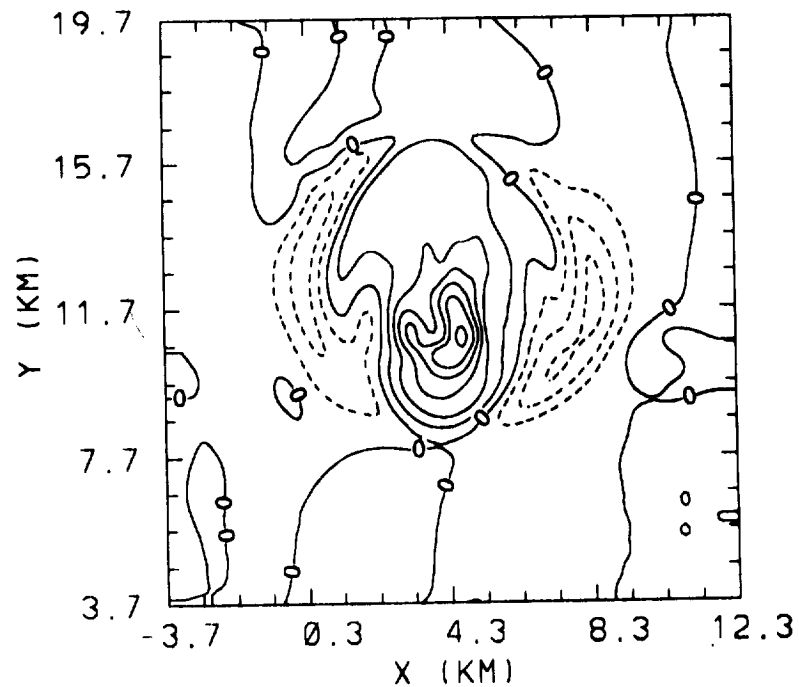
Figure A.2.24 Data Set #5-45: East-West $\bar{F}_{Km}$ at 50 meters elevation. Contours as in Figure A.2.1 with maximum value of about 0.16.

Case #6-14. Highly asymmetric Microburst
N-S 1 Km Averaged F Factor at Z= 300.0 meters
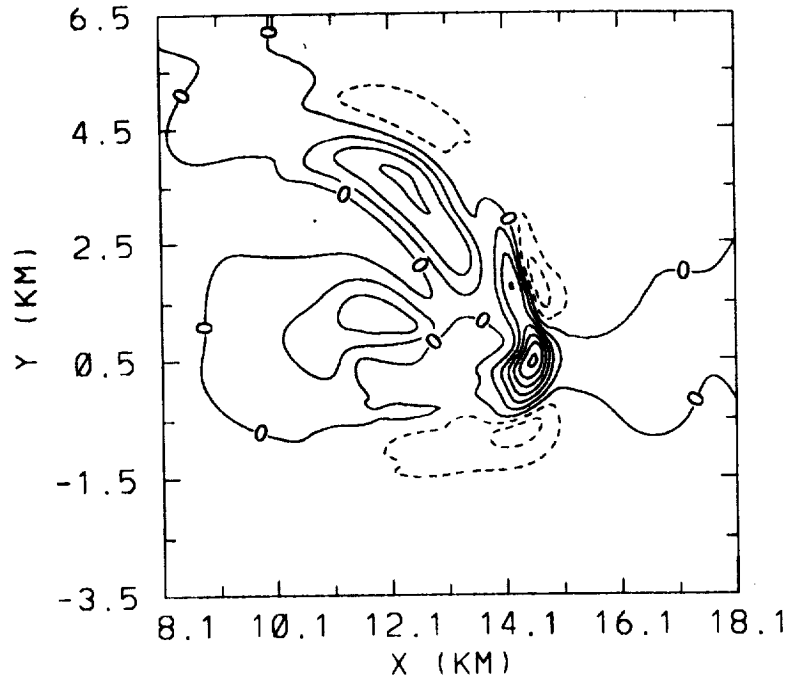
Figure A.2.25 Data Set #6-14: North-South $\bar{F}_{Km}$ at 300 meters elevation. Contours as in Figure A.2.1 with maximum value of about 0.16.

Case #6-14. Highly asymmetric Microburst
N-S 1 Km Averaged F Factor at Z= 50.0 meters
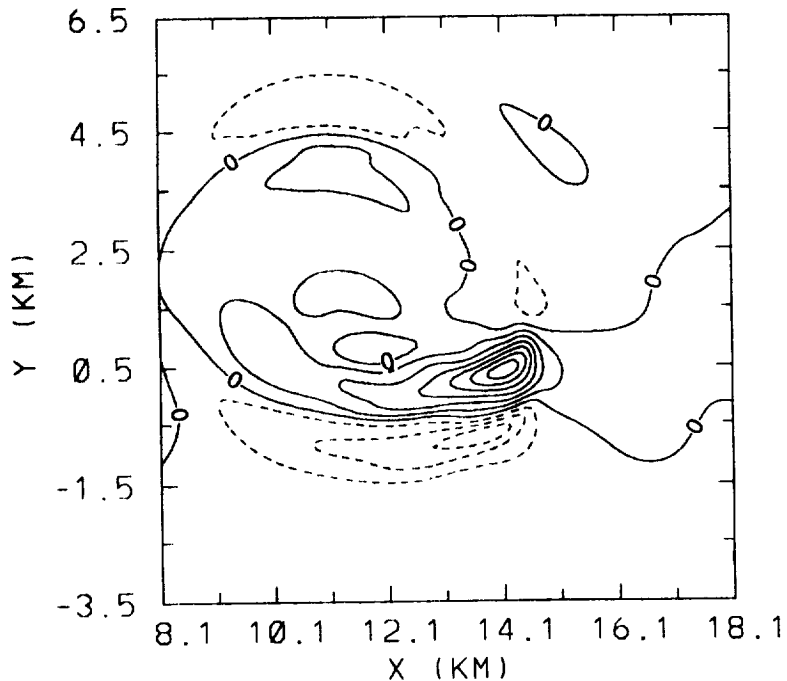
Figure A.2.26 Data Set #6-14: North-South $\bar{F}_{Km}$ at 50 meters elevation. Contours as in Figure A.2.1 with maximum value of about 0.17.

Case #6-14: Highly asymmetric Microburst
E-W 1 Km Averaged F Factor at Z= 300.0 meters
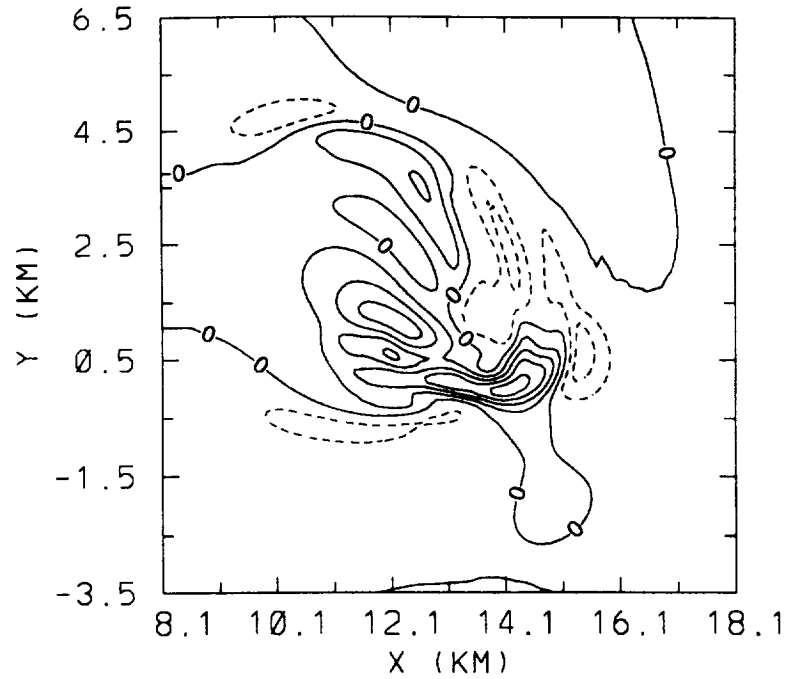
Figure A.2.27 Data Set #6-14: East-West $\overline{F}_{Km}$ at 300 meters elevation. Contours as in Figure A.2.1 with maximum value of about 0.12.

Case #6-14: Highly asymmetric Microburst
E-W 1 Km Averaged F Factor at Z= 50.0 meters
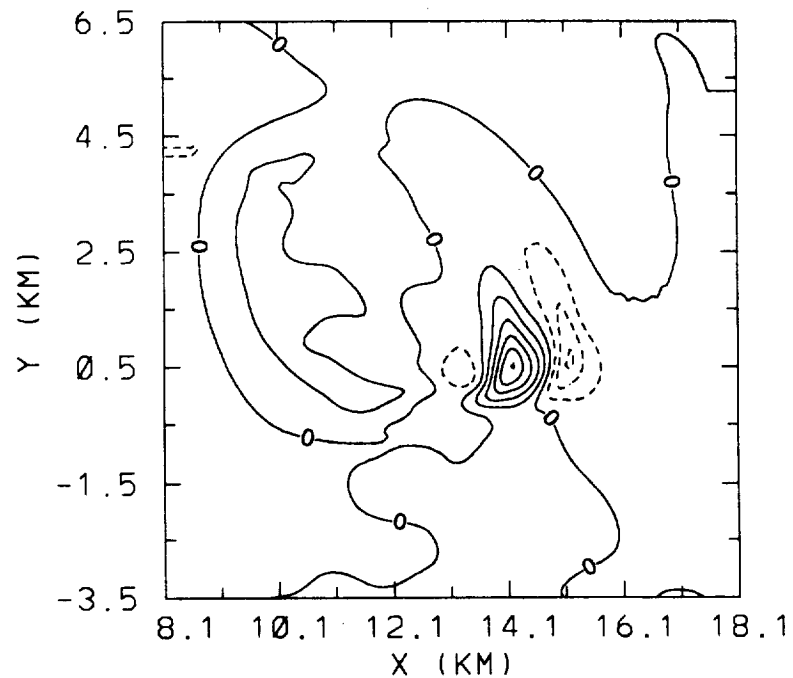
Figure A.2.28 Data Set #6-14: East-West $\overline{F}_{Km}$ at 50 meters elevation. Contours as in Figure A.2.1 with maximum value of about 0.13.

Case #7-27, Gust Front

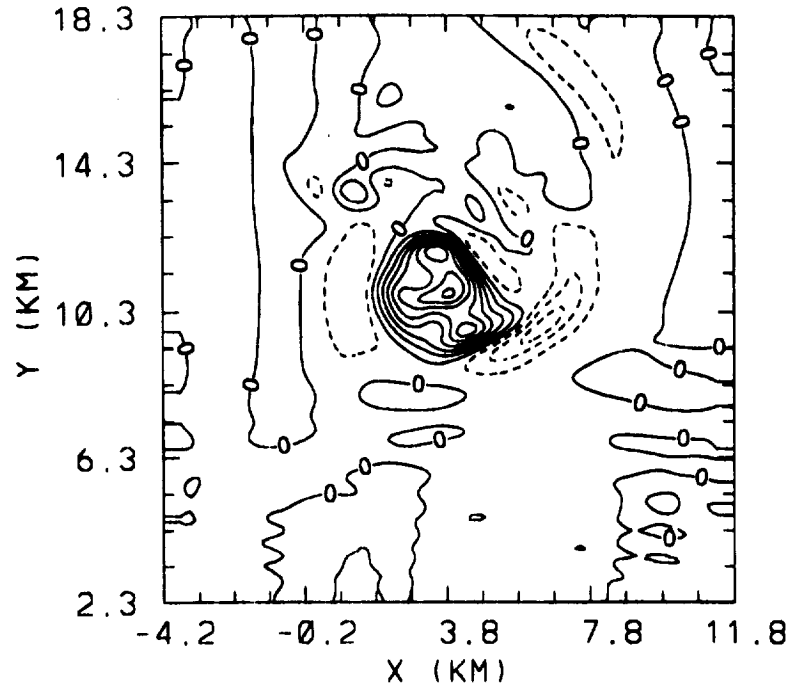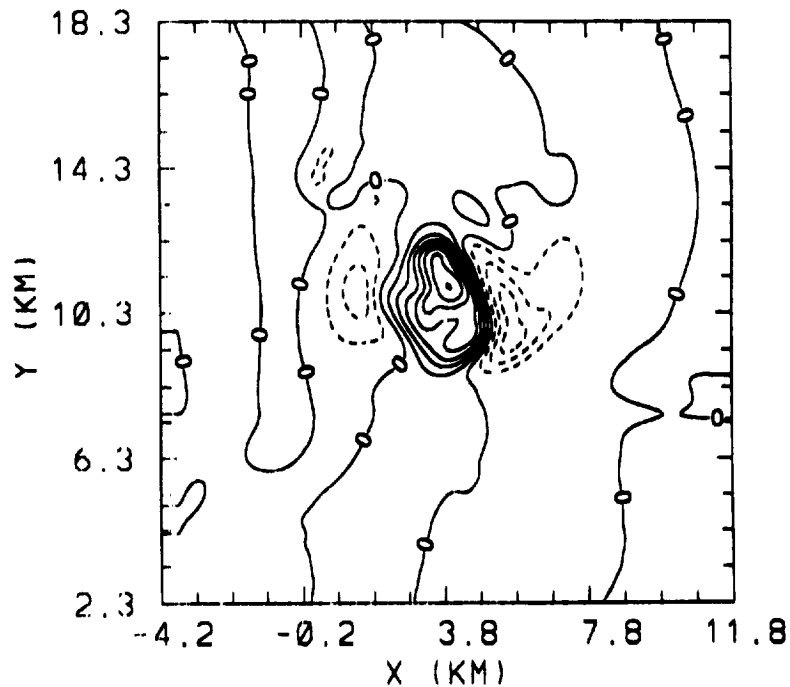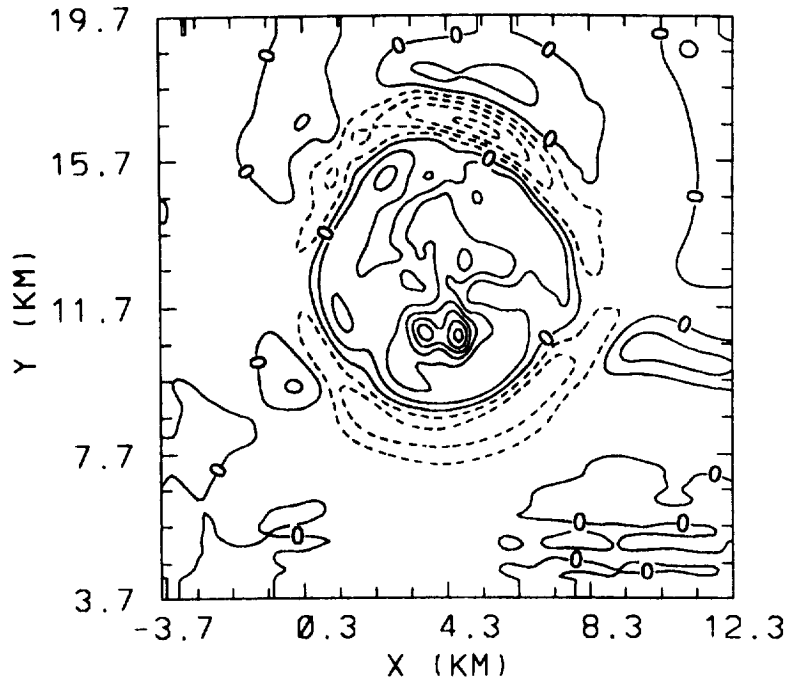E-W 1 Km Averaged F Factor at Z= 300.0 meters
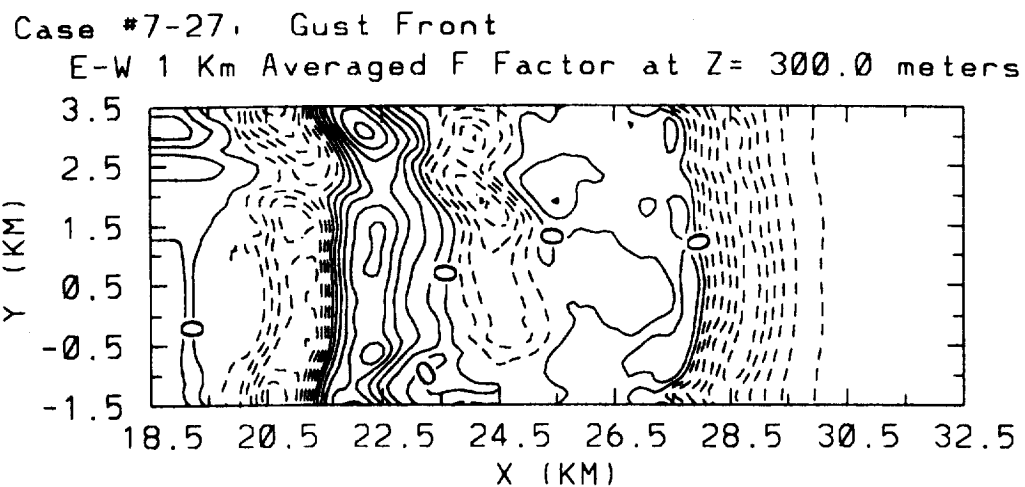
Figure A.2.29 Data Set #7-27: East-West $\bar{F}_{Km}$ at 300 meters elevation. Contours as in Figure A.2.1 with maximum value of about 0.16.

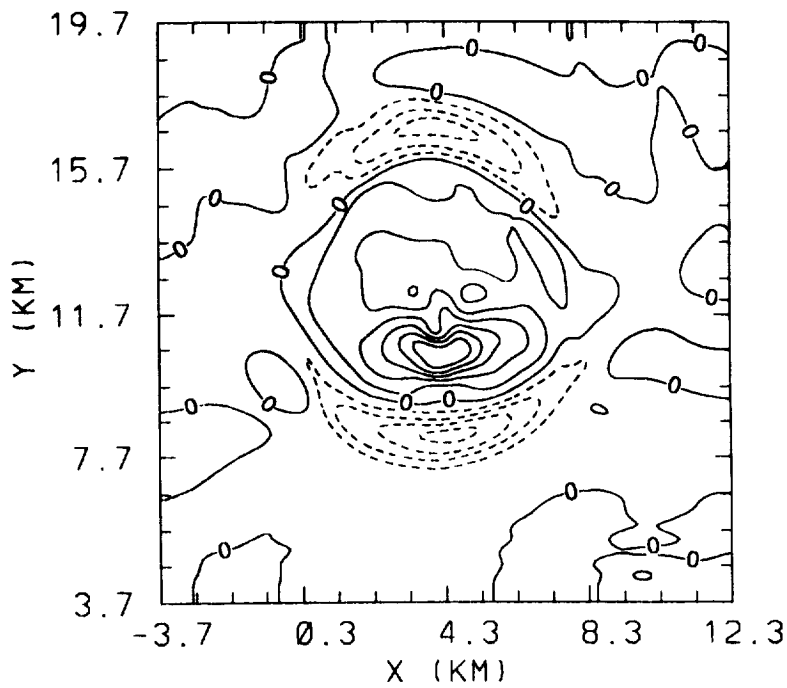Case #7-27, Gust Front

E-W 1 Km Averaged F Factor at Z= 50.0 meters
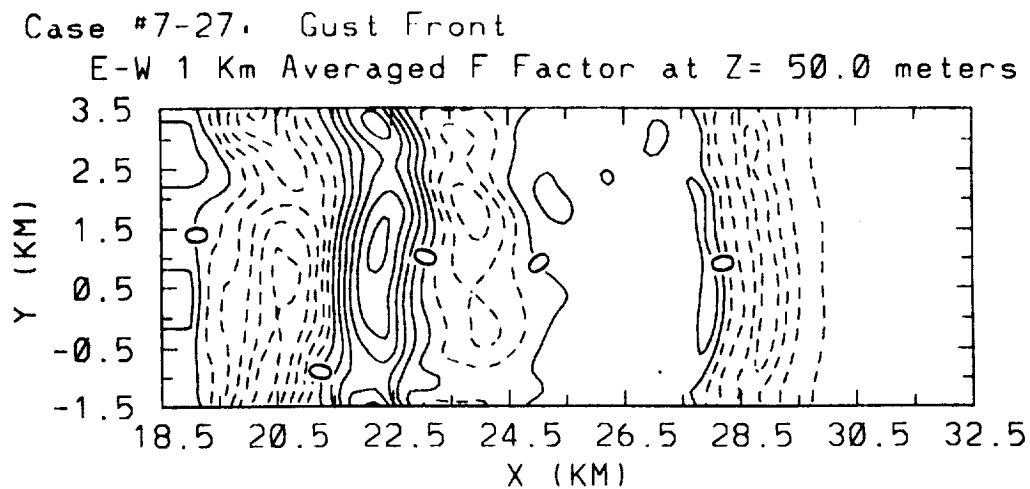
Figure A.2.30 Data Set #7-27: East-West $\bar{F}_{Km}$ at 50 meters elevation. Contours as in Figure A.2.1 with maximum value of about 0.13.

Appendix A.3

Radar Reflectivity Contour Plots

Case #1-11, DFW Accident Case, Wet Microburst
Radar Reflectivity (Dbz) at Z= 150.0 meters
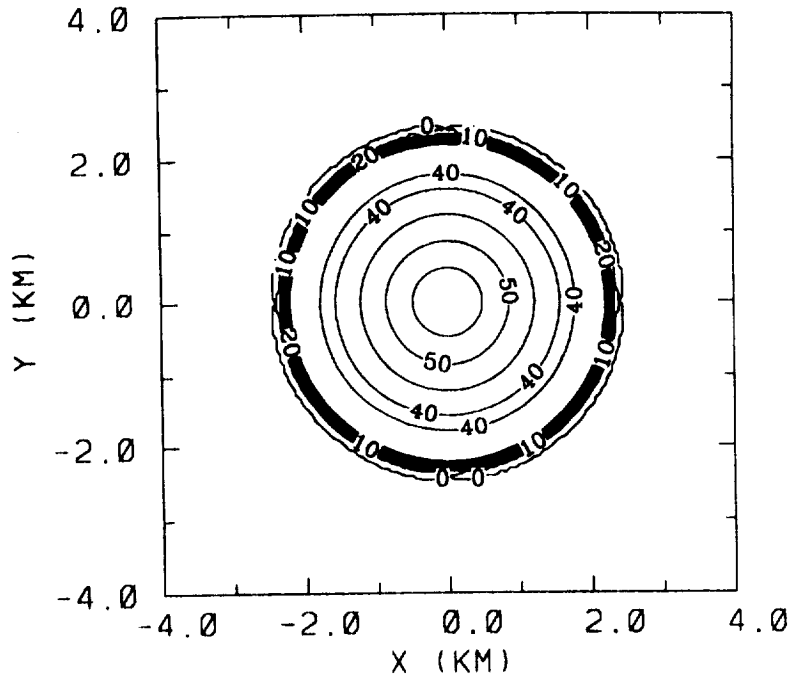
Figure A.3.1 Data Set #1-11: radar reflectivity. The contour interval is 5.0. Maximum value is about 56.

Case #2-37, 06/20/91 Orlando - NASA Event #143
Radar Reflectivity (Dbz) at Z= 150.0 meters
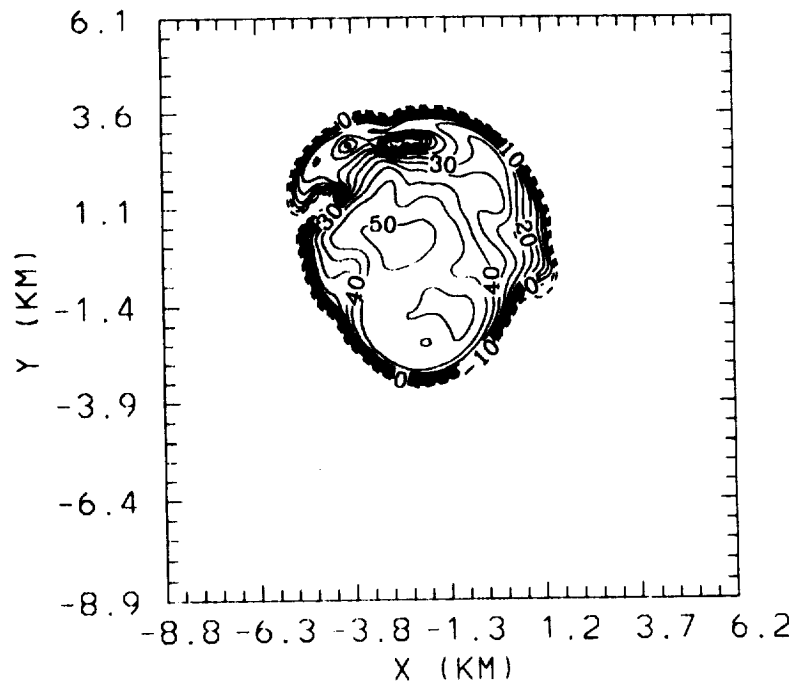
Figure A.3.2 Data Set #2-37: radar reflectivity. Contours as in Figure A.3.1 but contours with a negative value are dashed. Maximum value is about 53.

Case #3-49: 07/11/88 Denver - Multiple Microburst
Radar Reflectivity (Dbz) at Z= 150.0 meters
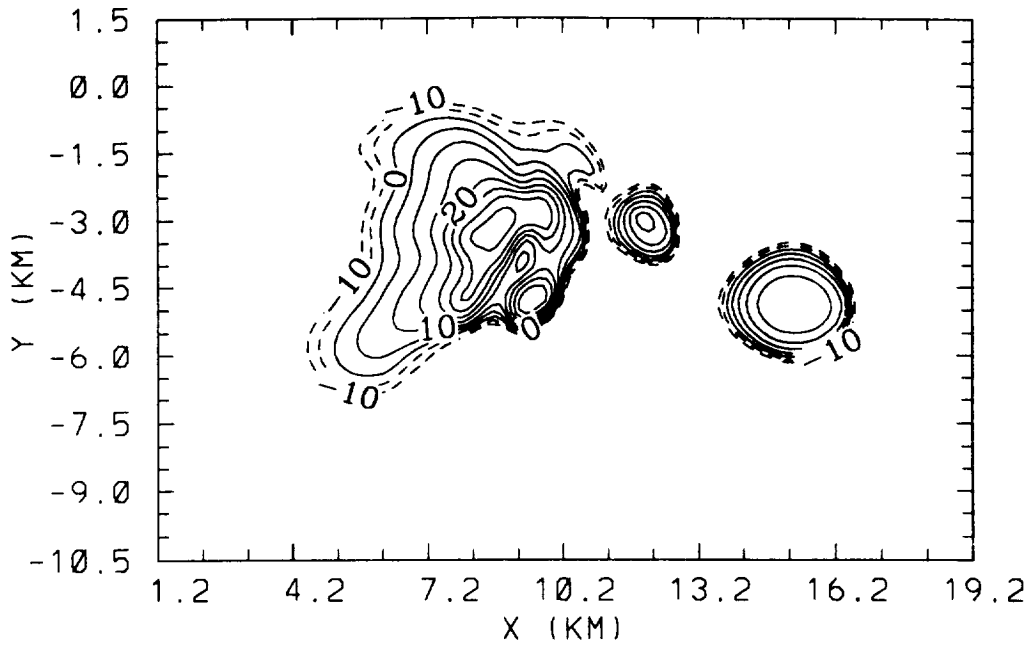
Figure A.3.3 Data Set #3-49: radar reflectivity. Contours as in Figure A.3.2 with maximum value of about 37.

Case #3-51: 07/11/88 Denver - Multiple Microburst
Radar Reflectivity (Dbz) at Z= 150.0 meters
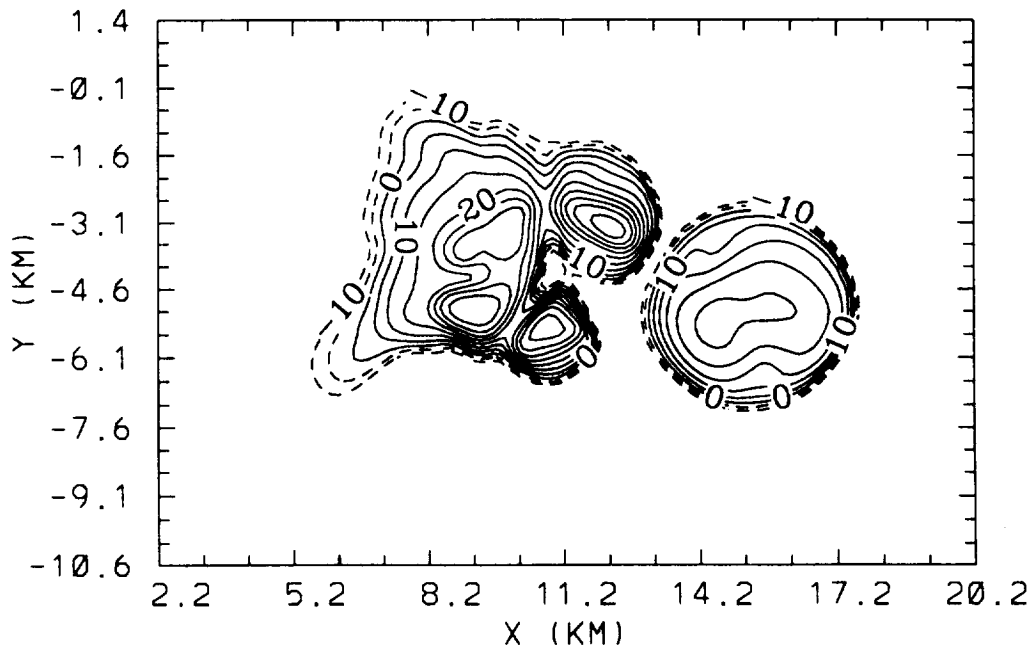
Figure A.3.4 Data Set #3-51: radar reflectivity. Contours as in Figure A.3.2 with maximum value of about 43.

Case #4-36: 07/14/82 Denver - Temperature Inversion
Radar Reflectivity (Dbz) at Z= 150.0 meters
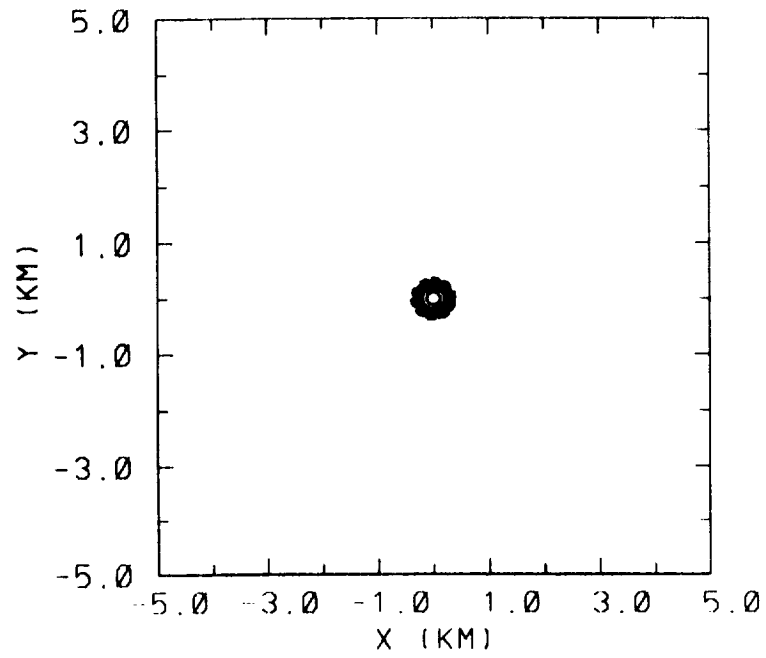
Figure A.3.5 Data Set #4-36: radar reflectivity. Contours as in Figure A.3.2 with maximum value of about 28.

Case #5-40: DRY - Microburst NASA Derived
Radar Reflectivity (Dbz) at Z= 150.0 meters
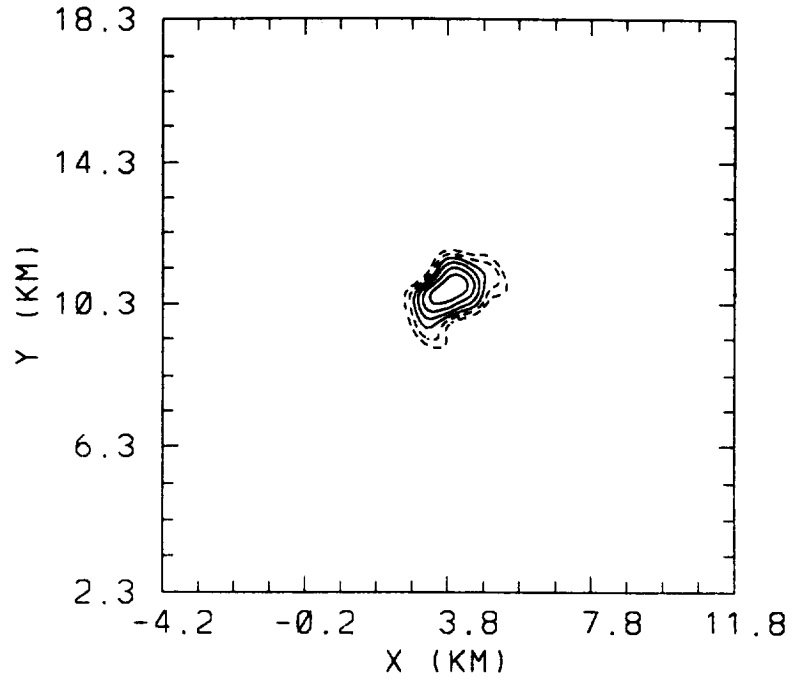
Figure A.3.6 Data Set #5-40: radar reflectivity. Contours as in Figure A.3.2 with maximum value of about 20.

Case #5-45: DRY - Microburst NASA Derived
Radar Reflectivity (Dbz) at Z= 150.0 meters
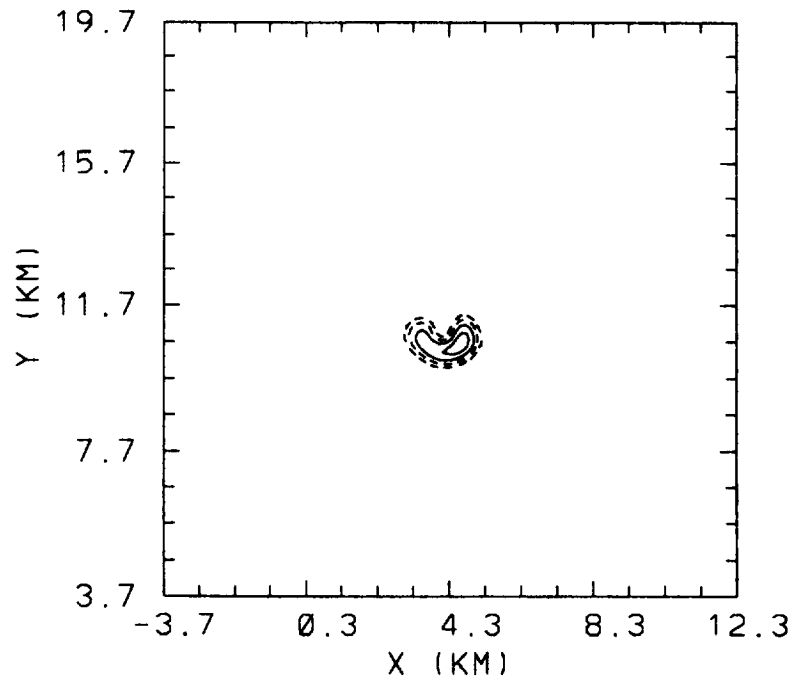
Figure A.3.7 Data Set #5-45: radar reflectivity. Contours as in Figure A.3.2 with maximum value of about 8.

Case #6-14. Highly asymmetric Microburst
Radar Reflectivity (Dbz) at Z= 150.0 meters
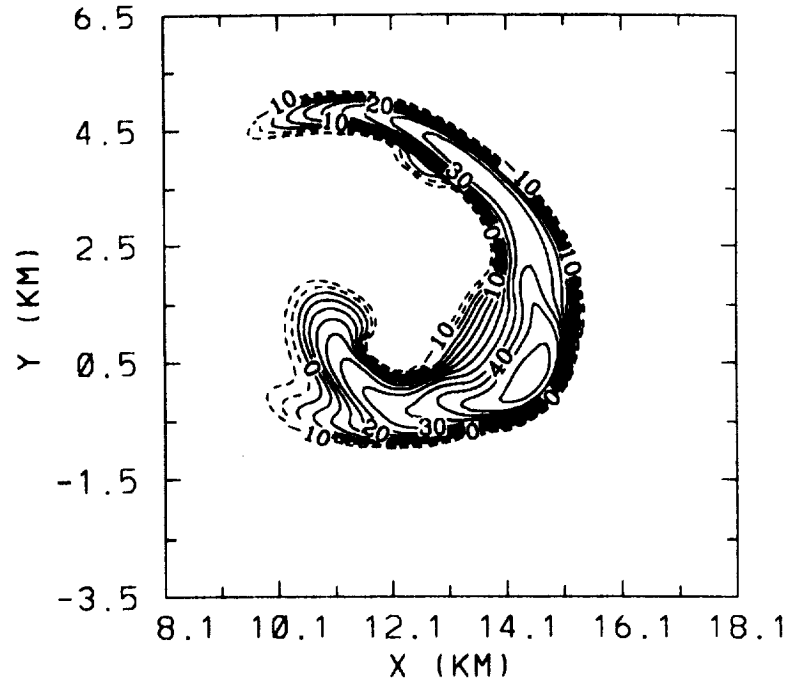
Figure A.3.8 Data Set #6-14: radar reflectivity. Contours as in Figure A.3.2 with maximum value of about 52.

Case #7-27. Gust Front
Radar Reflectivity (Dbz) at Z= 150.0 meters
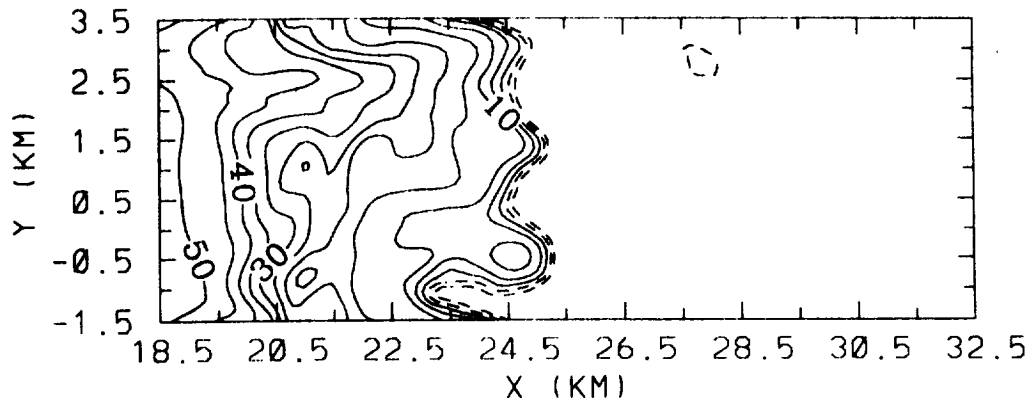
Figure A.3.9 Data Set #7-27: radar reflectivity. Contours as in Figure A.3.2 with maximum value of about 54.

Appendix A.4

Wind Vectors

Case #1-11.   DFW Accident Case, Wet Microburst
Velocity Vectors at Z= 50.0 meters
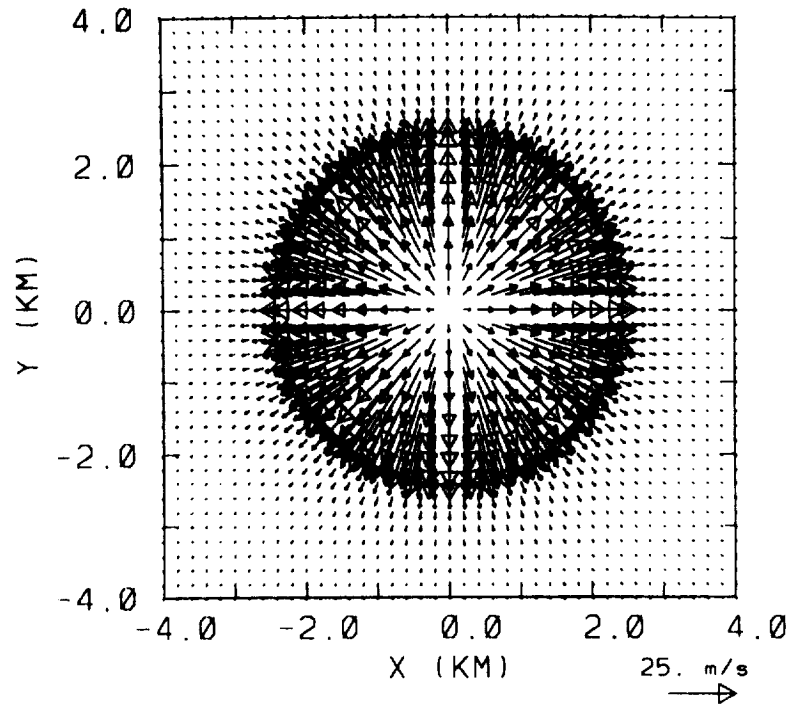
Figure A.4.1 Data Set #1-11: horizontal wind vectors at 50 meters elevation.

Case #1-11.   DFW Accident Case, Wet Microburst
Velocity Vectors at Y=   0.000 kilometers
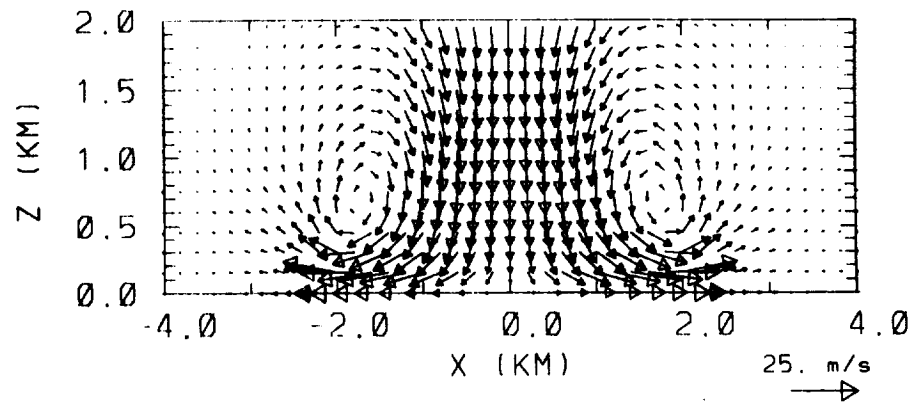
Figure A.4.2 Data Set #1-11: East-West vertical wind vectors at y = 0 Km.

Case #2-37: 06/20/91 Orlando - NASA Event #143
Velocity Vectors at Z= 50.0 meters
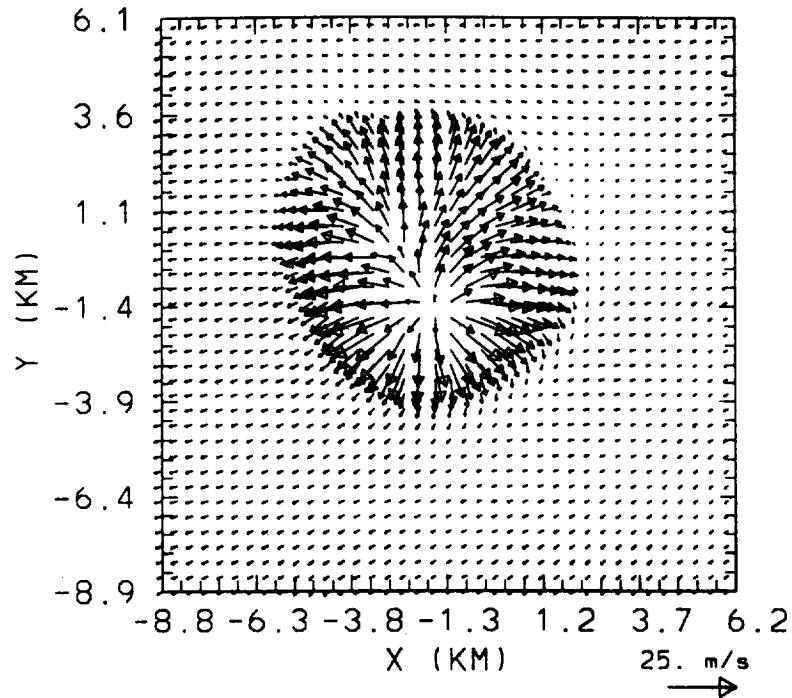
Figure A.4.3 Data Set #2-37: horizontal wind vectors at 50 meters elevation.

Case #2-37: 06/20/91 Orlando - NASA Event #143
Velocity Vectors at Y= -1.380 kilometers
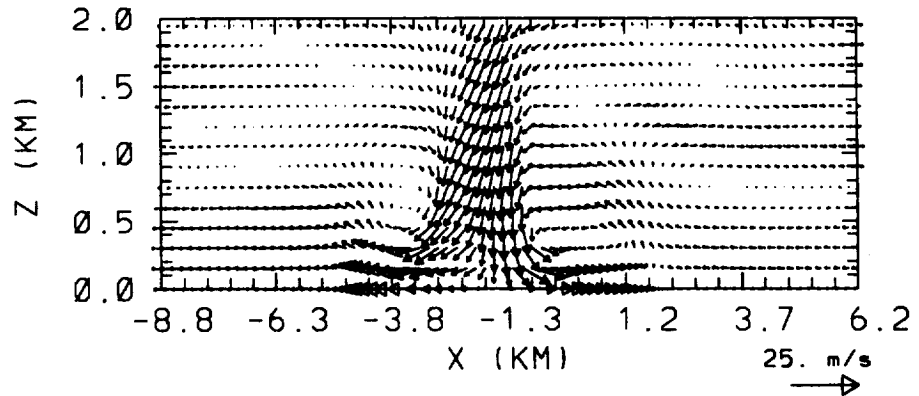
Figure A.4.4 Data Set #2-37: East-West vertical wind vectors at y = -1.4 Km.

Case #3-49: 07/11/88 Denver - Multiple Microburst
Velocity Vectors at Z= 50.0 meters
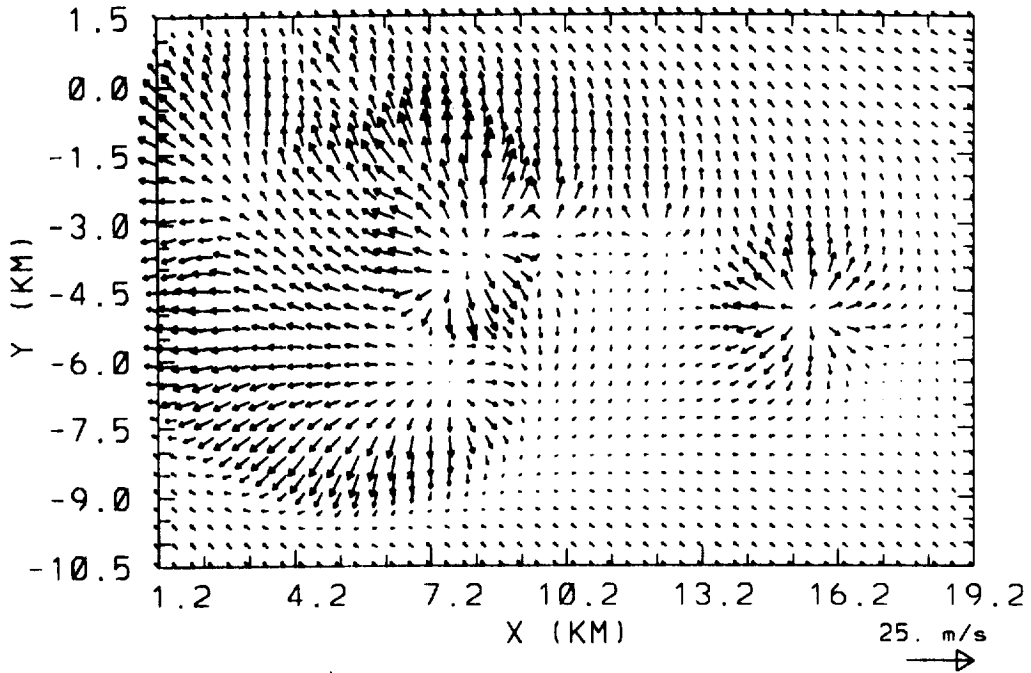
Figure A.4.5 Data Set #3-49: horizontal wind vectors at 50 meters elevation.

Case #3-49: 07/11/88 Denver - Multiple Microburst
Velocity Vectors at X=   8.490 kilometers
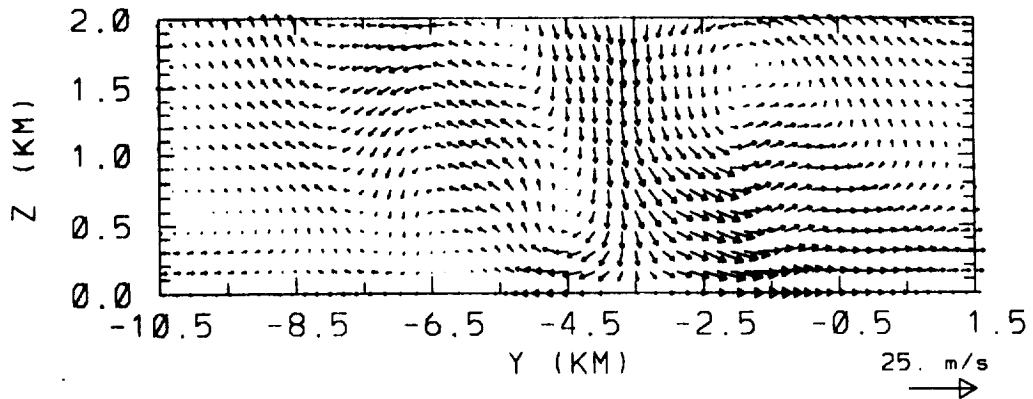
Figure A.4.6 Data Set #3-49: North-South vertical wind vectors at x = 8.5 Km.
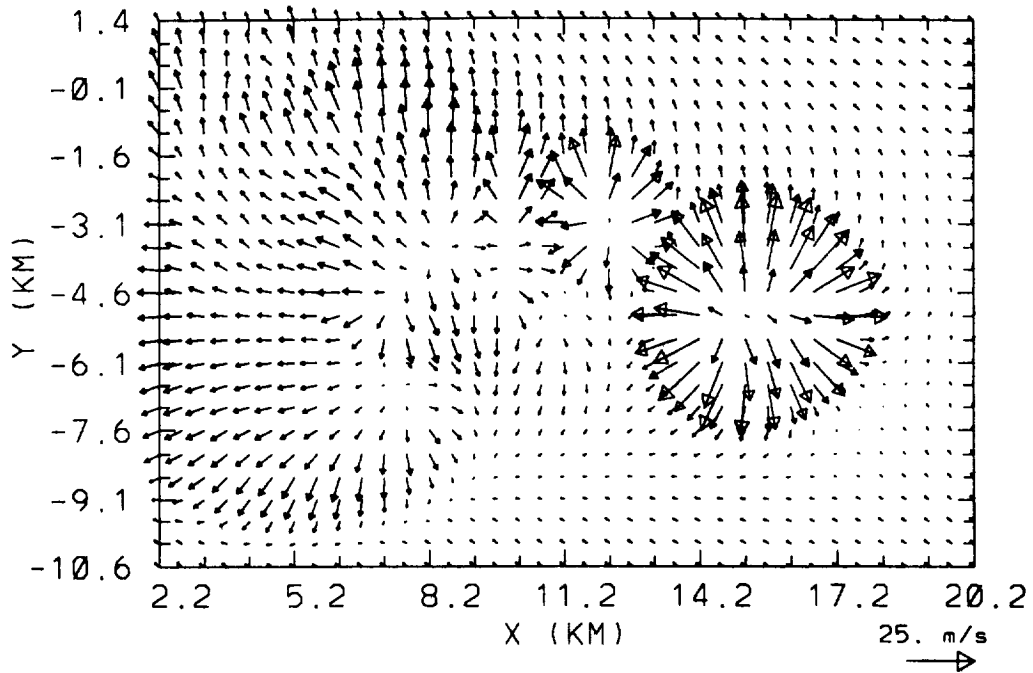
Figure A.4.7 Data Set #3-51: horizontal wind vectors at 50 meters elevation.
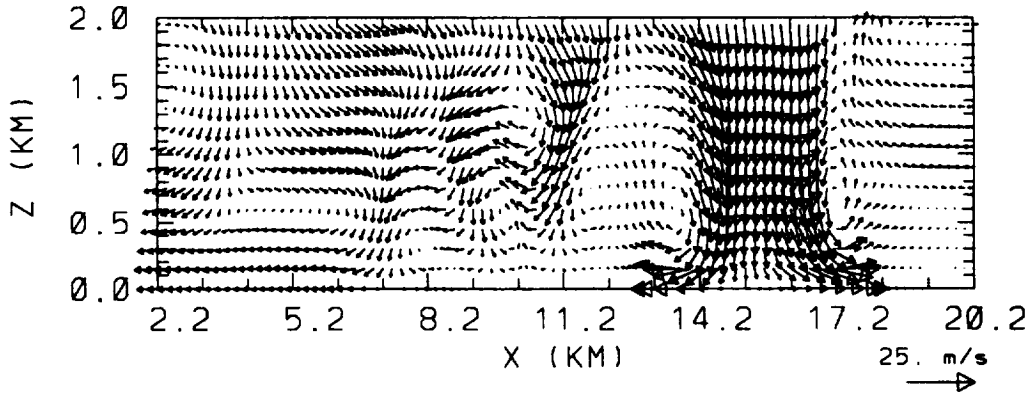
Figure A.4.8 Data Set #3-51: East-West vertical wind vectors at y = -5.1 Km.

Case #4-36: 07/14/82 Denver - Temperature Inversion
Velocity Vectors at Z= 50.0 meters
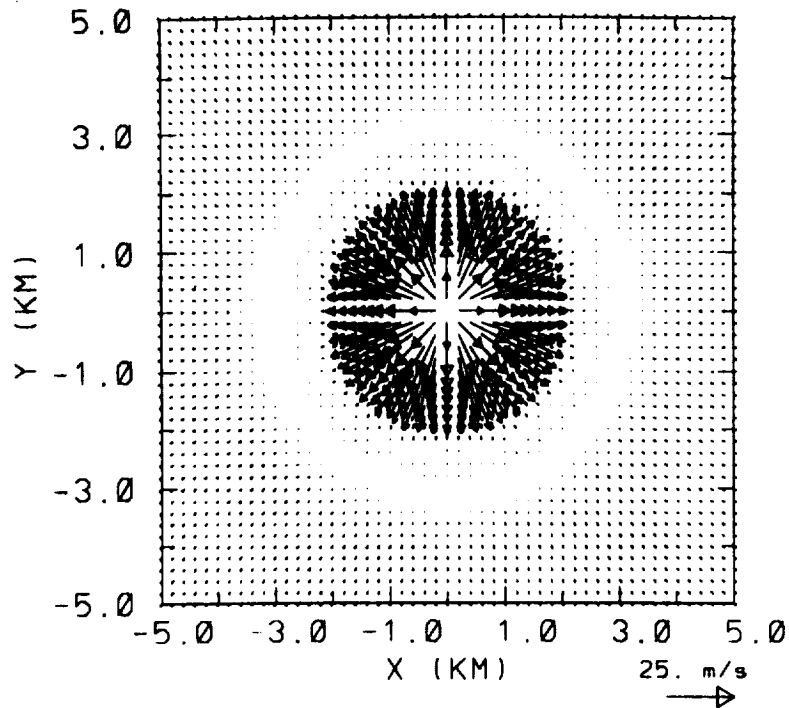
Figure A.4.9 Data Set #4-36: horizontal wind vectors at 50 meters elevation.

Case #4-36: 07/14/82 Denver - Temperature Inversion
Velocity Vectors at Y 0.000 kilometers
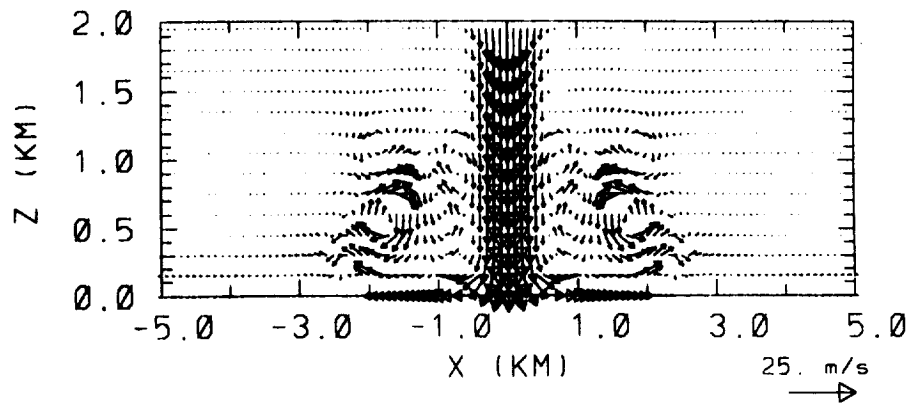
Figure A.4.10 Data Set #4-36: East-West vertical wind vectors at y = 0 Km.

Case #5-40: DRY - Microburst NASA Derived
Velocity Vectors at Z= 50.0 meters
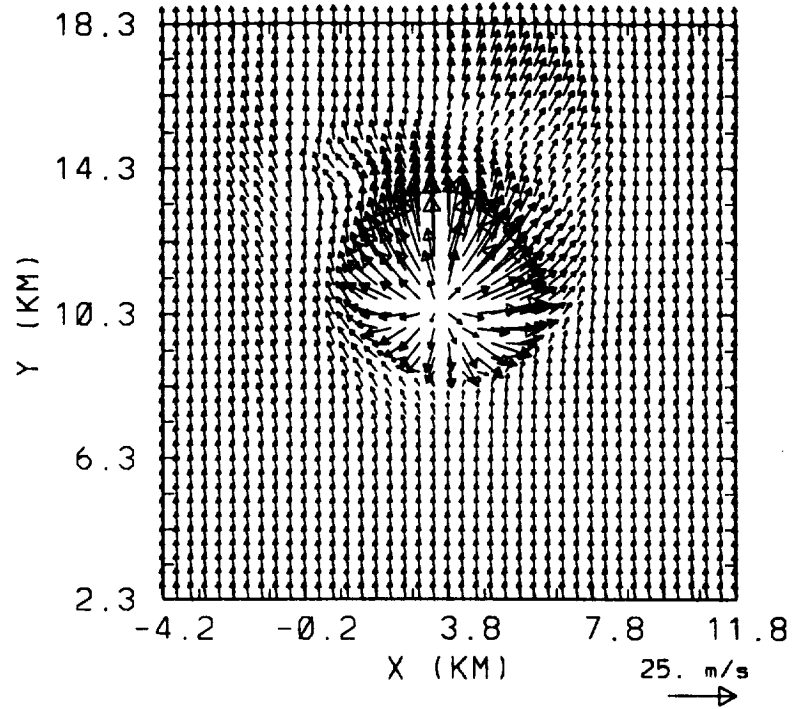
Figure A.4.11 Data Set #5-40: horizontal wind vectors at 50 meters elevation.

Case #5-40: DRY - Microburst NASA Derived
Velocity Vectors at X=   3.790 kilometers
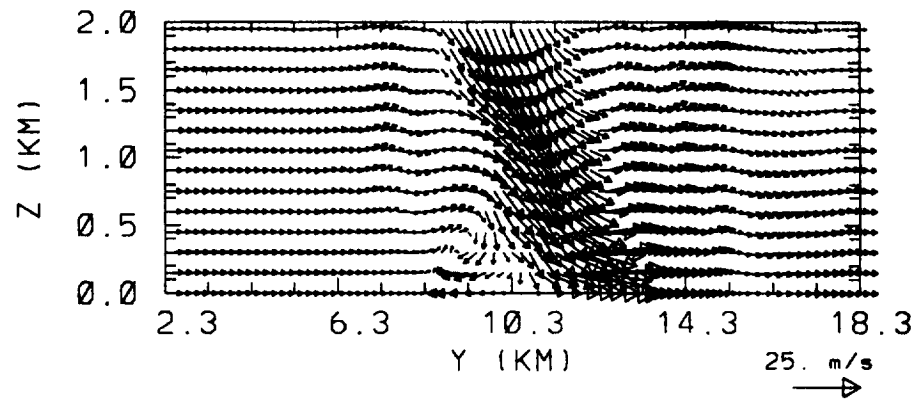
Figure A.4.12 Data Set #5-40: North-South vertical wind vectors at x = 3.8 Km.

Case #5-45: DRY - Microburst NASA Derived
Velocity Vectors at Z= 50.0 meters
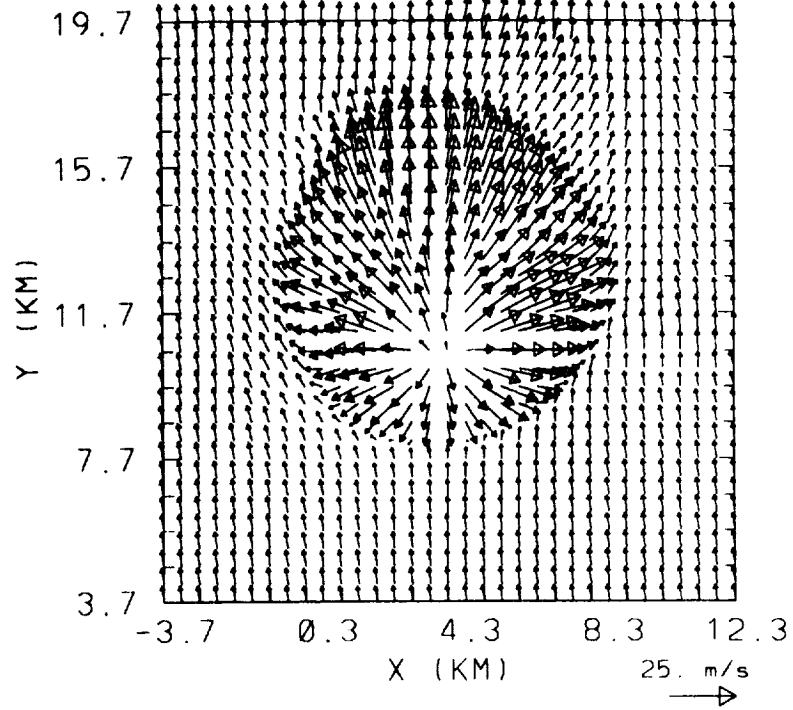
Figure A.4.13 Data Set #5-45: horizontal wind vectors at 50 meters elevation.

Case #5-45: DRY - Microburst NASA Derived
Velocity Vectors at X: 4.262 kilometers
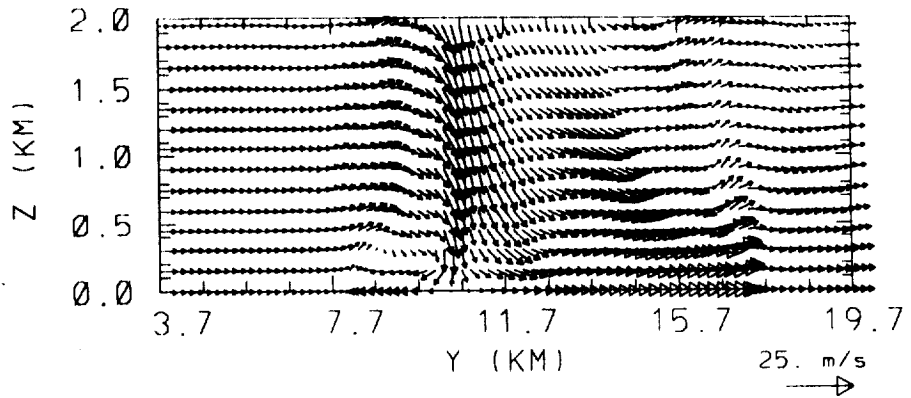
Figure A.4.14 Data Set #5-45: North-South vertical wind vectors at x = 4.3 Km.

Case #6-14: Highly asymmetric Microburst
Velocity Vectors at Z= 50.0 meters
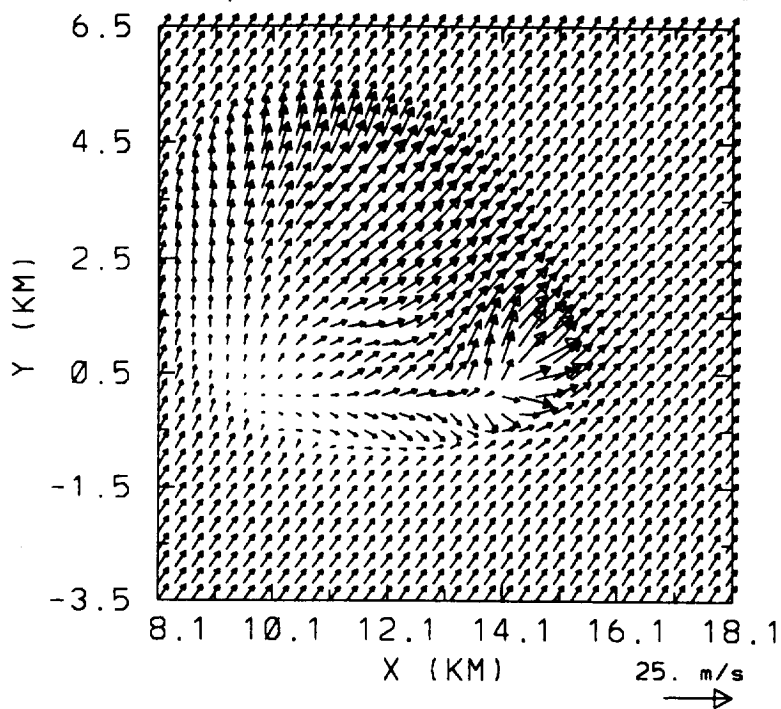
Figure A.4.15 Data Set #6-14: horizontal wind vectors at 50 meters elevation.

Case #6-14: Highly asymmetric Microburst
Velocity Vectors at X= 14.471 kilometers
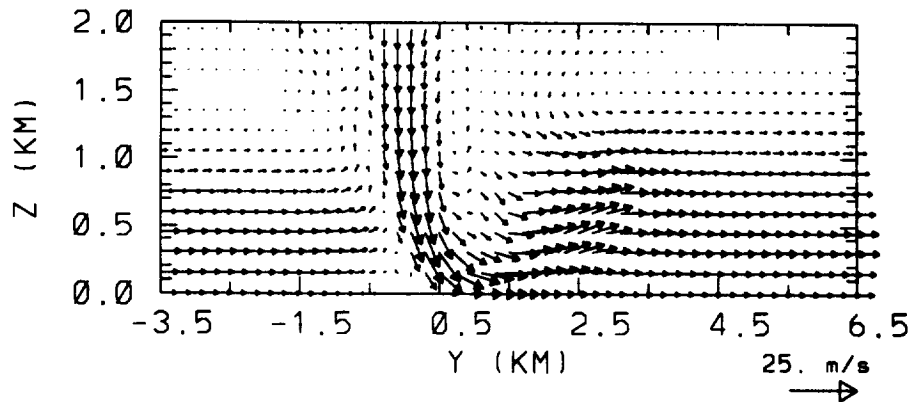
Figure A.4.16 Data Set #6-14: North-South vertical wind vectors at x = 14.5 Km.

Case #7-27, Gust Front
Velocity Vectors at Z= 50.0 meters
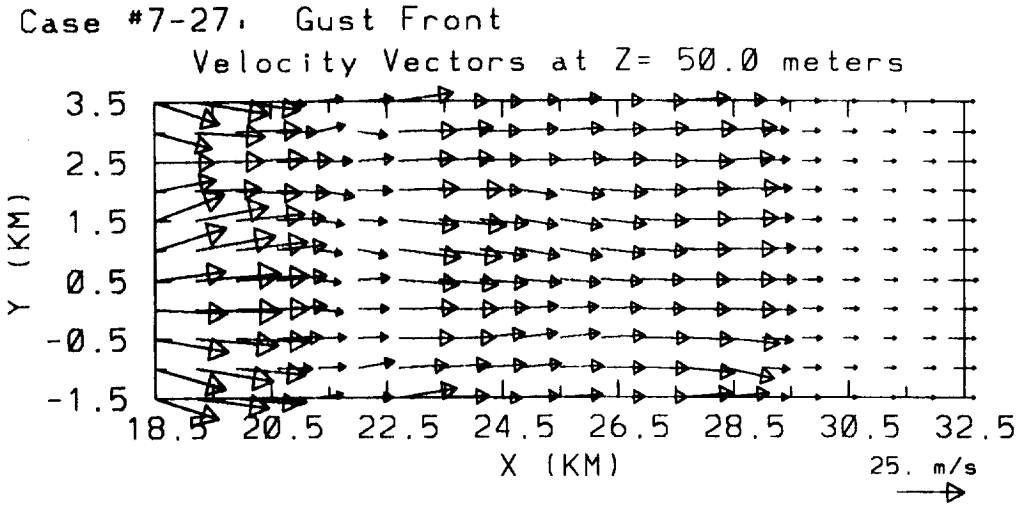
Figure A.4.17 Data Set #7-27: horizontal wind vectors at 50 meters elevation.

Case #7-27, Gust Front
Velocity Vectors at Y=   1.000 kilometers
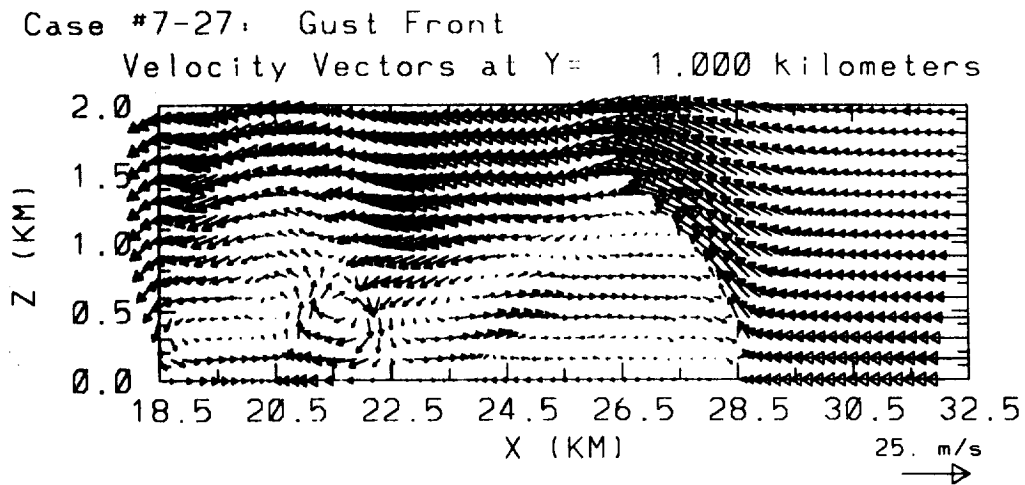
Figure A.4.18 Data Set #7-27: East-West vertical wind vectors at y = 1.0 Km. U velocity is biased by 21 m/s to show winds relative to translation of gust front.

Appendix A.5

Along Path Flight Scenario Plots

Data Set #1: DFW Accident Case, Wet Microburst

Aligned for Takeoff, Far Microburst

Time = 11 min.
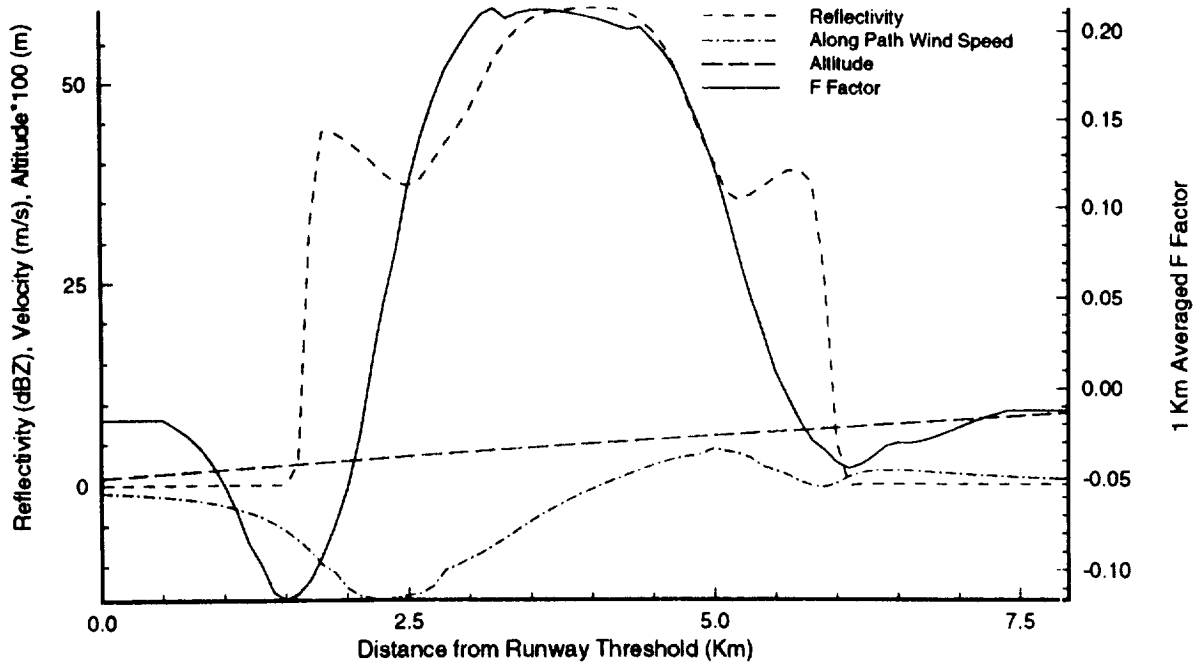
Figure A.5.1 Data Set #1-11: aligned for takeoff scenario (far microburst) on track 90. The solid line represents the 1 Kilometer averaged F factor, the short-dashed line represents the reflectivity in dBZ, the long dashed line represents the altitude of the sensor, and the dash-dot line represents the wind speed along the flight path.wind speed.

Data Set #1: DFW Accident Case, Wet Microburst

ILS Approach

Time = 11 min.

Figure A.5.2 Data Set #1-11: as in figure A.5.1 but for ILS approach scenario on track 90.

Data Set #2: 6/20/91 Orlando, Wet Microburst

ILS Approach (Track 180)   Time = 37 min.
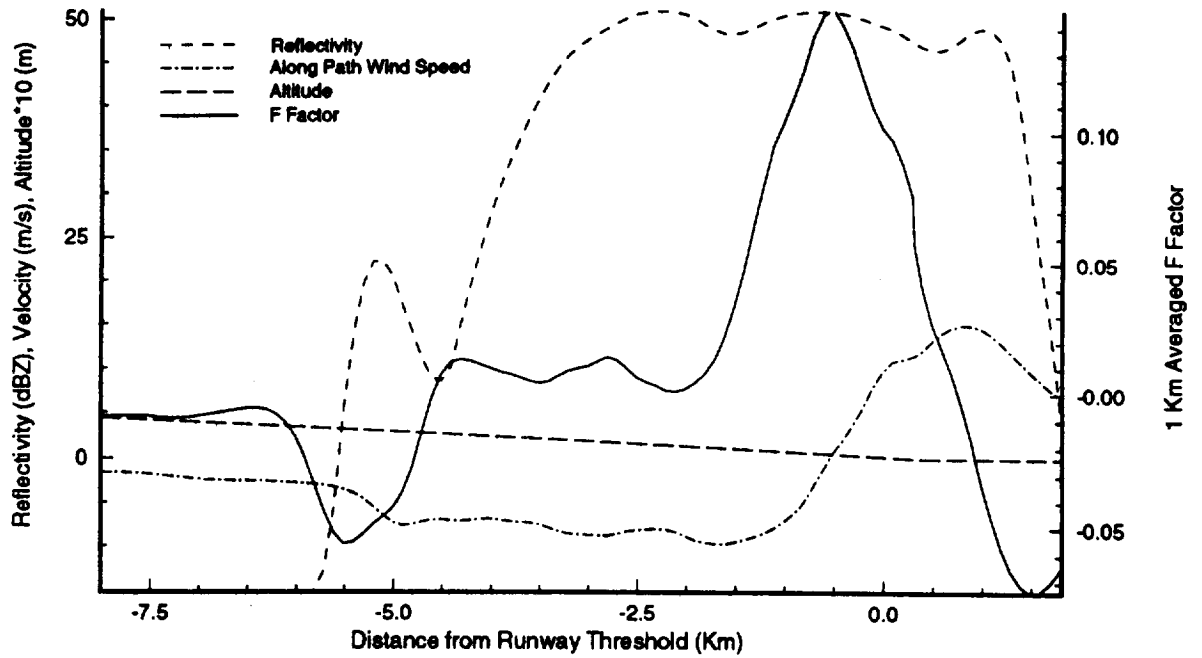
Figure A.5.3 Data Set #2-37: as in figure A.5.1 but for ILS approach scenario on track 180.

Data Set #2: 6/20/91 Orlando, Wet Microburst

Go-around Maneuver   Time = 37 min.
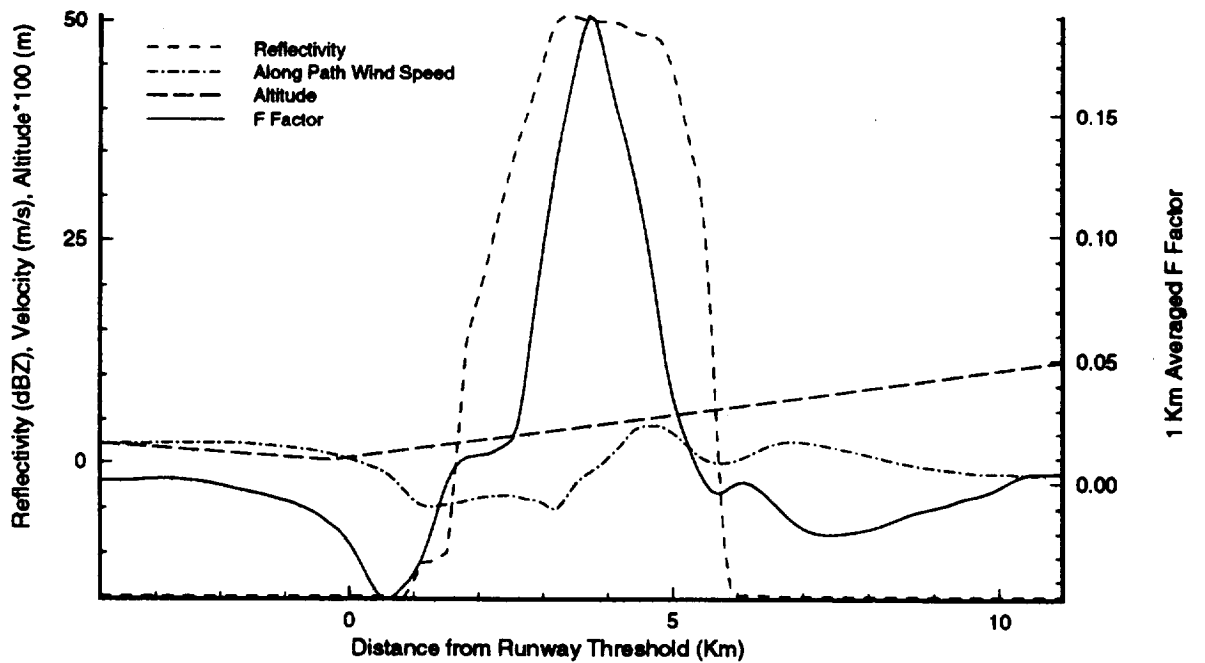
Figure A.5.4 Data Set #2-37: as in figure A.5.1 but for go-around scenario on track 270.

Data Set #2: 6/20/91 Orlando, Wet Microburst

ILS Approach (Below Alert Threshold Shear)   Time = 37 min.

Legend:
- - - - - Reflectivity
- · - · · - · - Along Path Wind Speed
- - - - Altitude
———— F Factor

X-axis: Distance from Runway Threshold (Km)
Left Y-axis: Reflectivity (dBZ), Velocity (m/s), Altitude*100 (m)
Right Y-axis: 1 Km Averaged F Factor
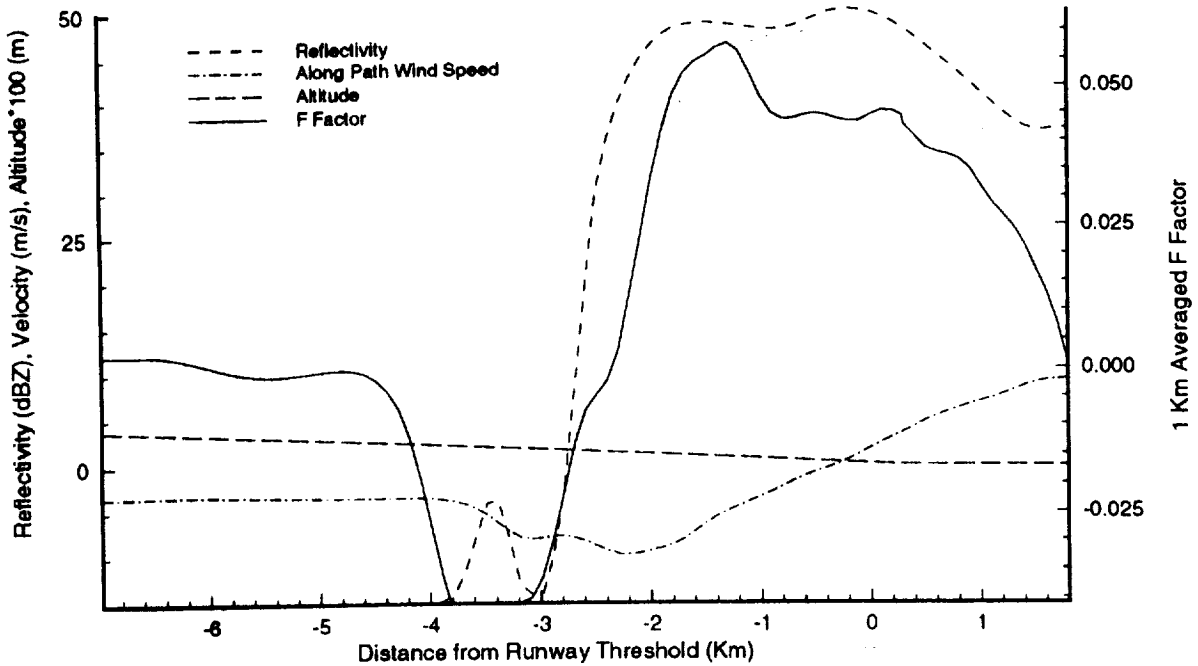
Figure A.5.5 Data Set #2-37: as in figure A.5.1 but for ILS approach scenario (below alert threshold shear) on track 90.

Data Set #3: 7/11/88 Denver, Multiple Microbursts

ILS Approach (Below Alert Threshold Shear)   Time = 49 min.

Legend:
- - - - - Reflectivity
- · - · · - · - Along Path Wind Speed
- - - - Altitude
———— F Factor

X-axis: Distance from Runway Threshold (Km)
Left Y-axis: Reflectivity (dBZ), Velocity (m/s), Altitude*100 (m)
Right Y-axis: 1 Km Averaged F Factor
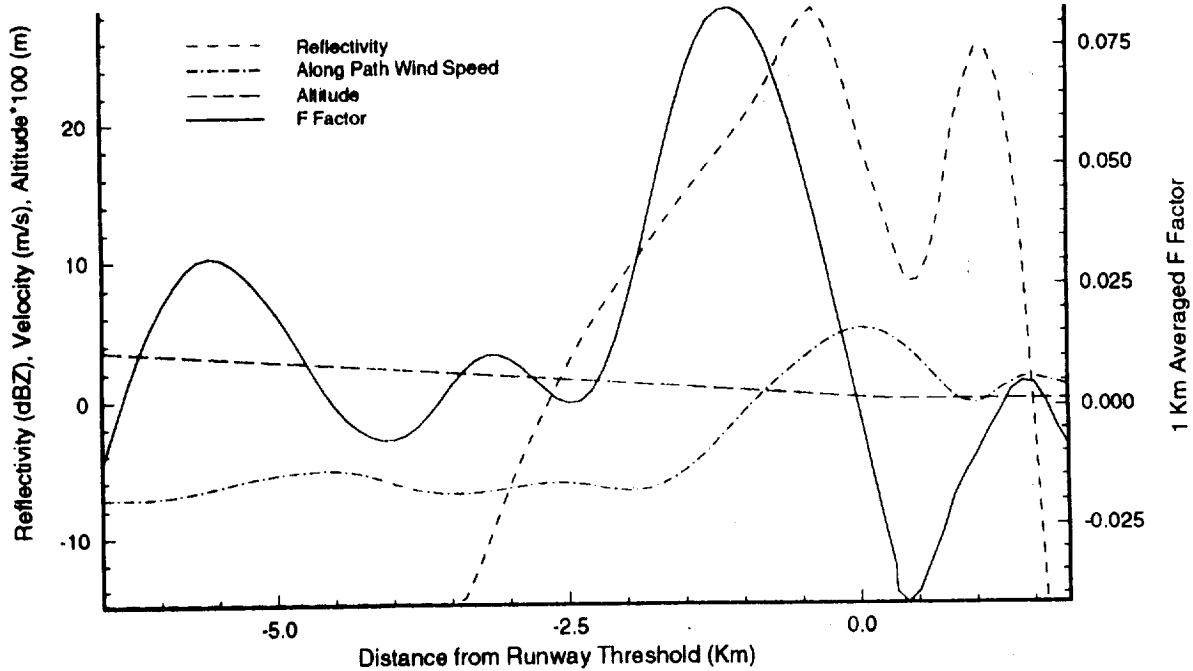
Figure A.5.6 Data Set #3-49: as in figure A.5.1 but for ILS approach scenario (below alert threshold shear) on track 90.

Data Set #3: 7/11/88 Denver, Multiple Microbursts

ILS Approach (Developing Microburst)   Time = 49 min.
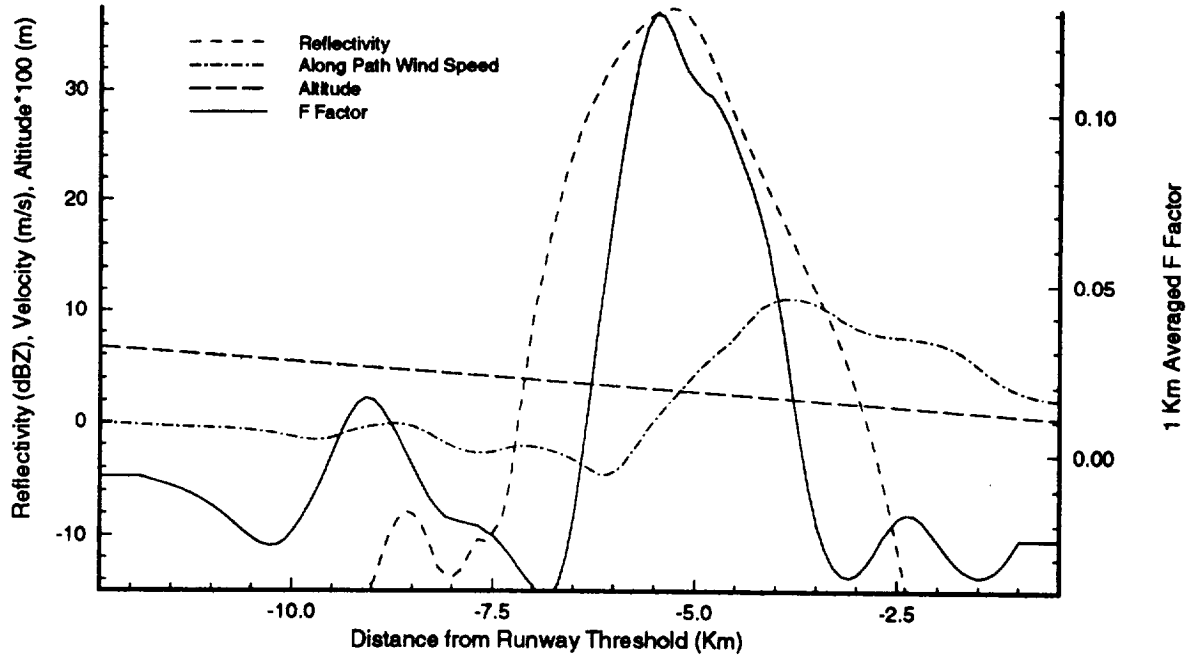
Figure A.5.7 Data Set #3-49: as in figure A.5.1 but for ILS approach scenario (must alert) on track 360.

Data Set #3: 7/11/88 Denver, Multiple Microbursts

Aligned for Takeoff, Near Microburst   Time = 51 min.
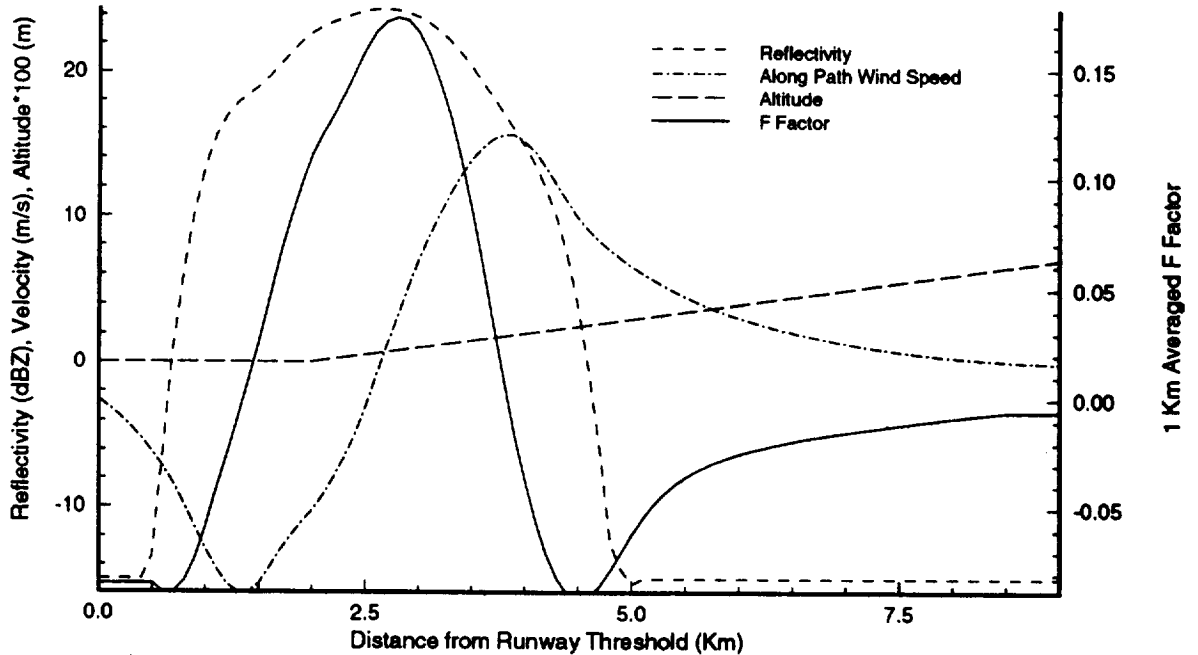
Figure A.5.8 Data Set #3-51: as in figure A.5.1 but for aligned for takeoff (near microburst) scenario on track 360.

Data Set #3: 7/11/88 Denver, Multiple Microbursts

Aligned for Takeoff, Far Microburst   Time = 51 min.

Reflectivity (dBZ), Velocity (m/s), Altitude*100 (m)

- - - - Reflectivity
-·-··-·- Along Path Wind Speed
- - - Altitude
——— F Factor

1 Km Averaged F Factor

Distance from Runway Threshold (Km)
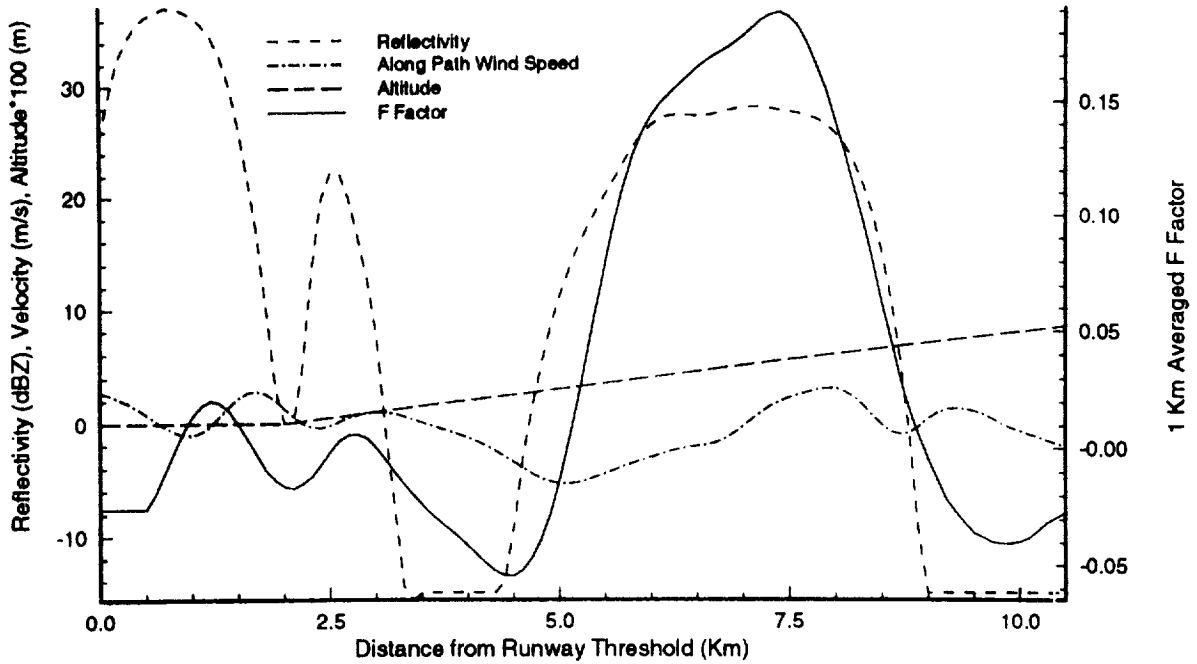
Figure A.5.9 Data Set #3-51: as in figure A.5.1 but for aligned for takeoff scenario (far microburst) on track 90.

Data Set #3: 7/11/88 Denver, Multiple Microbursts

ILS Approach (Track 360)   Time = 51 min.

Reflectivity (dBZ), Velocity (m/s), Altitude*100 (m)

- - - - Reflectivity
-·-··-·- Along Path Wind Speed
- - - Altitude
——— F Factor

1 Km Averaged F Factor

Distance from Runway Threshold (Km)
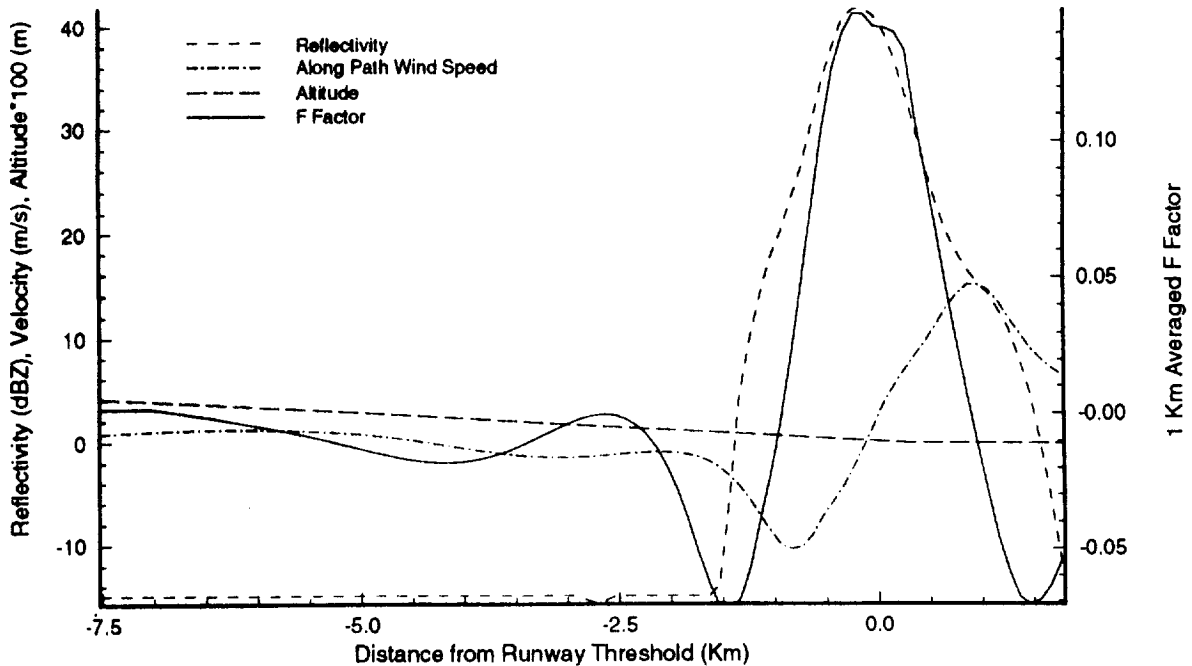
Figure A.5.10 Data Set #3-51: as in figure A.5.1 but for ILS approach scenario on track 360.

Data Set #3: 7/11/88 Denver, Multiple Microbursts

ILS Approach (Track 045)

Time = 51 min.
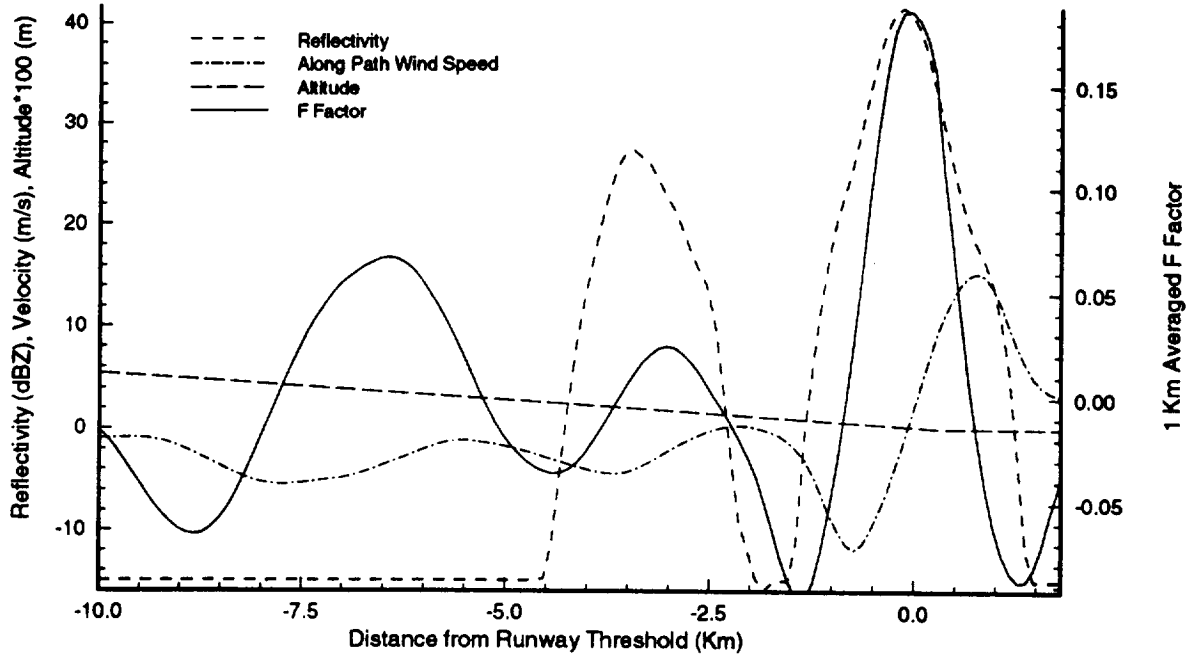
Figure A.5.11 Data Set #3-51: as in figure A.5.1 but for ILS approach scenario on track 45.

Data Set #3: 7/11/88 Denver, Multiple Microbursts

ILS Approach (Track 090)

Time = 51 min.
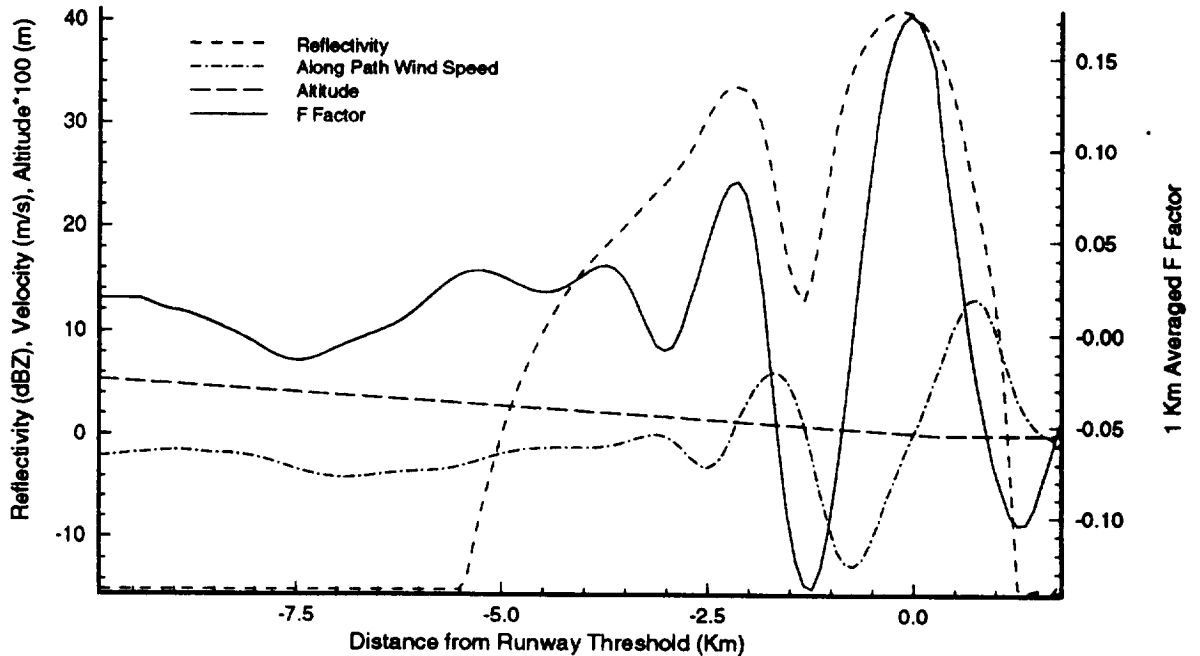
Figure A.5.12 Data Set #3-51: as in figure A.5.1 but for ILS approach scenario on track 90.

A-47

Data Set #3: 7/11/88 Denver, Multiple Microbursts

ILS Approach (Track 135)   Time = 51 min.
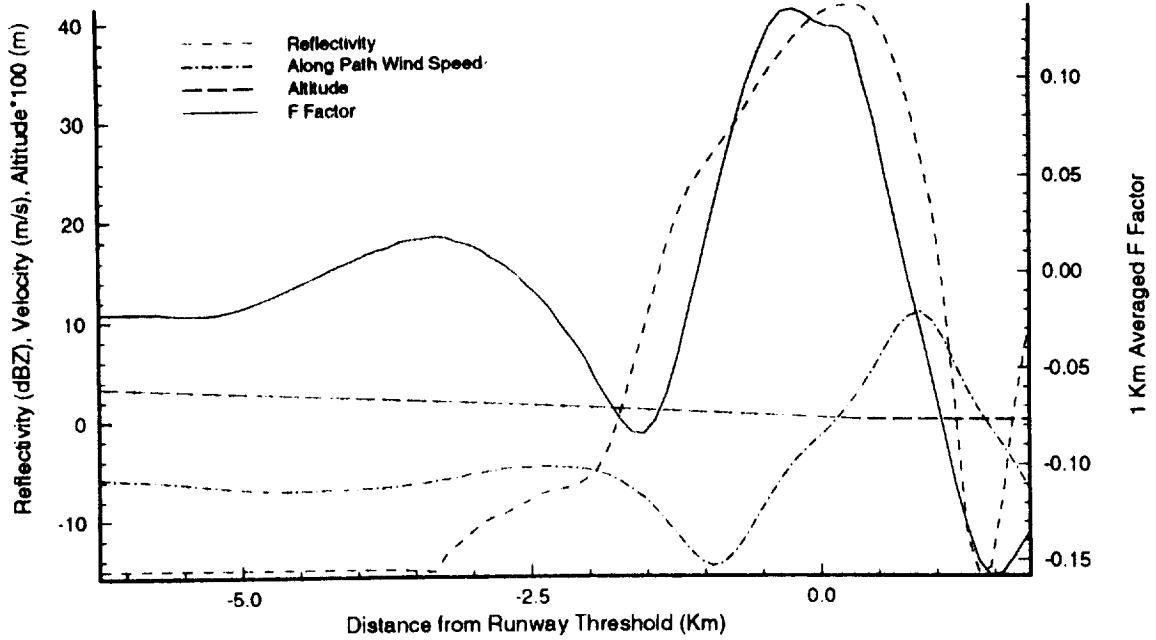
Figure A.5.13 Data Set #3-51: as in figure A.5.1 but for ILS approach scenario on track 135.

Data Set #3: 7/11/88 Denver, Multiple Microbursts

ILS Approach (Track 270)   Time = 51 min.
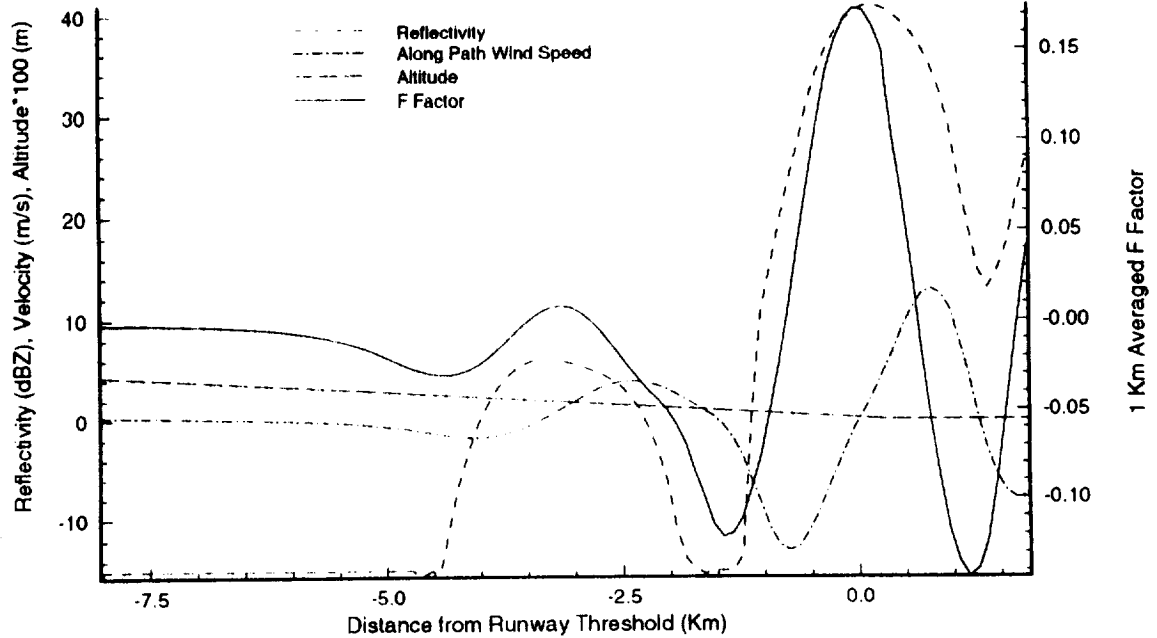
Figure A.5.14 Data Set #3-51: as in figure A.5.1 but for ILS approach scenario on track 270.

A-48

Data Set #3: 7/11/88 Denver, Multiple Microbursts

ILS Approach (Track 315)   Time = 51 min.

Reflectivity
Along Path Wind Speed
Altitude
F Factor

Reflectivity (dBZ), Velocity (m/s), Altitude*100 (m)

1 Km Averaged F Factor

Distance from Runway Threshold (Km)
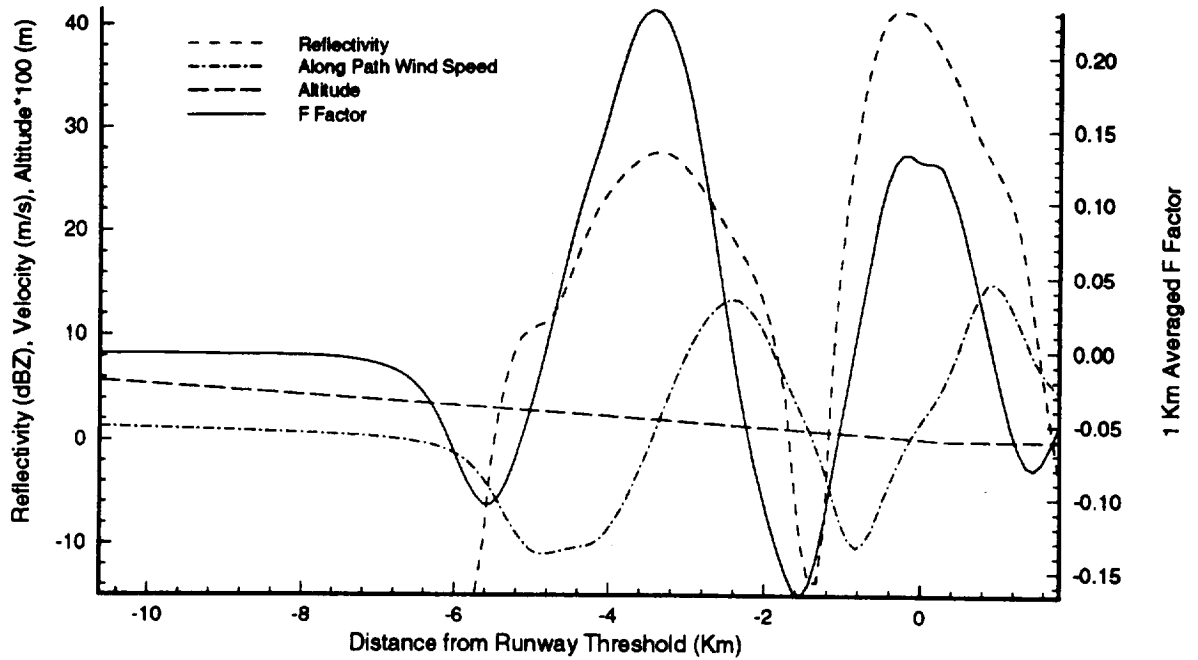
Figure A.5.15 Data Set #3-51: as in figure A.5.1 but for ILS approach scenario on track 315.

Data Set #3: 7/11/88 Denver, Multiple Microbursts

Curved Approach at 200 knots   Time = 51 min.

Reflectivity
Along Path Wind Speed
F Factor

Reflectivity (dBZ), Velocity (m/s)

1 Km Averaged F Factor

Distance from Beginning of Localizer Course (Km)
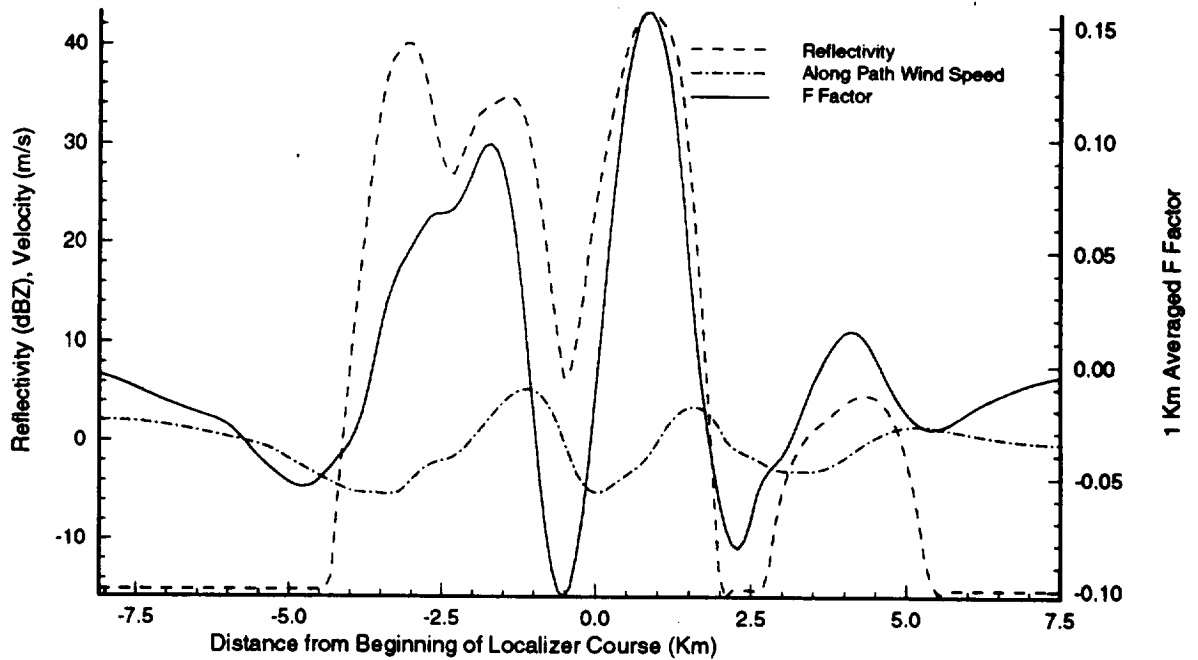
Figure A.5.16 Data Set #3-51: curved approach flight scenario (right turn) with localizer on track 90. The solid line represents the 1 Kilometer averaged F Factor, the dashed line represents the Reflectivity in dBZ, and the dash-dot line represents the wind speed along the flight path.wind speed.

Data Set #4: 7/14/82 Denver, Temperature Inversion

Aligned for Takeoff, Near Microburst

Time = 36 min.
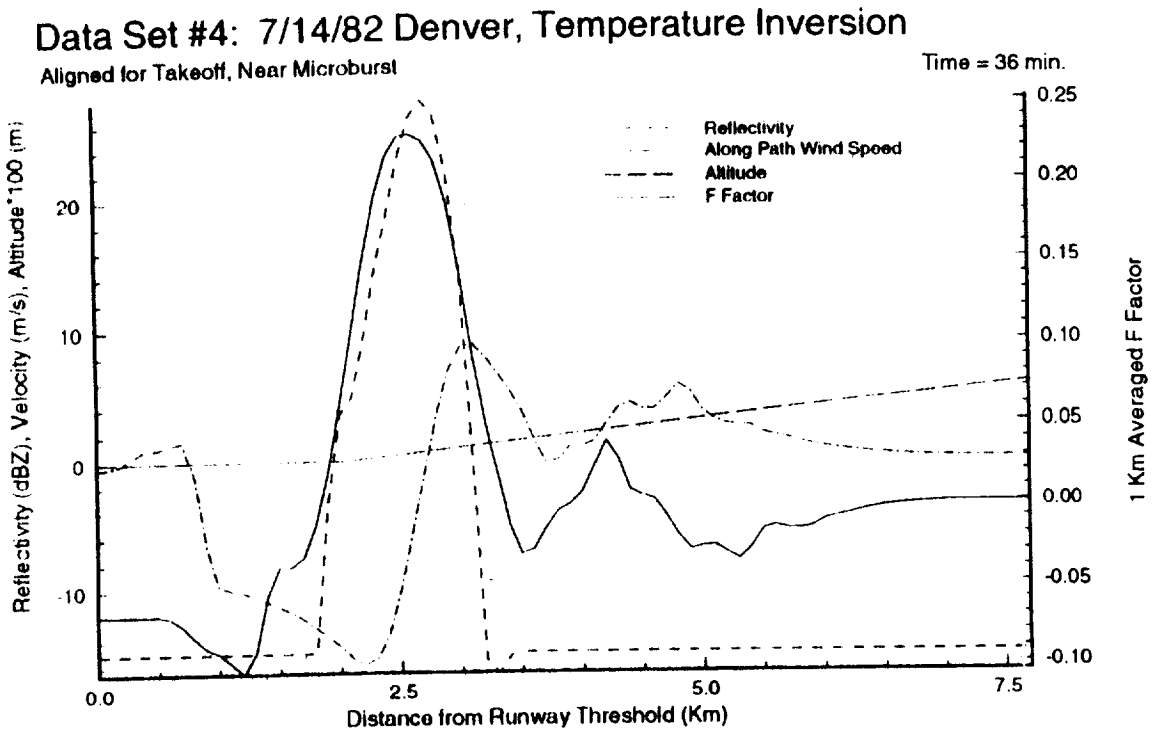
Figure A.5.17 Data Set #4-36: as in figure A.5.1 but for aligned for takeoff scenario (near microburst) on track 90.

Data Set #4: 7/14/82 Denver, Temperature Inversion

ILS Approach
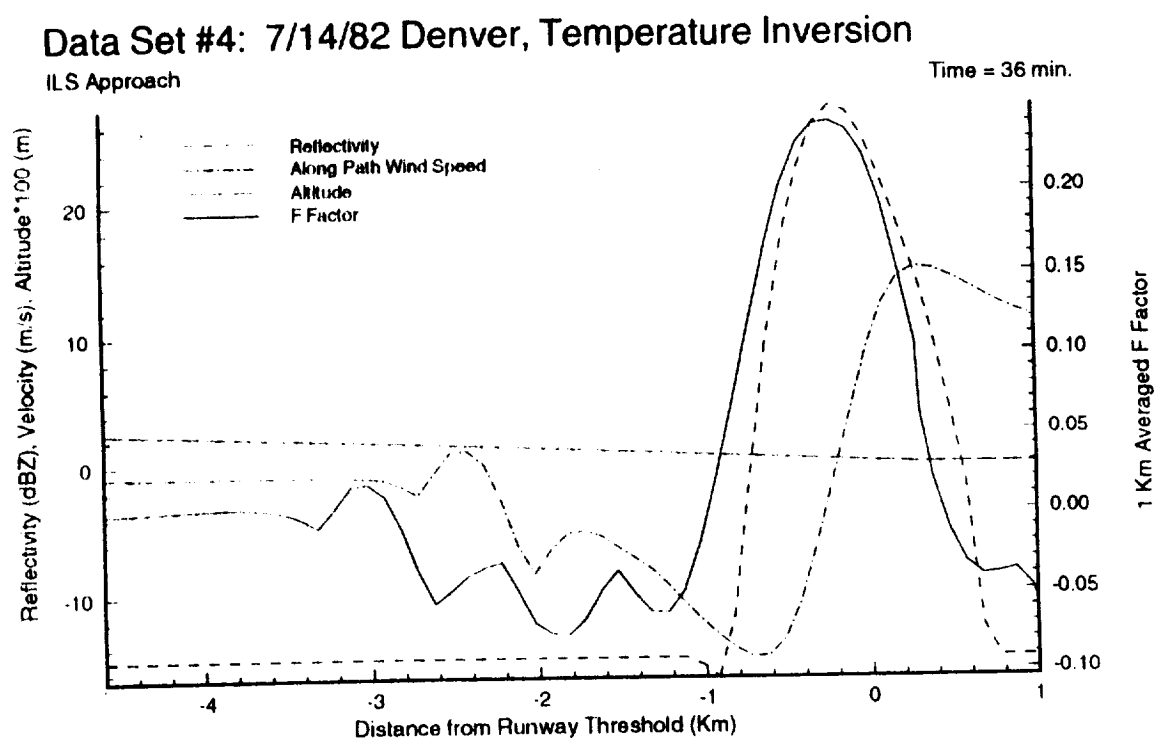
Time = 36 min.

Figure A.5.18 Data Set #4-36: as in figure A.5.1 but for ILS approach scenario on track 90.

Data Set #4: 7/14/82 Denver, Temperature Inversion

Worst-case Drift Approach at 120 knots   Time = 36 min.
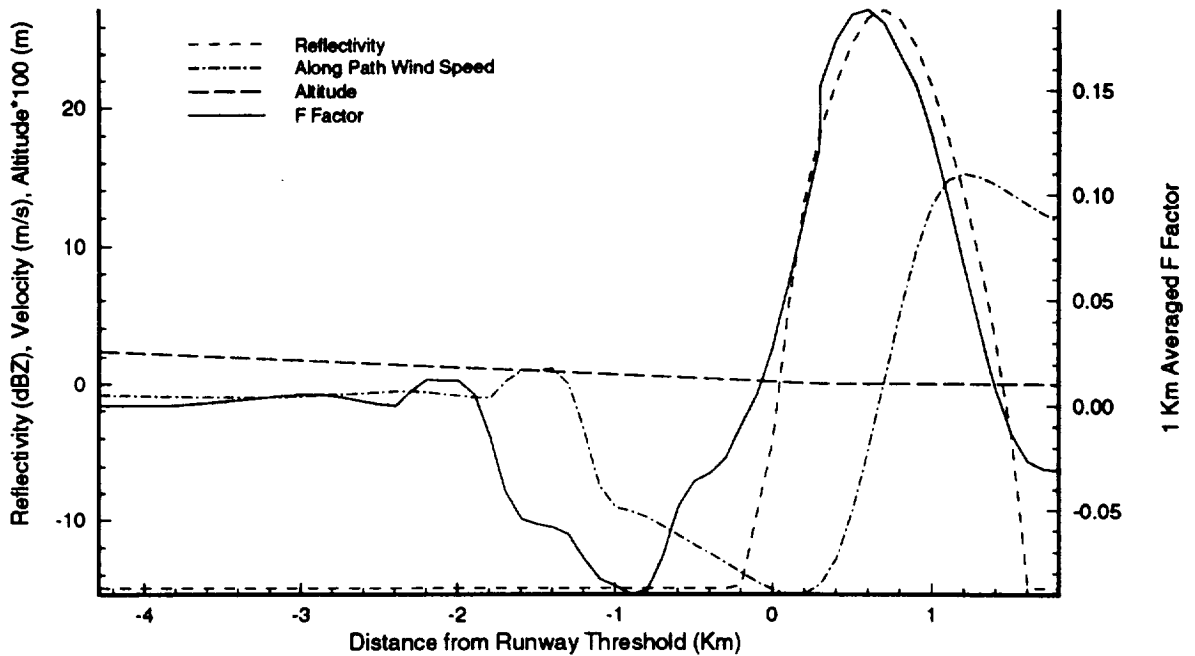
Figure A.5.19 Data Set #4-36: as in figure A.5.1 but for worst-case drift ILS approach on track 90.

Data Set #5: 7/8/89 Denver, Very Dry Microburst

Aligned for Takeoff, Far Microburst   Time = 40 min.
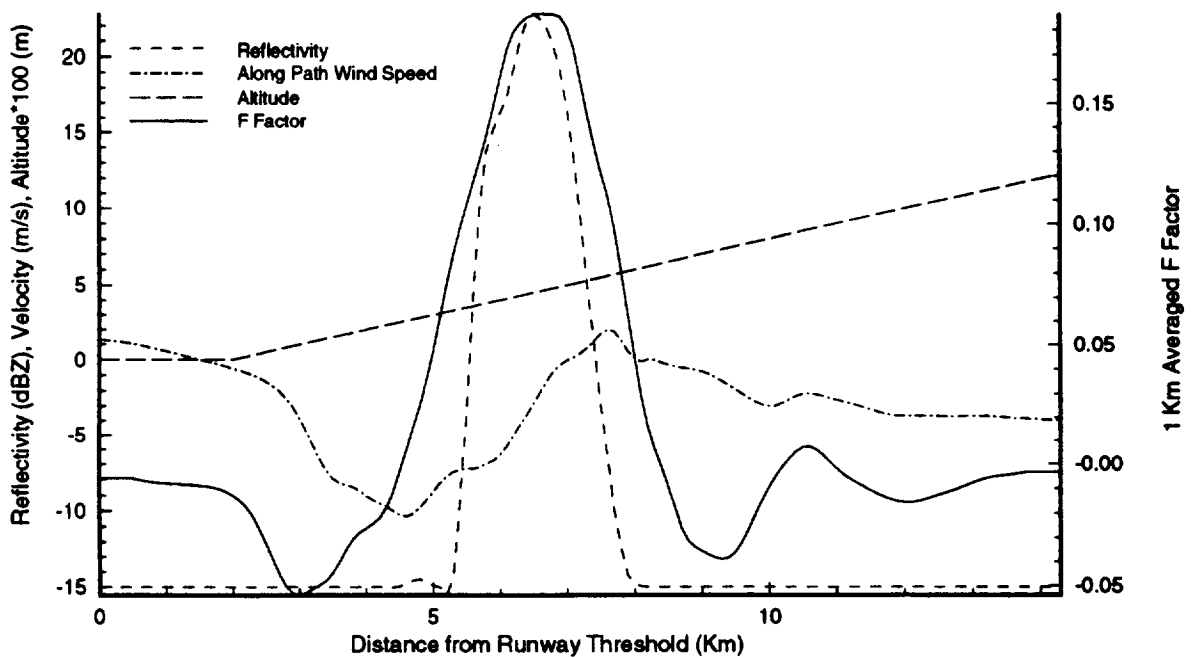
Figure A.5.20 Data Set #5-40: as in figure A.5.1 but for aligned for takeoff scenario (far microburst) on track 270.

Data Set #5: 7/8/89 Denver, Very Dry Microburst

ILS Approach   Time = 40 min.
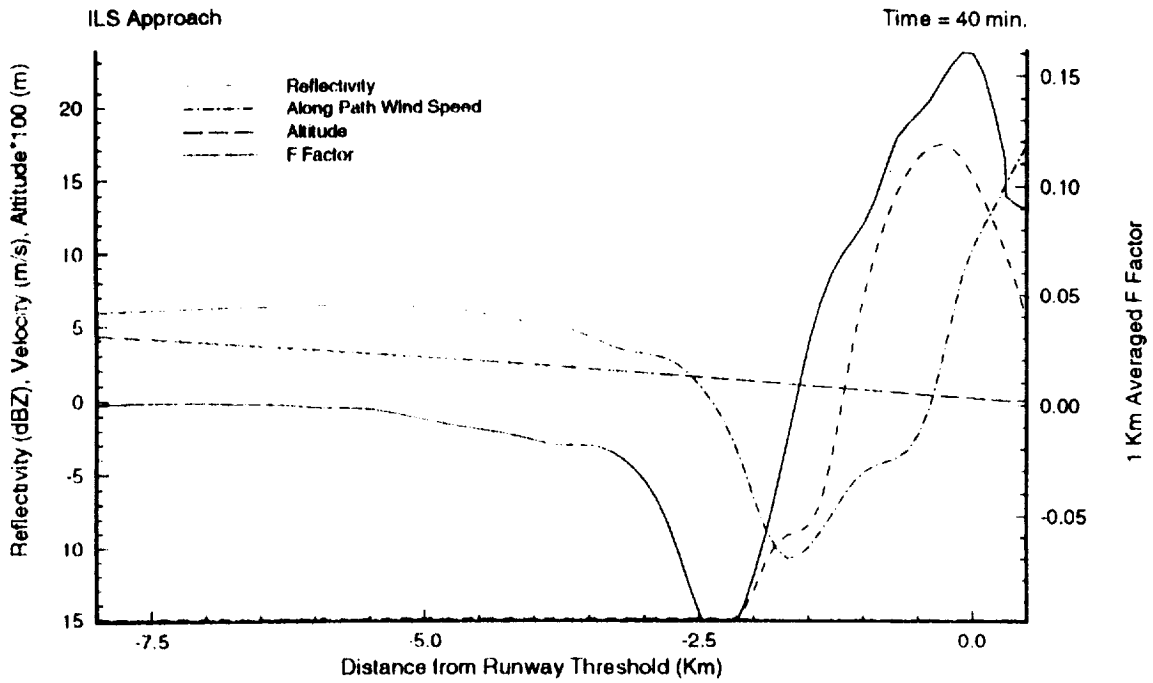
Figure A.5.21 Data Set #5-40: as in figure A.5.1 but for ILS approach on track 360.

Data Set #5: 7/8/89 Denver, Very Dry Microburst

Worst-case Drift Approach at 120 knots   Time = 40 min.
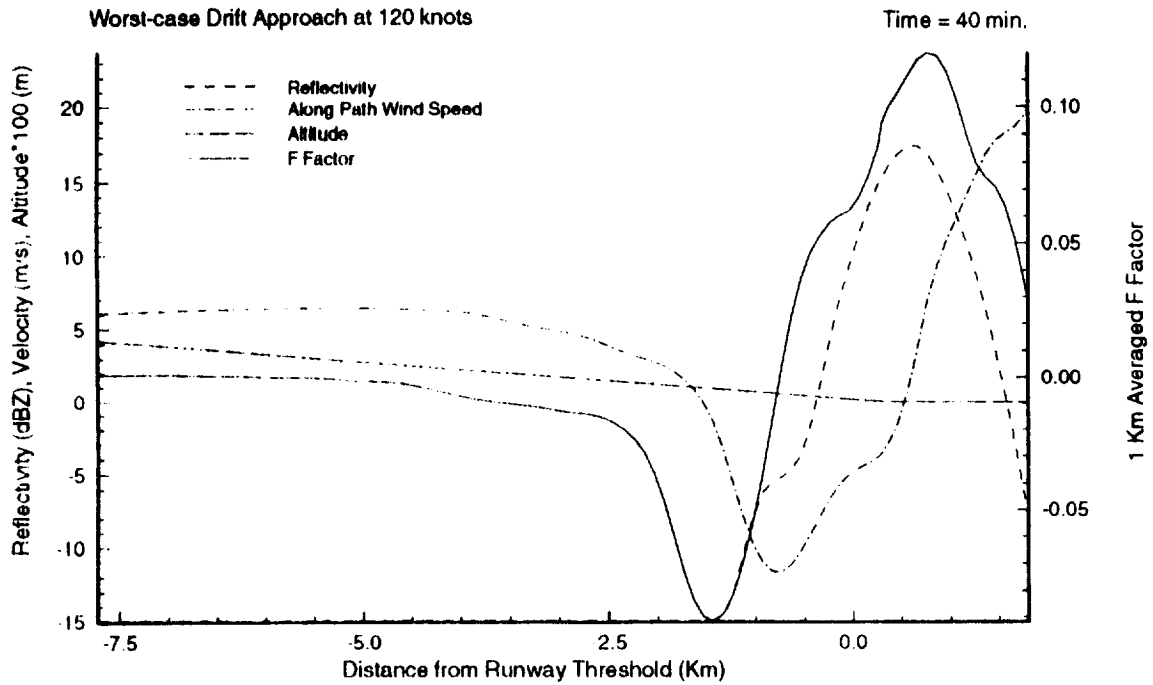
Figure A.5.22 Data Set #5-40: as in figure A.5.1 but for worst-case drift ILS approach on track 360.

Data Set #5: 7/8/89 Denver, Very Dry Microburst

Go-around Maneuver   Time = 40 min.
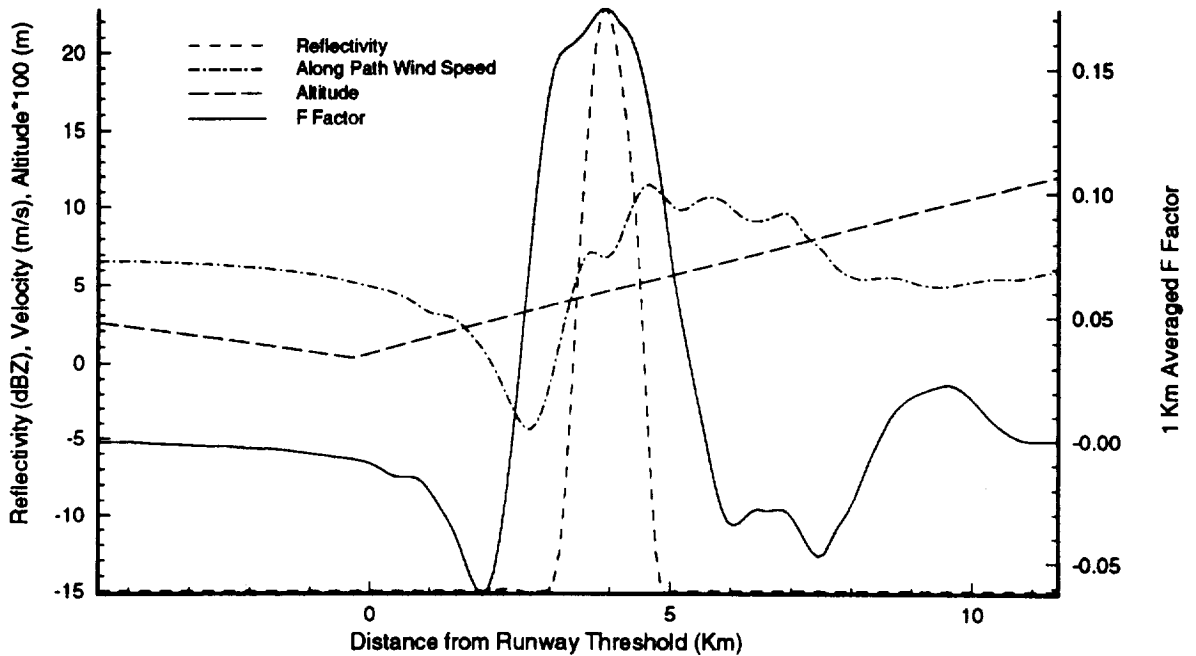
Figure A.5.23 Data Set #5-40: as in figure A.5.1 but for go-around scenario on track 360.

Data Set #5: 7/8/89 Denver, Very Dry Microburst

Curved Approach at 200 knots (Left Turn)   Time = 40 min.
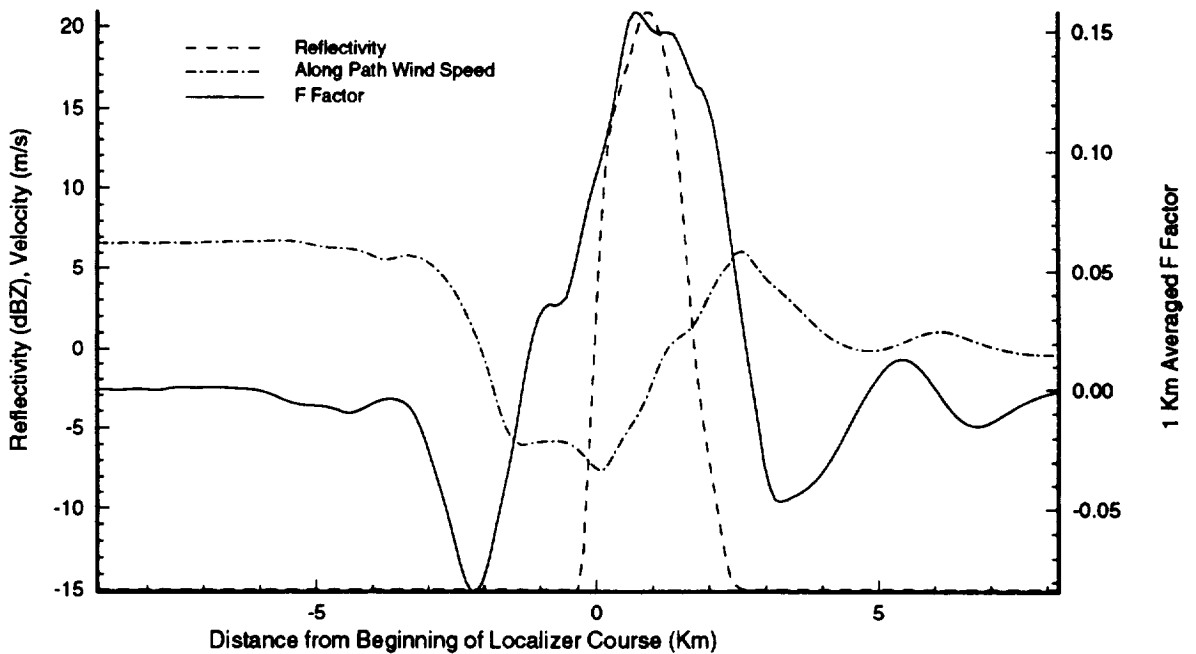
Figure A.5.24 Data Set #5-40: as in figure A.5.16 but curved approach flight scenario (left turn) with localizer on track 270.

Data Set #5: 7/8/89 Denver, Very Dry Microburst

Curved Approach at 200 knots (Right Turn)   Time = 40 min.
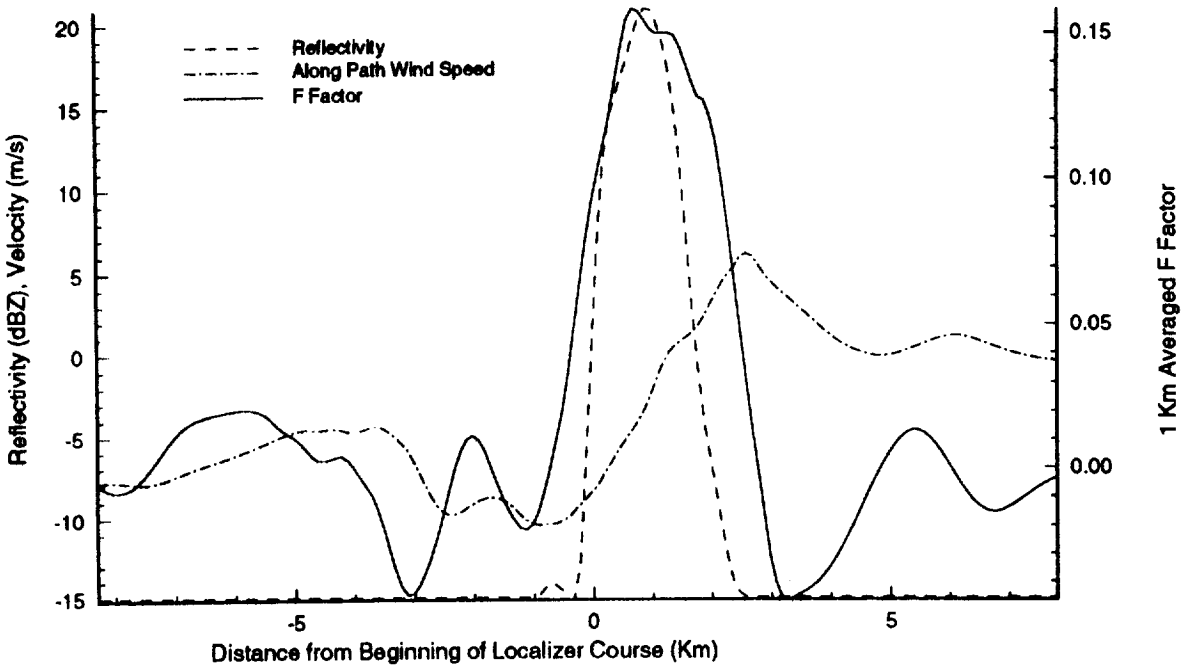
Figure A.5.25 Data Set #5-40: as in figure A.5.16 but curved approach flight scenario (right turn) with localizer on track 270.

Data Set #5: 7/8/89 Denver, Very Dry Microburst

ILS Approach (Second Microburst Pulse)   Time = 45 min.
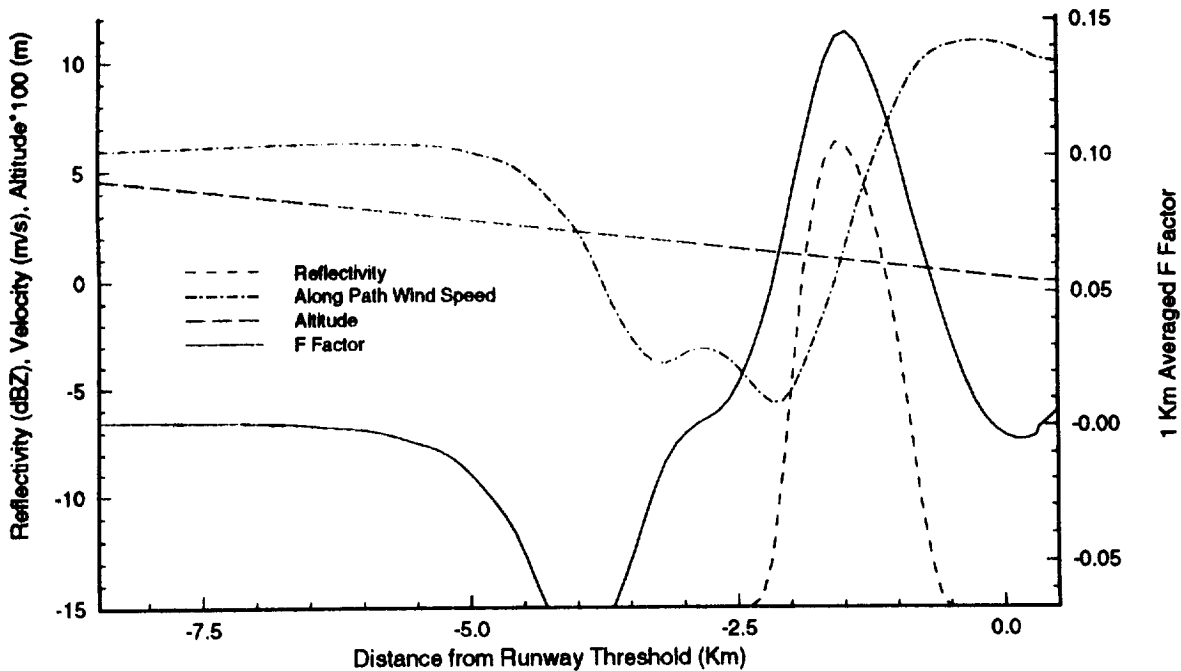
Figure A.5.26 Data Set #5-45: as in figure A.5.1 but for ILS approach on track 360.

Data Set #6: Highly Asymmetric Microburst

Curved Approach at 200 knots   Time = 14 min.
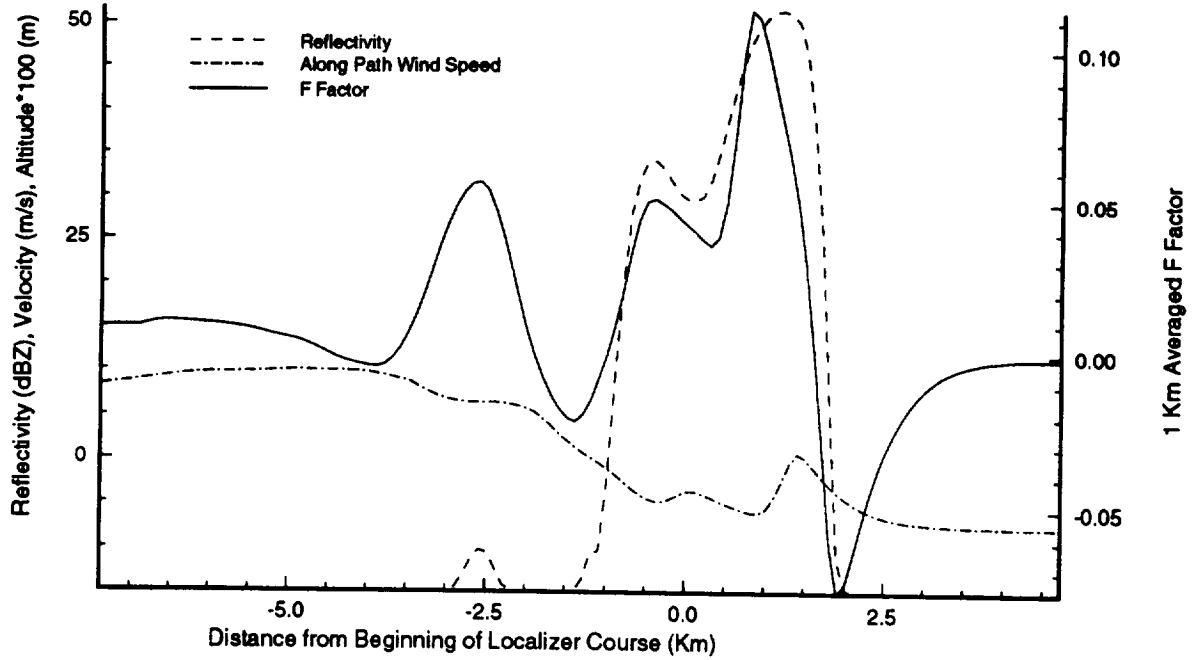
Figure A.5.27 Data Set #6-14: as in figure A.5.16 but curved approach flight scenario (right turn) with localizer on track 180.

Data Set #6: Highly Asymmetric Microburst

ILS Approach (Track 360)   Time = 14 min.
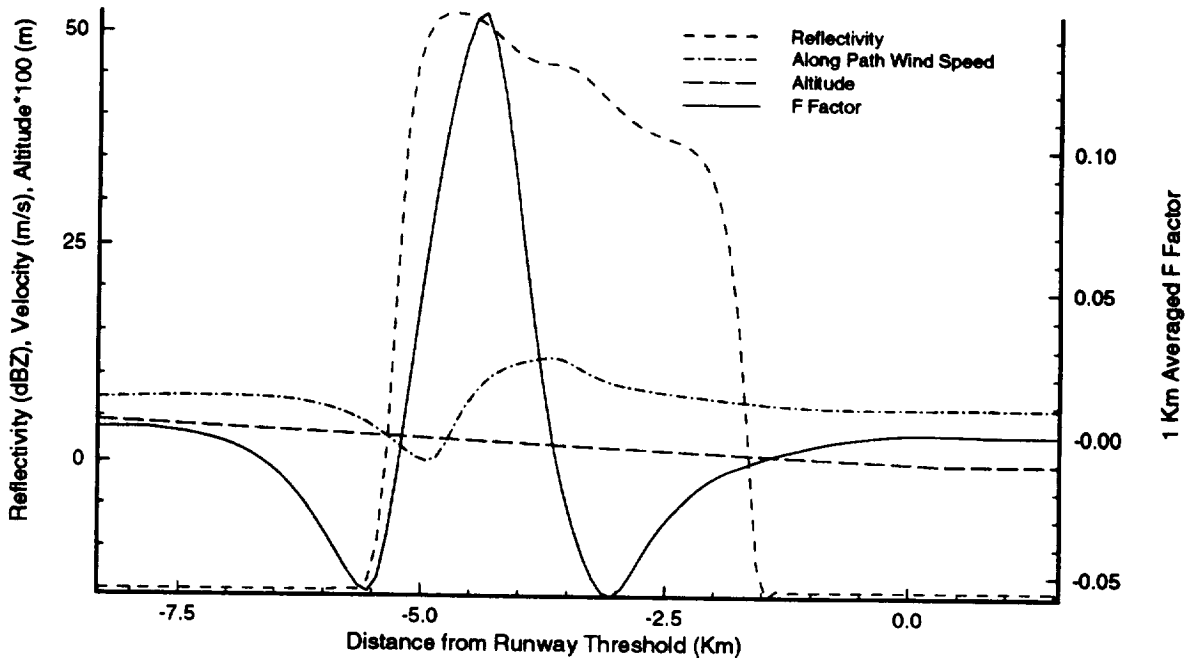
Figure A.5.28 Data Set #6-14: as in figure A.5.1 but for ILS approach scenario on track 360.

A-55

Data Set #6: Highly Asymmetric Microburst

ILS Approach (Track 045)   Time = 14 min.
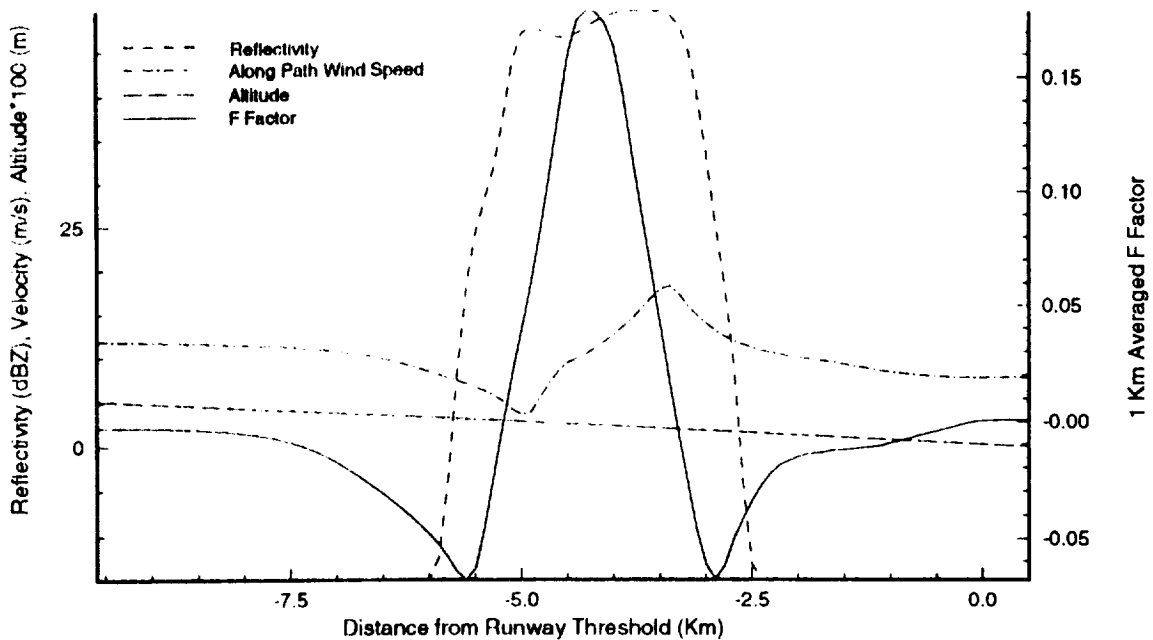
Figure A.5.29 Data Set #6-14: as in figure A.5.1 but for ILS approach scenario on track 45.

Data Set #6: Highly Asymmetric Microburst

ILS Approach (Track 090)   Time = 14 min.
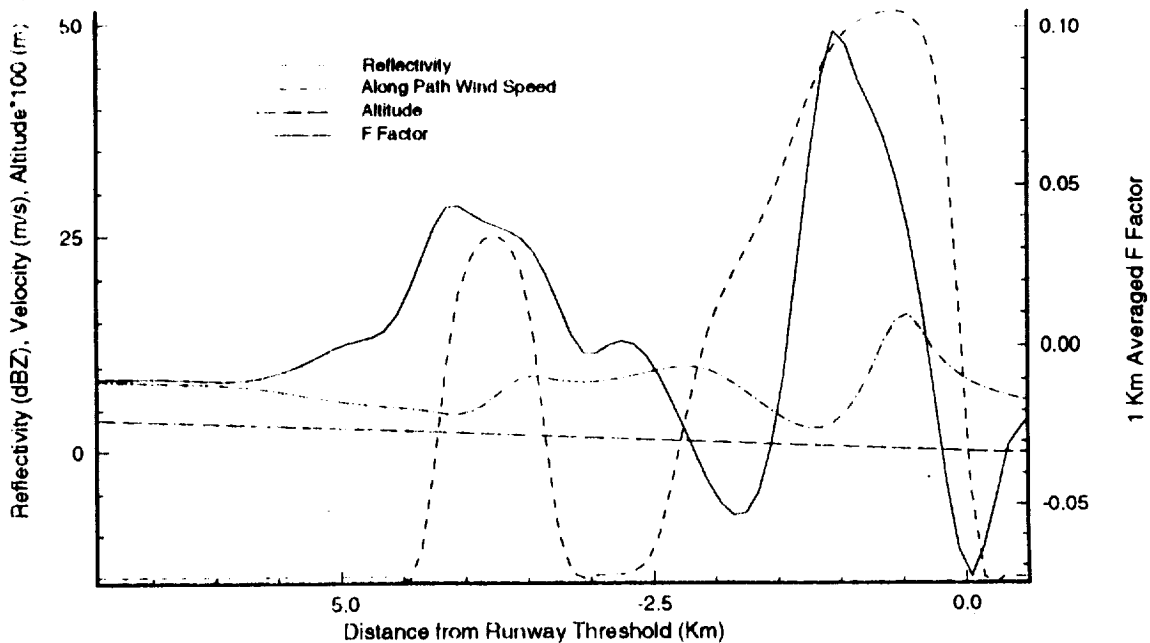
Figure A.5.30 Data Set #6-14: as in figure A.5.1 but for ILS approach scenario on track 90.

Data Set #6: Highly Asymmetric Microburst

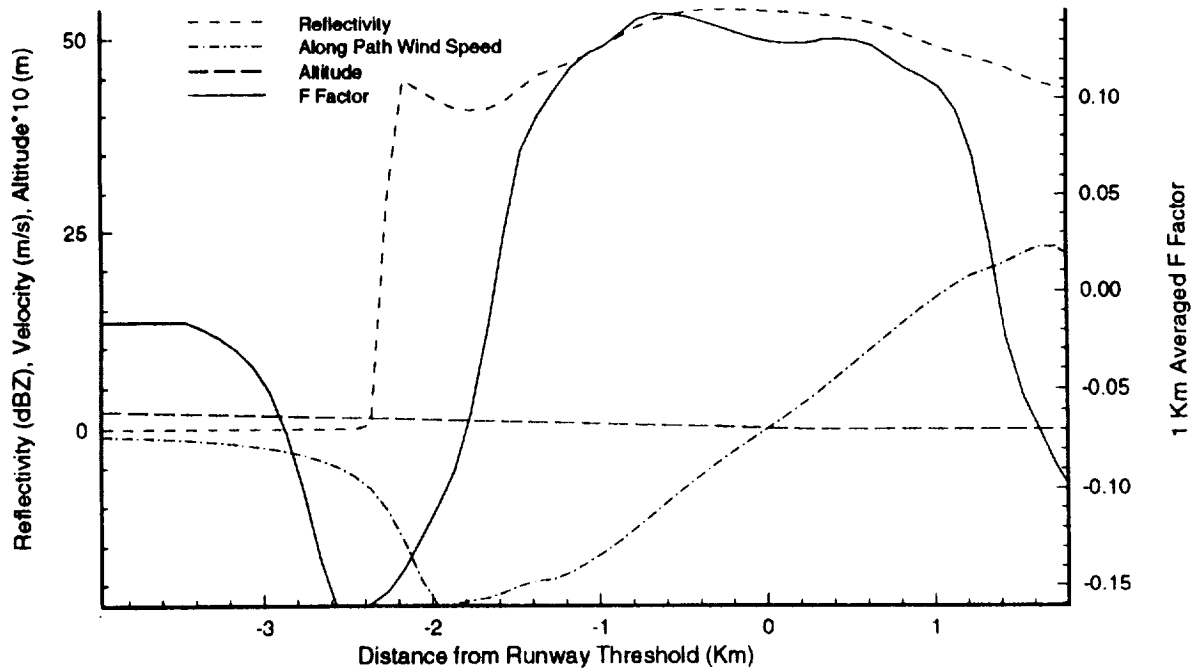ILS Approach (Track 180)   Time = 14 min.
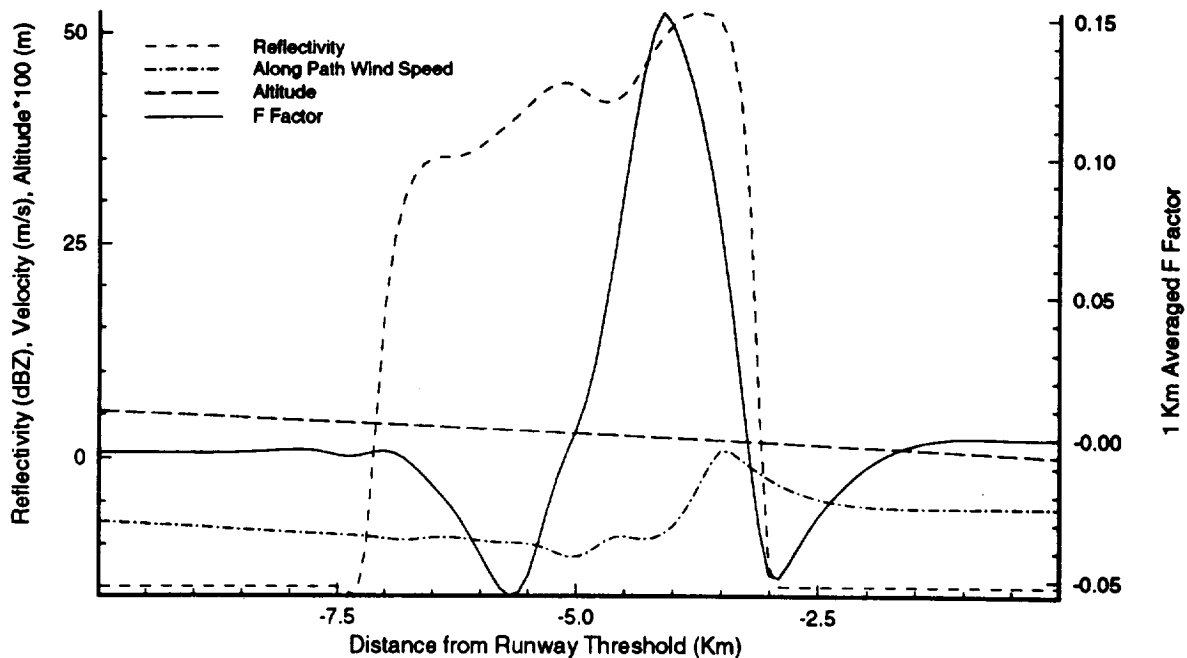
Figure A.5.31 Data Set #6-14: as in figure A.5.1 but for ILS approach scenario on track 180.

Data Set #6: Highly Asymmetric Microburst

ILS Approach (Track 225)   Time = 14 min.
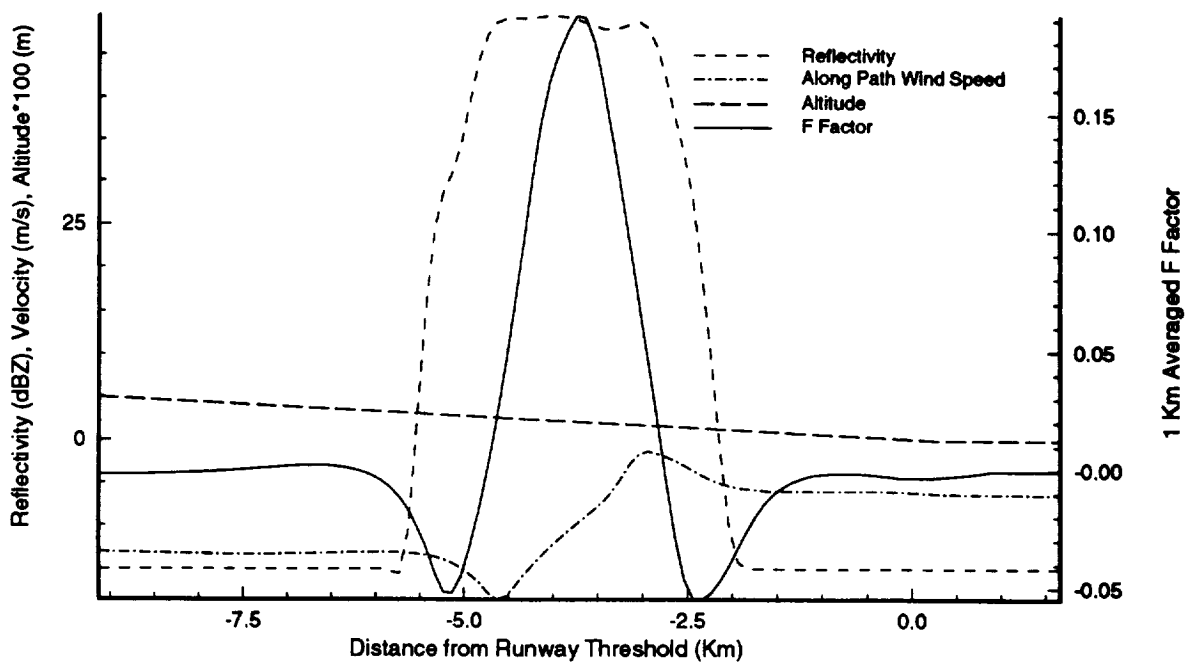
Figure A.5.32 Data Set #6-14: as in figure A.5.1 but for ILS approach scenario on track 225.

Data Set #6: Highly Asymmetric Microburst

ILS Approach (Track 270)   Time = 14 min.
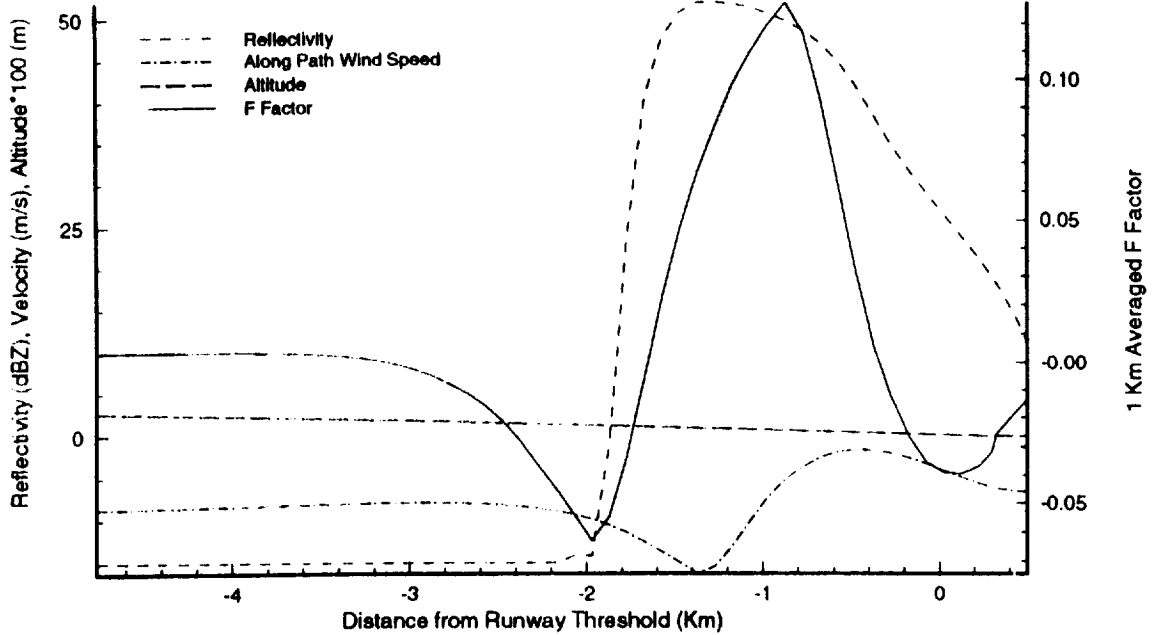
Figure A.5.33 Data Set #6-14: as in figure A.5.1 but for ILS approach scenario on track 270.

Data Set #6: Highly Asymmetric Microburst

ILS Approach (Track 315)   Time = 14 min.
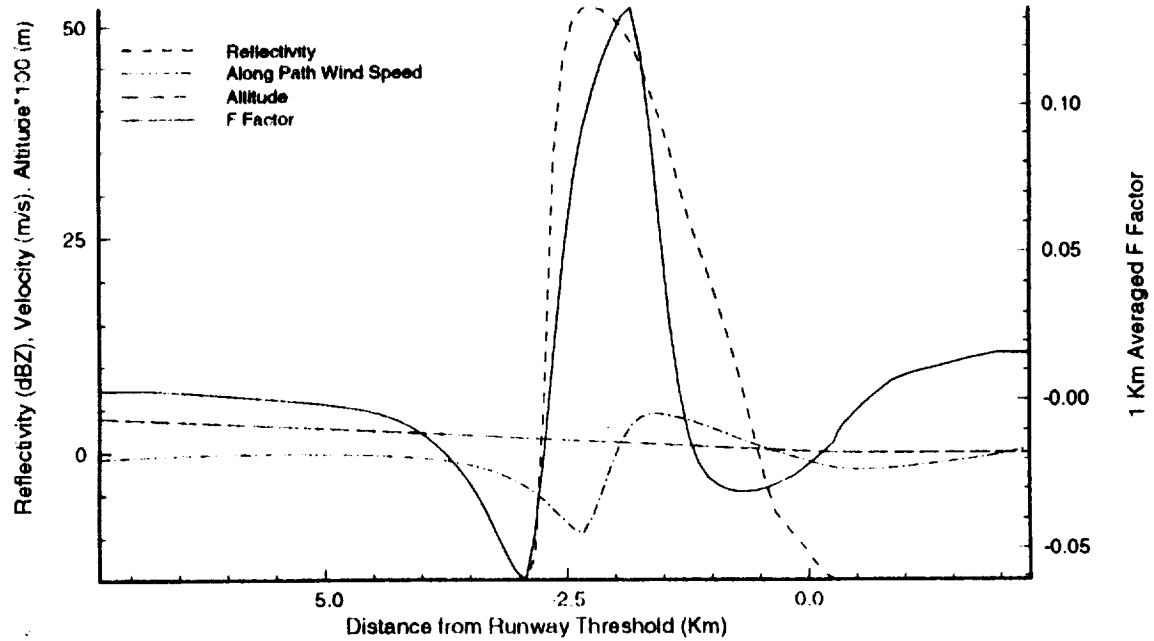
Figure A.5.34 Data Set #6-14: as in figure A.5.1 but for ILS approach scenario on track 315.

A-58

Data Set #7: Montana Sounding, Gust Front

Aligned for Takeoff   **Time = 27 min.**
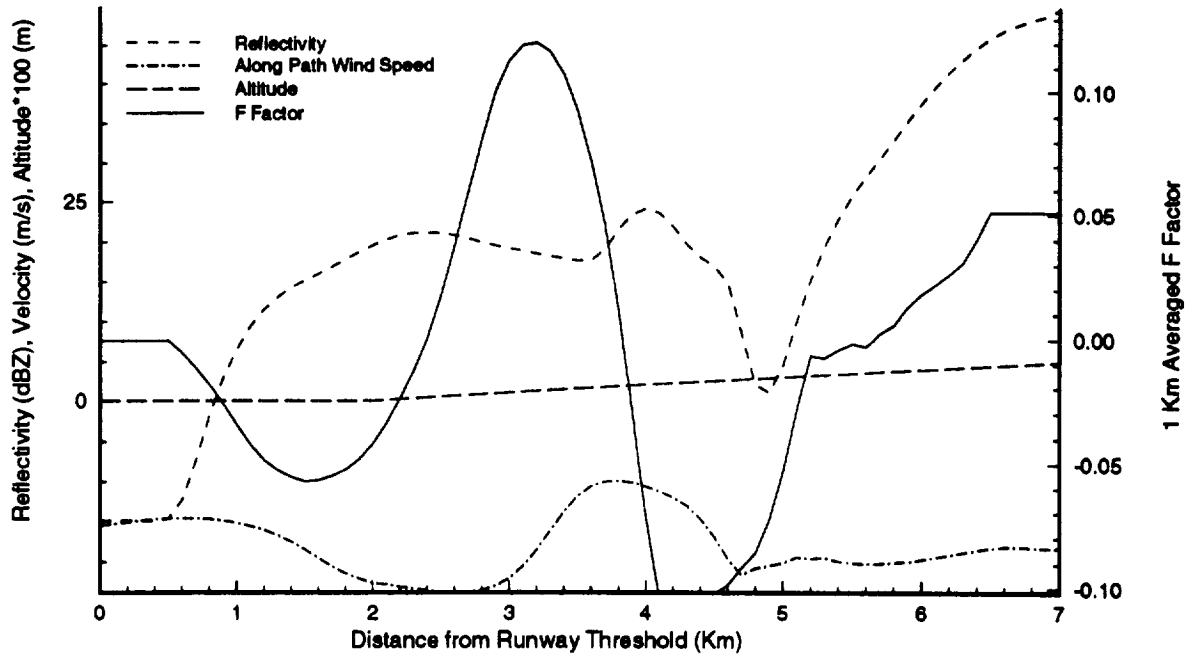
Figure A.5.35 Data Set #7-27: as in figure A.5.1 but for aligned for takeoff scenario (gust front near departure end of runway) on track 270.

Data Set #7: Montana Sounding, Gust Front

ILS Approach   **Time = 27 min.**
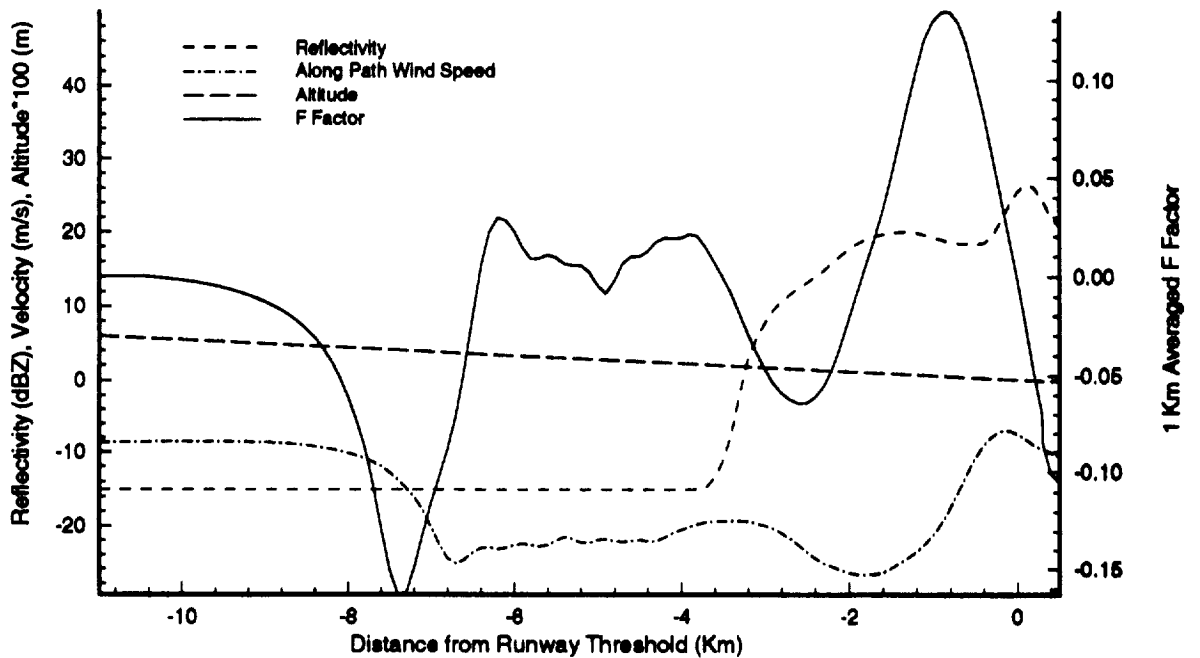
Figure A.5.36 Data Set #7-27: as in figure A.5.1 but for ILS approach scenario on track 270.

APPENDIX B

SKEW-T DIAGRAMS[1]

The chief data source for upper atmospheric data is the twice-daily (0000 and 1200 UTC) release of balloon-borne radiosondes from rawinsonde sites all over the globe. This data is collected and archived by the World Meteorological Organization (WMO - a part of the United Nations). A radiosonde is a balloon-borne package which contains temperature, humidity and pressure sensors. Data measured from these sensors is transmitted back to the ground station by telemetry. Altitude information is not explicitly measured, but is derived from the radiosonde data by use of the ideal gas law and integration of the hypsometric equation. The tracking of the balloons position by the rawinsonde system's radar or radio direction finder, allows for the trigonometric computation of upper-atmospheric wind data. The wind speed and direction, temperature, dewpoint, pressure, and altitude data is used by weather forecasters and is input into weather models, as well as being forwarded to the WMO.

To analyze rawinsonde data, a Skew-T (formally a Skew-T/Log-P) diagram is used. This type of thermodynamic chart, which is widely used in meteorology, has its ordinate proportional to ln P and it abscissa proportional to (T + ln P), where P is atmospheric pressure and T is temperature. In order to understand the wealth of information that it provides, we shall construct a Skew-T diagram by overlaying its parts. The left side of Fig. B.1 shows the base of the Skew-T diagram --- the isobars (constant pressure levels), the isotherms (lines of constant temperature), and the dry adiabats. The isobars are represented on a logarithmic scale in order to approximate a linear altitude axis:

$$\frac{dP}{dz} = -\rho g = -\frac{gP}{RT},$$

$$\frac{dP}{P} = -\frac{g}{RT}dz, \qquad (B-1)$$

where z is height, ρ is air density, g is acceleration due to gravity, and R is the gas constant for dry air. If g/RT is assumed constant (a reasonable zeroth-order assumption), then:

$$ln\ P \propto z. \qquad (B-2)$$

---

[1]The following text is extracted with minor modification from Appendix A of Bacon et al. (1991).

The isotherms are "skewed" to improve the readability of the diagram. Finally, the dry adiabats represent the decrease in temperature that a dry air parcel should experience if it were to be expanded via an adiabatic process:

$$\frac{P}{P_o} = \left(\frac{\rho}{\rho_o}\right)^{\frac{1}{\gamma}}$$

where: $\gamma = \frac{c_p}{c_v}$, the ratio of the specific heats of dry air,

$$\Rightarrow \quad P = P_o\left(\frac{T}{T_o}\right)^{\frac{\gamma}{\gamma-1}} \tag{B-3}$$

Note that in Fig. B.1 that the dry adiabats (dotted lines in left figure) are not straight lines, but are slightly curved and run from the lower right to the upper left corner of the diagram. The angle between isotherms and dry adiabats is nearly $90°$.

Vertical profiles of atmospheric temperature through clouds rarely follow that of a dry adiabat because of the presence of moisture. At a given temperature and pressure, there exists a maximum amount of moisture which can remain in the atmosphere as vapor; the remainder must condense out, and in doing so release latent heat. The right side of Fig. B.1 shows lines that represent this process. Lines of constant mixing ratio (a mixing ratio is the amount of a given quantity divided by the amount of dry air) are shown as straight dashed lines. [The vapor mixing ratio of a parcel of air is conserved in absence of turbulence mixing, condensation, and evaporation.] Because of the large number of lines which appear on a typical Skew-T diagram, we show the lines of constant mixing ratio at regular multiplicative increments of a factor of two starting at 0.5 g/kg (grams of water vapor per kilogram of dry air). Thus the dashed line which starts just above $10°$ C near the surface represents a constant mixing ratio of 8 g/kg.

As we mentioned, the water vapor in excess of the saturation mixing ratio must condense out of the atmosphere releasing latent heat. Thus if we start with a saturated air parcel and expand it adiabatically it would not have the temperature behavior of the dry adiabat; the latent heat release would tend to make the *saturation adiabat* warmer. This is shown by the gently-curved solid lines on the left side of Fig. B.2. Note that at cold temperatures where the amount of water vapor in the air parcel must be small, the saturation adiabats asymptotically approach the dry adiabats.

Finally, on the right side of Fig. B.2 we show the Skew-T diagram for the 1200 UTC sounding taken at Moscow on July 18, 1974. Note that once the temperature (solid line) and dewpoint (dashed line) are known as functions of pressure, then it is possible to determine an altitude axis to go along with the sounding. Starting from the

surface, we note that the surface air was very humid, but that it was not saturated. Thus the temperature lapse rate of the atmosphere near the surface was approximated by a dry adiabat. If we extend the surface dewpoint along a line of constant mixing ratio, the point at which it intersects this dry adiabat represents the altitude at which condensation would begin (approximately cloud base). If you look closely at this sounding, you will see that this is precisely where the temperature begins to diverge from a dry adiabat and begin to follow a saturation adiabat. A region from 4 to 5 km altitude where the temperature and dewpoint are nearly the same is indicative of existing cloud cover. Above roughly 5.5 km there is virtually no measurable water vapor as indicated by the dew point profile.
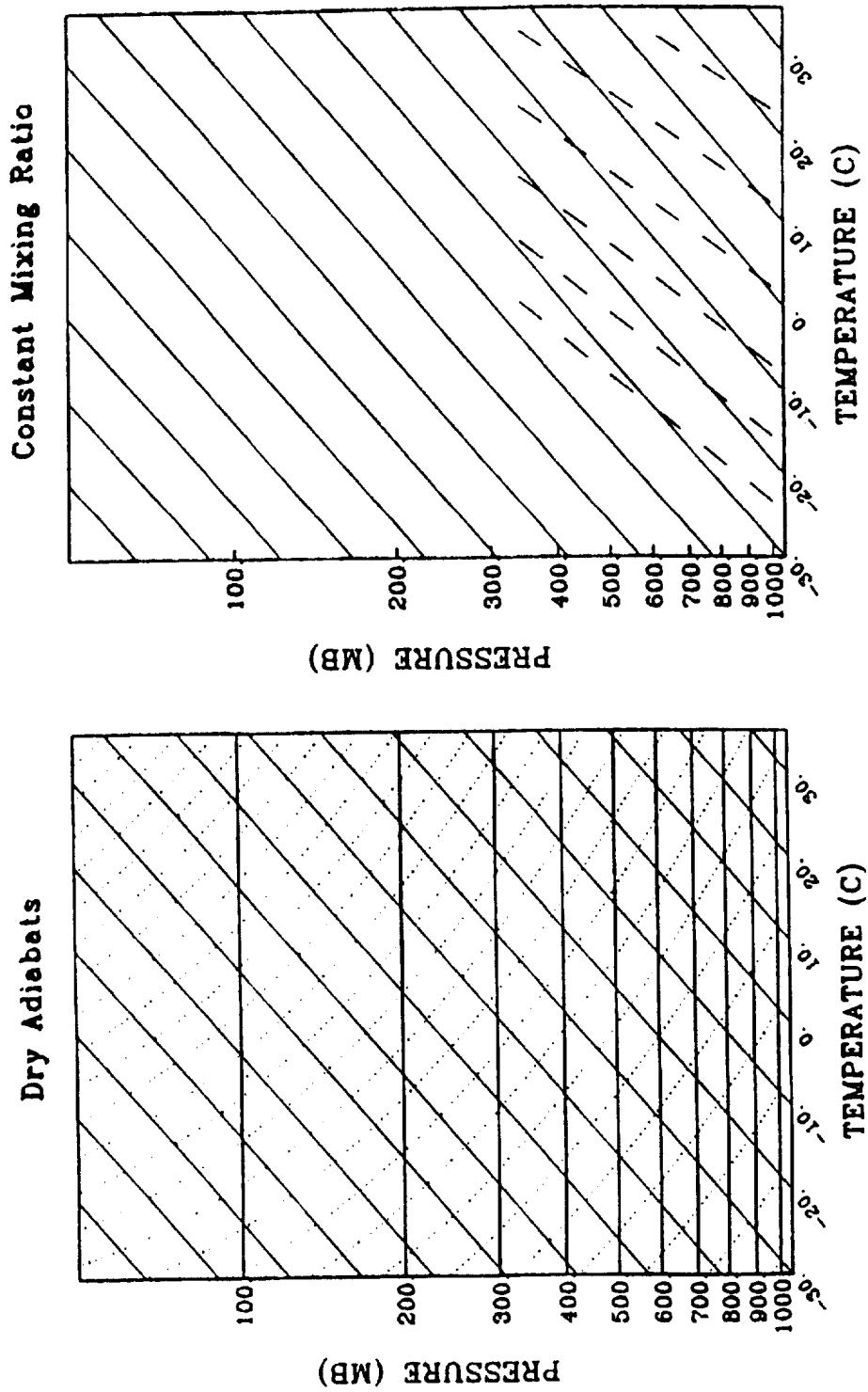
Figure B.1 Skew-T diagrams with isobars, isotherms, and dry adiabats (left) and isotherms and saturation mixing ratios (right).

C-2

GEOPOTENTIAL ALTITUDE (KM-AGL)

MOSCOW DATA 1200Z 7-18-74

Dry + Saturation Adiabats

TEMPERATURE (C)

TEMPERATURE (C)

PRESSURE (MB)

PRESSURE (MB)
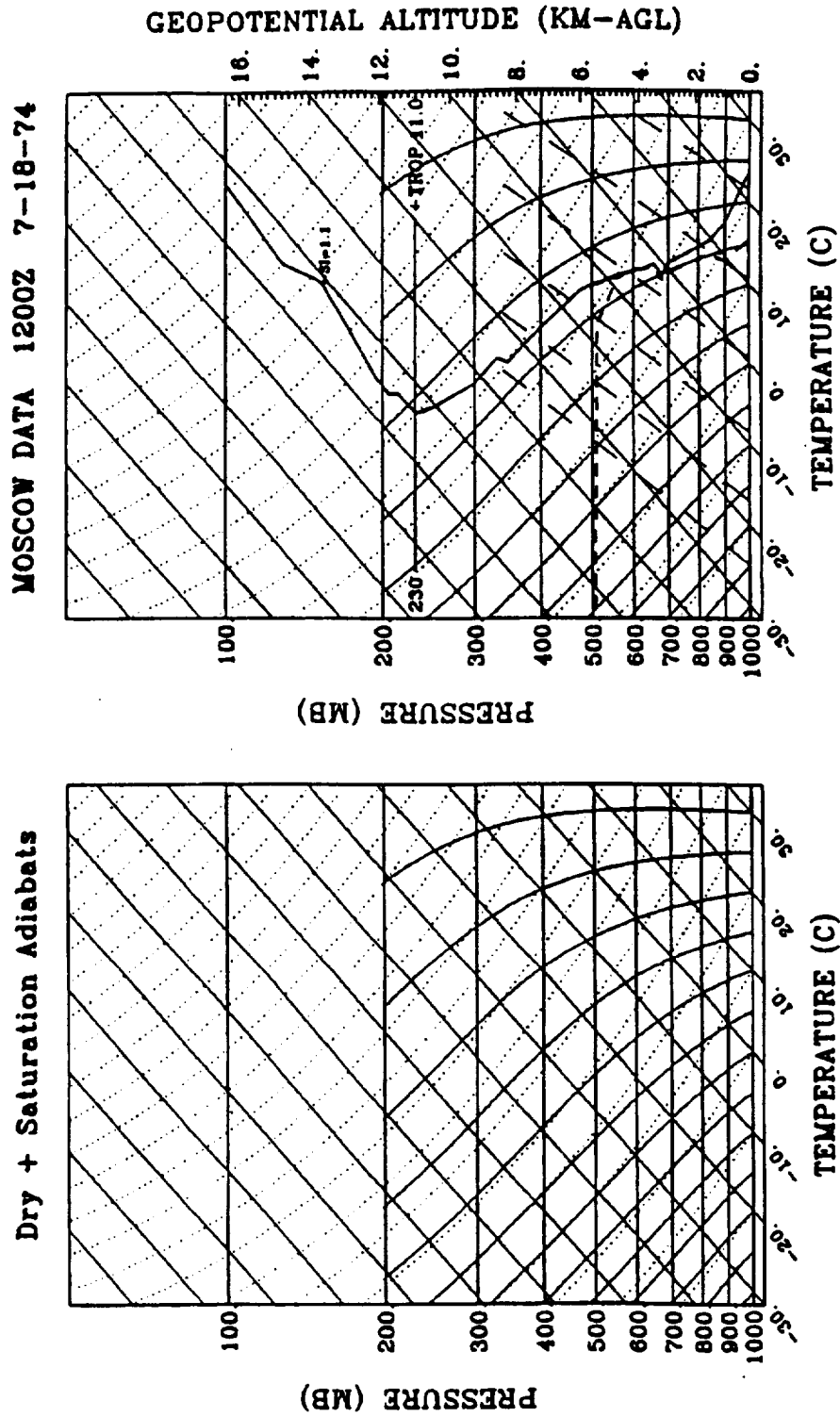
Figure B.2 Skew-T diagram with isobars, isotherms, and both dry and saturation adiabats (left). The right shows a full Skew-T diagram of the 1200 UTC sounding from Moscow on July 18, 1974.

Appendix C

Aircraft Hazard Factor or F-factor Equations

The primary threat of microbursts to aircraft is the single or combined effect of the horizontal velocity shear and downdraft motion. Either of these effects can penalize the performance of an aircraft, and possibly result in a critical loss of altitude for arriving or departing aircraft. A nondimensional index based on the fundamentals of flight mechanics that quantifies the effect of wind shear on the aircraft energy state is the F-factor (Bowles 1990):

$$F = \frac{1}{g}\frac{DU_H}{Dt} - \frac{w}{\left|\bar{V}_a\right|} \qquad (C-1)$$

where g is gravitational acceleration, U_H is the horizontal component of wind velocity along the flight path, w is the vertical component of wind velocity, and $\bar{V}_a$ is airplane velocity relative to the air mass. For the data shown in this document the term U_H is calculated by the dot product of the horizontal wind velocity and a unit vector that is the aircraft velocity unit vector constrained to the horizontal plane at the airplane's position. The first term on the right side of (C-1) represents the contribution of horizontal wind shear to the performance of the aircraft, while the second term represents the contribution due to vertical wind. *Positive* values of F indicate a *performance-decreasing* condition, whereas *negative* values indicate a *performance-increasing* situation. The F-factor can be interpreted as the gain or loss of an aircraft's potential climb angle due to atmospheric winds. Note that with an airspeed of 75 m/s, a headwind loss of 0.1 g (2 knots/sec) has the same effect on aircraft performance as a downdraft of 7.5 m/s. The above formula can be simplified by noting that the database wind fields are frozen in time. With this constraint DU_H/Dt is then:

$$\nabla\bar{U}_H \bullet \bar{V}_a \qquad (C-2)$$

Therefore for frozen wind fields the equation for the F-factor becomes:

$$F = \frac{1}{g}\left[\nabla\bar{U}_H \bullet \bar{V}_a\right] - \frac{w}{\left|\bar{V}_a\right|} \qquad (C-3)$$

The instantaneous equation above is then averaged over a 1-km segment resulting in the following equation for the 1-km averaged F-factor or "FBAR" at point $\bar{R}$ (x,y,z):

$$FBAR = \bar{F}(\bar{R}) = \frac{1}{L}\int_{-L/2}^{L/2} F(\bar{R}')ds \qquad (C-4)$$

where:

$$\vec{R}' = \vec{R} + \hat{n}_a(\vec{R})s$$

$\hat{n}_a$ = unit vector along the aircraft flight path

L = 1 km

For this application, the F-factor in (C-3) is calculated in three steps. First the quantity U_H is computed at the airplane's position and at a point 100 meters ahead in the direction of flight[1]. The gradient of this quantity in the given direction is approximated by taking the difference of these two values and dividing by 100 meters. This value is multiplied by the airspeed, and divided by g to arrive at the complete value of the horizontal term. The last term of (C-3) is the vertical wind speed at the airplane's position over the airspeed. For this document the airspeed is assumed equal to the groundspeed and is constant along a path. Finally (C-4) is applied to the calculated values from (C-3). The along path F-factor plots are shown in appendix A-5.

Equation (C-4) allows the computation of F-factors along any segment. Additional restrictions to the flight path can be made to give a quantitative assessment of the hazard to aircraft throughout each of the data set domains without specifying specific flight paths. These restrictions are to fix the airspeed and groundspeed at 77.2 m/s (150 knots), hold the airplane altitude constant, and assume parallel paths through the data set in north to south or east to west directions. These restrictions result in North-South and East-West F-factor fields. Note that with the above assumptions FBAR would be the same for an aircraft flying south as for one flying north along the same path. F-factor calculations with these constraints reduces to:

$$FBAR_{N-S} = \frac{V_a}{g\,L}\left(v_{y+\frac{L}{2}} - v_{y-\frac{L}{2}}\right) - \frac{dxy}{L\,V_a}\sum_{y-\frac{L}{2}}^{y+\frac{L}{2}} w \qquad \text{(C-5)}$$

$$FBAR_{E-W} = \frac{V_a}{g\,L}\left(u_{x+\frac{L}{2}} - u_{x-\frac{L}{2}}\right) - \frac{dxy}{L\,V_a}\sum_{x-\frac{L}{2}}^{x+\frac{L}{2}} w \qquad \text{(C-6)}$$

where V_a is the magnitude of airspeed; u, v, and w are the velocity components of the wind (explained in table 2.2); and dxy is the horizontal spacing of the data set (explained in section 5). The second term in (C-5) and (C-6) is the average vertical wind speed over the airspeed. The above equations are used to generate the F-factor field plots shown in appendix A-2.

---

[1]The IMSL Math/Library (1989) routine "QD3VL" is used to interpolate for the necessary velocity components for along path calculations.

APPENDIX D

Supplementary Equations

Section D.1 discusses the relevant hydrometeor-size distributions that are used in TASS, along with the subsequent diagnostic equations for radar reflectivity factor and surface precipitation rate. Section D.2 lists empirical relationships between visibility and rainfall rate; and formulas for converting temperature between Celsius, Kelvin and Fahrenheit are provided in the final section for the users convenience.

D.1 Model Drop-Size Distributions and Subsequent Diagnostic Equations

In the TASS model formulation, the cloud hydrometeors are subdivided into 5 bulk categories compromising nonprecipitating or suspended particles such as 1) liquid cloud droplets and 2) ice crystal, as well as precipitating particles such as 3) raindrops, 4) snow, and 5) hail/graupel. The distributions and contribution to the simulated radar reflectivity factor are described below for only those variables which are included in the database. [The variables not described in this section, such as cloud ice, melt before falling within the windowed domain of the database.]

D.1.1 Size Distributions for Rain and Hail

The hydrometeor size distributions for both rain and hail are assumed to be inverse exponential. Specifically, the size distribution for rain is (Marshall and Palmer 1948)

$$N(D_R) = N_{OR} \exp(-\frac{D_R}{\Lambda_R}),\qquad\text{(D-1)}$$

where $N(D_R)$ is the number of raindrops per unit diameter per unit volume, D_R is the raindrop diameter, Λ_R is the inverse of the slope of the rain distribution and N_{OR} is the intercept. Similarly, the size distribution for hail is (Federer and Waldvogel 1975)

$$N(D_H) = N_{OH} \exp(-\frac{D_H}{\Lambda_H}),\qquad\text{(D-2)}$$

where $N(D_H)$ is the number of hail particles per unit diameter per unit volume, D_H is the hail particle diameter, Λ_H is the inverse of the slope of the hail distribution and N_{OH} is the intercept.

The slope factors can be determined from the above distributions as (Kessler 1969):

$$\Lambda_R = \left(\frac{M_R}{\pi N_{OR}\, \delta_w}\right)^{0.25}, \quad and \quad \Lambda_H = \left(\frac{M_H}{\pi N_{OH}\, \delta_H}\right)^{0.25} \tag{D-3}$$

where δ_w is the density of water, δ_H is the average density of the hail particles, M_R is the rainwater content (rainwater mass contained per unit volume of air), and M_H is the hailwater content (hail mass contained per unit volume of air).

D.1.2 Parameterization of Raindrop Intercept

Based on a survey of observed drop-size distributions, the well-known **Marshal-Palmer Intercept value of** $N_{OR} = 8 \times 10^6\, m^{-4}$ (which was empirically-based on size distributions measured in steady light rain) is both small and inappropriate for most thunderstorm rainfalls. Furthermore, raindrop spectrum data obtained from Doppler radar suggest that the intercept value depends on rainfall rate (e.g. Hodson 1986). One-dimensional microphysics models (e.g, List et al. 1987) imply that the intercept should increase with rainwater content (and rainfall rate) for moderate to heavy rainfall due to the continuous production of small drops from the collisional breakup of drops.

The TASS model formulation, assumes a N_{OR} that depends on rainwater content, as based on measured data. The relationship is

$$N_{OR} = 2.5 \times 10^8\ M_R^{\,0.375} \tag{D-4}$$

where N_{OR} has units of [m^{-4}], and M_R has units of [$kg\ m^{-3}$]. The above formula is obtained from radar drop-size data within thunderstorms as reported in Sekhon and Srivastava (1971). [Note that for rainwater contents less than $10^{-4}\ Kg\ m^{-3}$ $(0.1\ g\ m^{-3})$, Eq. (D-4) gives value less than Marshal Palmer.]

D.1.3 Contribution to Radar Reflectivity Factor From Rain

The contribution of radar reflectivity from rain can be determined from any continuous drop spectrum by assuming Rayleigh scattering as:

$$Z_R = \int_0^\infty N(D_R) \; D_R^6 \; dD_R \; .$$ (D-5)

Integrating (D-5) with (D-1) and substituting (D-3) and (D-4) yields:

$$Z_R = 1.1 \; x \; 10^4 \; M_R^{1.47}$$ (D-6)

where Z_R has the conventional units of [$mm^6 \; m^{-3}$], and M_R has units of [$g \; m^{-3}$].

D.1.4 Parameterization of Surface Rainfall Rate

A diagnostic equation for rainfall rate from either rainwater content or radar reflectivity can be determined with the aid of the above equations.

The surface rainfall rate [$mm \; hr^{-1}$] in terms of the raindrop spectrum is

$$R_R = 3.6 \; x \; 10^6 \; \frac{\pi}{6} \int_0^\infty W(D_R) \; D_R^3 \; N(D_R) \; dD_R \; ,$$ (D-7)

where $W(D_R)$ is the fall velocity of a raindrop with diameter D_R. An approximation for the fall velocity that is fitted from Gunn and Kinzer's (1949) experimental data (units MKS) is

$$W(D_R) = 386.6 \; D_R^{2/3} \; .$$ (D-8)

With (D-1), and (D-8), Eq. (D-7) may be integrated giving:

$$R_R = 1.072 \; x \; 10^{10} \; N_{OR} \; \Lambda^{4.6667} \; .$$ (D-9)

By substituting (D-3) and (D-4) into (D-9), the rainfall rate may be expressed in terms of the rainwater content as:

$$R_R = 17.3 \; M_R^{1.104},$$ (D-10)

where again M_R is in units of [$g \; m^{-3}$]. Note that the rainfall rate is *almost* linerally-proportional to the rainwater content.

D-3

With (D-6) and (D-11) the radar reflectivity factor can be expressed in terms of surface rainfall rate as:

$$Z_R = 245 \; R_R^{1.33} \; .$$

(D-11)

A comparison of (D-11) and the relation attributed to Marshall and Palmer,

$$Z_{mp} = 200 \; R_R^{1.6} \; ,$$

is shown in Fig. D.1.

D.1.5 Formulas for Hailwater

Similar relationships between radar reflectivity, precipitation rate, and hailwater content can be developed for hail, but are less general than those for rain since N_{OH} and δ_H may vary substantially with case. Care must be taken in developing these formulas to include the effects of Mie scattering from wet hailstones. Formulas for hail, as well as those already derived for rain, are summarized in D.1.6
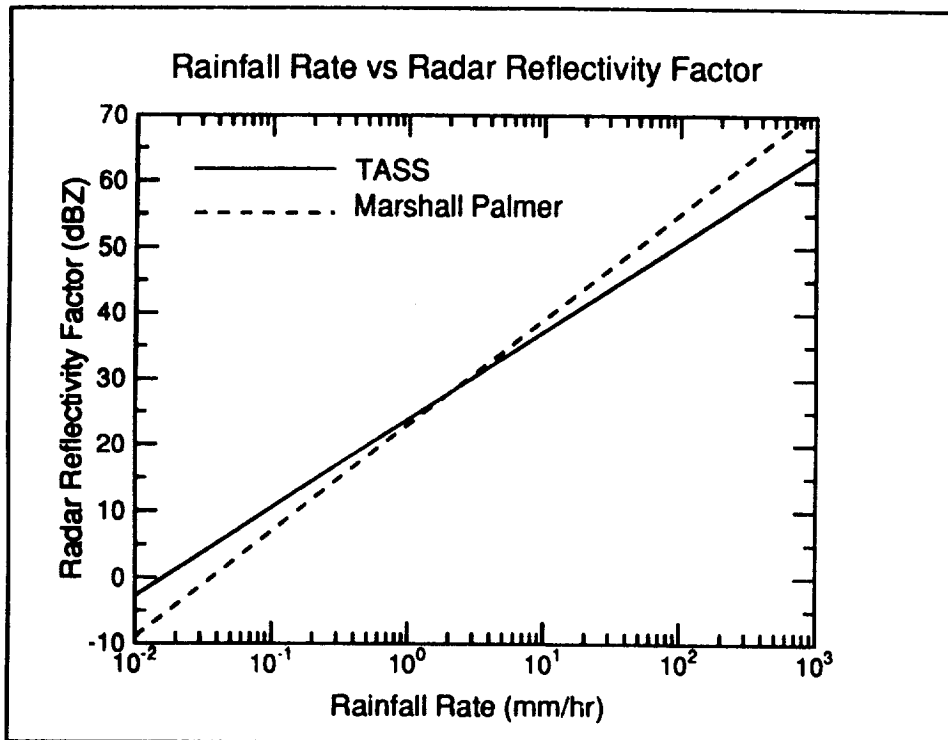
Figure D.1 Comparison between Eq. (D-11) (which is derived from TASS formulations) and Marshal-Palmer's empirical relationship for rainfall rate vs radar reflectivity.

D.1.6 Summary of Equations for Radar Reflectivity and Precipitation Rate

Relationships between radar reflectivity and precipitation rate for rain and for wet hail are as follows:

Rain:

$$R_R = 17.3 \, M_R^{1.104}$$

$$R_R = 0.016 \, Z_R^{0.75}$$

$$Z_R = 245 \, R_R^{1.333}$$

$$Z_R = 1.1 \times 10^4 \, M_R^{1.47}$$

Hail:

$$R_H = 52 \, M_H^{1.125}$$

$$R_H = 6.8 \times 10^{-3} \, Z_H^{0.68}$$

$$Z_H = 1591 \, R_H^{1.48}$$

$$Z_H = 5.5 \times 10^5 \, M_H^{1.66}$$

where:

M_R = Rain content [g m^{-3}]

M_H = Hail content [g m^{-3}]

R_R = Surface rainfall rate [mm/hr]

R_H = Surface precipitation rate for hail [mm/hr]

Z_R = Radar reflectivity factor for rain [mm^6 m^{-3}]

Z_H = Radar reflectivity factor for wet hail [mm^6 m^{-3}]

Notes: 1 mm/hr = 0.03937 in/hr

$$dBZ = 10 \, \log_{10}(Z_R + Z_H)$$

D.2 Visibility

An empirical relationship between visual range and surface rainfall rate has been formulated by Huffman and Haines (1984) and is listed below:

$$h = 18.5 \, R_R^{-0.63} \, ,$$

where:

h = Visibility [km],

and

R_R = Rainfall rate [mm/hr].

D.3 Temperature

Formulas for converting between degrees Celsius, Kelvin and Fahrenheit:

degrees Fahrenheit = 32 + 1.8 degrees Celsius

degrees Fahrenheit = 32 + 1.8 (degrees Kelvin - 273.15)

degrees Celsius = 5/9 (degrees Fahrenheit - 32)

degrees Celsius = degrees Kelvin - 273.15

Appendix E

Sample FORTRAN Program to Read and Verify the Database

```
          PROGRAM DATACHK
C••••••••••••••••••••••••••••••••••••••••••••••••••••••••••••••••••••••••••••
C
C  THIS IS A PROGRAM TO CHECK 3-D DATA SETS IN FAA FORMAT.
C
C••••••••••••••••••••••••••••••••••••••••••••••••••••••••••••••••••••••••••••
          PARAMETER(IMAX=201, JMAX=201, KMAX=41, NVAR=5)
          INTEGER FTIN, QLOC
          DIMENSION QXYZ(IMAX,JMAX,KMAX,NVAR)
          DIMENSION VARMAX(KMAX),VARMIN(KMAX)
          INTEGER LOCMAX(3,KMAX),LOCMIN(3,KMAX)
          LOGICAL UREAD,VREAD,WREAD
          CHARACTER*80 INFILE,TITLE
          CHARACTER*4 VAR
          DATA QLOC /1/
          DATA UREAD/.FALSE./, VREAD /.FALSE./, WREAD/.FALSE./
C
10        WRITE(*,*) 'ENTER THE NAME OF THE DATA FILE TO CHECK'
          READ(5,'(A)') INFILE
          WRITE(6,'(A,A)')' READING FROM DATA FILE = ',INFILE
20        WRITE(6,*) 'IS THE FILE FORMATTED OR BINARY?'
          WRITE(6,*) ' 1 = FORMATTED'
          WRITE(6,*) ' 0 = BINARY  '
          READ(5,*) FTIN
          IF(FTIN.NE.1 .AND. FTIN.NE.0) GOTO 20
          IF(FTIN.EQ.1) THEN
             OPEN(UNIT=1,FILE=INFILE,ERR=10,FORM='FORMATTED',STATUS='OLD')
             READ(1,1000,ERR=998) TITLE
             READ(1,2000,ERR=998) VAR,IX,IY,IZ,TIME,XSTART,YSTART,DXY,DZ
          ELSE
             OPEN(UNIT=1,FILE=INFILE,ERR=10,FORM='UNFORMATTED',STATUS='OLD')
             READ(1,ERR=998) TITLE
             READ(1,ERR=998) VAR,IX,IY,IZ,TIME,XSTART,YSTART,DXY,DZ
          ENDIF
          REWIND(1)
          IF(IX.GT.IMAX .OR. IY.GT.JMAX .OR. IZ.GT.KMAX) THEN
             WRITE(*,*)' ARRAY TOO LARGE!'
             WRITE(*,'(A,3I5)')' IMAX,JMAX,KMAX = ',IMAX,JMAX,KMAX
             WRITE(*,'(A,3I5)')' IX,IY,IZ = ',IX,IY,IZ
             CLOSE(1)
             STOP
          ENDIF
          REWIND(1)
          IF(FTIN.EQ.1) THEN
             READ(1,1000) TITLE
          ELSE
             READ(1) TITLE
          ENDIF
          WRITE(*,'(A)')' TITLE LINE:'
          WRITE(*,'(A)') TITLE
50        WRITE(*,*)' ENTER THE TYPE OF ANALYSIS TO PERFORM.'
          WRITE(*,*)' 1 = GLOBAL MINIMUM AND MAXIMUM'
          WRITE(*,*)' 2 = PLANAR MINIMUM AND MAXIMUM (IN Z PLANES)'
          READ(*,*) ICALC
```

```fortran
         IF(ICALC.NE.1 .AND. ICALC.NE.2) GOTO 50
         IVAR = 1
C
C LOOP OVER ALL VARIABLES STORED ON TAPE
C
300      CONTINUE
         IF(FTIN.EQ.1) THEN
           READ(1,2000,END=999) VAR,IX,IY,IZ,TIME,XSTART,YSTART,DXY,DZ
           READ(1,3000,END=999) (((QXYZ(I,J,K,QLOC),I=1,IX),J=1,IY),K=1,IZ)
         ELSE
           READ(1,END=999) VAR,IX,IY,IZ,TIME,XSTART,YSTART,DXY,DZ,
     1       (((QXYZ(I,J,K,QLOC),I=1,IX),J=1,IY),K=1,IZ)
         ENDIF
C
         IF(VAR(1:1) .EQ. 'U' .OR. VAR(1:1).EQ.'V' .OR.
     1 VAR(1:1).EQ.'W') THEN
           CALL DATFILL(QXYZ,IX,IY,IZ,UREAD,VREAD,WREAD,VAR,
     1       IMAX,JMAX,KMAX,NVAR,QLOC,DXY)
         ENDIF
350      IVAR = IVAR + 1
         IF(QLOC.EQ.2) VAR = 'EWFF'
         IF(QLOC.EQ.3) VAR = 'NSFF'
         IF(QLOC.NE.1) THEN
           IF(QLOC.EQ.3)
     1     WRITE(*,'(A,A,A)')' EXAMINING THE CALCULATED VARIABLE : ',
     2     'NORTH-SOUTH 1 KM AVERAGED F FACTOR'
           IF(QLOC.EQ.2)
     1     WRITE(*,'(A,A,A)')' EXAMINING THE CALCULATED VARIABLE : ',
     2     'EAST-WEST 1 KM AVERAGED F FACTOR'
         ENDIF
         L = 1
         VARMAX(L) = -9.99E50
         VARMIN(L) =  9.99E50
         DO 400 K = 1, IZ
           IF(ICALC.EQ.2) THEN
             L = K
             VARMAX(L) = -9.99E50
             VARMIN(L) =  9.99E50
           ENDIF
           DO 400 J = 1, IY
             DO 400 I = 1, IX
               IF(QXYZ(I,J,K,QLOC) .GT. VARMAX(L)) THEN
                 VARMAX(L) = QXYZ(I,J,K,QLOC)
                 LOCMAX(1,L) = I
                 LOCMAX(2,L) = J
                 LOCMAX(3,L) = K
               ENDIF
               IF(QXYZ(I,J,K,QLOC) .LT. VARMIN(L)) THEN
                 VARMIN(L) = QXYZ(I,J,K,QLOC)
                 LOCMIN(1,L) = I
                 LOCMIN(2,L) = J
                 LOCMIN(3,L) = K
               ENDIF
400      CONTINUE
```

```
         IF(ICALC.EQ.1) THEN
           IF(QLOC.EQ.1) THEN
             WRITE(*,'(A,A,A)')' FOR THE VARIABLE = "',VAR,'"'
           ENDIF
           WRITE(*,'(A,G15.7)')' MAXIMUM VALUE IS = ',
     1        VARMAX(1)
           WRITE(*,'(A,3I15,A)')' MAXIMUM VALUE IS AT ',
     1        (LOCMAX(I,1),I=1,3),' (I,J,K)'
           XLOCMAX = XSTART + FLOAT(LOCMAX(1,1)-1)*DXY
           YLOCMAX = YSTART + FLOAT(LOCMAX(2,1)-1)*DXY
           ZLOCMAX = FLOAT(LOCMAX(3,1)-1)*DZ
           WRITE(*,'(A,3G15.7,A)')' MAXIMUM VALUE IS AT ',
     1        XLOCMAX,YLOCMAX,ZLOCMAX,' (X,Y,Z)'
           WRITE(*,'(A,G15.7)')' MINIMUM VALUE IS = ',
     1        VARMIN(1)
           WRITE(*,'(A,3I15,A)')' MINIMUM VALUE IS AT ',
     1        (LOCMIN(I,1),I=1,3),' (I,J,K)'
           XLOCMIN = XSTART + FLOAT(LOCMIN(1,1)-1)*DXY
           YLOCMIN = YSTART + FLOAT(LOCMIN(2,1)-1)*DXY
           ZLOCMIN = FLOAT(LOCMIN(3,1)-1)*DZ
           WRITE(*,'(A,3G15.7,A)')' MINIMUM VALUE IS AT ',
     1        XLOCMIN,YLOCMIN,ZLOCMIN,' (X,Y,Z)'
         ELSE IF(ICALC .EQ.2) THEN
           WRITE(*,'(A,A,A)')' FOR THE VARIABLE = "',VAR,'"'
           WRITE(*,'(A)')' VARIABLES = Z,X1,Y1,VALMAX,X2,Y2,VALMIN'
           DO 450 K = 1, IZ
             XLOCMAX = XSTART + FLOAT(LOCMAX(1,K)-1)*DXY
             YLOCMAX = YSTART + FLOAT(LOCMAX(2,K)-1)*DXY
             ZLOCMAX = FLOAT(LOCMAX(3,K)-1)*DZ
             XLOCMIN = XSTART + FLOAT(LOCMIN(1,K)-1)*DXY
             YLOCMIN = YSTART + FLOAT(LOCMIN(2,K)-1)*DXY
             WRITE(*,4000) ZLOCMAX,XLOCMAX,YLOCMAX,
     1          VARMAX(K),XLOCMIN,YLOCMIN,VARMIN(K)
450        CONTINUE
         ENDIF
         IF(QLOC.NE.1) GOTO 999
       GOTO 300
998      CONTINUE
         WRITE(*,'(A)')' ERROR ON INPUT'
         WRITE(*,'(A)')' RE-ENTER THE NAME OF THE DATA SET'
         REWIND(1)
         GOTO 10
999      CONTINUE
         IF(WREAD) THEN
           QLOC = QLOC + 1
           IF(UREAD .AND. VREAD) THEN
             IF(QLOC.LE.3) GOTO 350
           ENDIF
         ENDIF
         WRITE(6,*) 'END OF FILE . . . STOP'
         CLOSE(1)
         STOP
1000     FORMAT(A80)
2000     FORMAT(A4,/,3I4,/,5E12.4)
```

```
3000      FORMAT((8E10.4))
4000      FORMAT(F10.4,1X,2(F9.2,1X),F11.4,1X,2(F9.2,1X),F11.4)
          END
C••••••••••••••••••••••••••••••••••••••••••••••••••••••••••••••••••••••••
C
C  THIS IS A SUBROUTINE TO TAKE THE DATA AND PLACE IT INTO THE PROPER
C  LOCATION TO CALCULATE THE 1 KM AVERAGED F FACTOR
C
C••••••••••••••••••••••••••••••••••••••••••••••••••••••••••••••••••••••••
          SUBROUTINE DATFILL(QXYZ,IX,IY,IZ,UREAD,VREAD,WREAD,VAR,
     1                     IMAX,JMAX,KMAX,NVAR,QLOC,DXY)
          DIMENSION QXYZ(IMAX,JMAX,KMAX,NVAR)
          LOGICAL UREAD,VREAD,WREAD
          INTEGER QLOC
          CHARACTER*4 VAR
          DATA ITYPE /0/
          IF(VAR .EQ. 'U   ') THEN
            UREAD = .TRUE.
            DO 400 I = 1, IX
              DO 400 J = 1, IY
              DO 400 K = 1, IZ
                QXYZ(I,J,K,2) = QXYZ(I,J,K,QLOC)
400         CONTINUE
          ELSE IF(VAR .EQ. 'V   ') THEN
            VREAD = .TRUE.
            DO 410 I = 1, IX
              DO 410 J = 1, IY
                DO 410 K = 1, IZ
                QXYZ(I,J,K,3) = QXYZ(I,J,K,QLOC)
410         CONTINUE
          ELSE IF(VAR .EQ. 'W   ') THEN
            WREAD = .TRUE.
            DO 420 I = 1, IX
              DO 420 J = 1, IY
                DO 420 K = 1, IZ
                QXYZ(I,J,K,4) = QXYZ(I,J,K,QLOC)
420         CONTINUE
          ENDIF
          IF(WREAD .AND. VREAD) THEN
            LOC = 5
            IDIR = 2
            CALL FFACT(DXY,QXYZ,IX,IY,IZ,NVAR,LOC,IDIR,IMAX,JMAX,KMAX,
     1        ITYPE)
            DO 600 I = 1, IX
              DO 600 J = 1, IY
                DO 600 K = 1, IZ
                QXYZ(I,J,K,3) = QXYZ(I,J,K,LOC)
600         CONTINUE
          ENDIF
625       IF(WREAD .AND. UREAD) THEN
            LOC = 5
            IDIR = 1
            CALL FFACT(DXY,QXYZ,IX,IY,IZ,NVAR,LOC,IDIR,IMAX,JMAX,KMAX,
     1             ITYPE)
```

```
              DO 650 I = 1, IX
                DO 650 J = 1, IY
                  DO 650 K = 1, IZ
                    QXYZ(I,J,K,2) = QXYZ(I,J,K,LOC)
650           CONTINUE
            ENDIF
            RETURN
            END
C
            SUBROUTINE FFACT(DXY,Q,IX,IY,IZ,NVAR,LOC,IDIR,IMAX,JMAX,KMAX,
     1              ITYPE)
C
C THIS IS A SUBROUTINE TO COMPUTE THE NORTH-SOUTH OR EAST-WEST 1 KM
C AVERAGED F FACTOR AND STUFF IT INTO THE ARRAY Q.
C
C IDIR - PARAMETER TO DETERMINE THE DIRECTION TO CALCULATE THE F
C        FACTOR
C           = 1 EAST-WEST CALCULATION
C           = 2 NORTH-SOUTH CALCULATION
C ITYPE - PARAMETER TO DETERMINE WHAT GOES INTO THE F FACTOR
C        CALCULATION
C           = 0 INCLUDE BOTH VERTICAL AND HORIZONTAL COMPONENTS
C           = 1 INCLUDE ONLY HORIZONTAL COMPONENT
C           = 2 INCLUDE ONLY VERTICAL COMPONENT
C Q    = DATA ARRAY THAT CONTAINS THE VELOCITY COMPONENTS AS FOLLOWS:
C           Q(I,J,K,2) = U OR WEST TO EAST VELOCITY
C           Q(I,J,K,3) = V OR SOUTH TO NORTH VELOCITY
C           Q(I,J,K,4) = W OR VERTICAL (POSITIVE UP)
C
            DIMENSION Q(IMAX,JMAX,KMAX,NVAR)
C   WRITE(*,'(A)')' INSIDE FFACT'
C   WRITE(*,'(A,/,G10.4,7I10)')' DXY,IX,IY,IZ,NVAR,LOC,IDIR,ITYPE=',
C   1 DXY,IX,IY,IZ,NVAR,LOC,IDIR,ITYPE
            VAIR = 150.
            GRAV = 9.8
C
C CONVERT VAIR FROM KNOTS TO METERS/SEC
C
            VAIR = VAIR * 6080.27 * 12. * 2.54 / (100. * 3600.)
C
C DETERMINE THE NUMBER OF GRID CELLS IN 1000 METERS
C
            IF(FLOAT(INT(1000.0E0/DXY)) .EQ. 1000.0E0/DXY) THEN
              I1000 = INT(1000.0E0/DXY + 0.5)
            ELSE
              I1000 = INT(1000.0E0/DXY + 0.5)
              WRITE(*,'(A)')' WARNING FROM FFACT ******'
              WRITE(*,'(A,F10.1,A)')
     1          ' F FACTOR CALCULATION BASED ON DISTANCE OF ',
     2          (I1000)*DXY,' METERS!'
            ENDIF
C
C COMPUTE THE COEFFICIENT TO MULTIPLY BY
C
```

```fortran
          FFCOEF1 = VAIR/(GRAV*FLOAT(I1000)*DXY)
          FFCOEF2 =1.0E0/(FLOAT(I1000+1)*VAIR)
          SWITCH1 = 1.0E0
          SWITCH2 = 1.0E0
          IF(ITYPE.EQ.1) SWITCH2 = 0.0E0
          IF(ITYPE.EQ.2) SWITCH1 = 0.0E0
          IF(IDIR .EQ. 1) THEN
C
C COMPUTE EAST-WEST F FACTOR
C
          IDISP  = INT(FLOAT(I1000)/2.0E0)
          IEND   = IX - I1000
          DO 300 K = 1, IZ
            DO 300 J = 1, IY
              DO 200 I = 1, IEND
                WSUM = 0.0E0
                DO 100 L = 0, I1000
                  WSUM = WSUM + Q(I+L,J,K,4)
100             CONTINUE
                Q(I+IDISP,J,K,LOC) = FFCOEF1*SWITCH1*(Q(I+I1000,J,K,2)-
     1                              Q(I,J,K,2)) - FFCOEF2*WSUM*SWITCH2
200           CONTINUE
300         CONTINUE
C
C EXTRAPOLATE END VALUES TO COVER ENTIRE GRID
C
          DO 310 K = 1, IZ
            DO 310 J = 1, IY
              DO 310 I = 1, IDISP
                Q(I,J,K,LOC) = Q(IDISP+1,J,K,LOC)
310         CONTINUE
          DO 320 K = 1, IZ
            DO 320 J = 1, IY
              DO 320 I = IEND + 1, IX
                Q(I,J,K,LOC) = Q(IEND,J,K,LOC)
320         CONTINUE
          ELSE IF(IDIR.EQ.2) THEN
C
C COMPUTE NORTH-SOUTH F FACTOR
C
          JDISP  = INT(FLOAT(I1000)/2.0E0)
          JSTART = JDISP + 1
          JEND   = IY - I1000
          DO 600 K = 1, IZ
            DO 600 I = 1, IX
              DO 500 J = 1, JEND
                WSUM = 0.0E0
                DO 400 L = 0, I1000
                  WSUM = WSUM + Q(I,J+L,K,4)
400             CONTINUE
                Q(I,J+JDISP,K,LOC) = FFCOEF1*SWITCH1*(Q(I,J+I1000,K,3)-
     1                              Q(I,J,K,3)) - FFCOEF2*WSUM*SWITCH2
500           CONTINUE
600         CONTINUE
```

```
C
C  EXTRAPOLATE END VALUES TO COVER ENTIRE GRID
C
            DO 610 K = 1, IZ
              DO 610 I = 1, IX
                DO 610 J = 1, JDISP
                  Q(I,J,K,LOC) = Q(I,JDISP+1,K,LOC)
610         CONTINUE
            DO 620 K = 1, IZ
              DO 620 I = 1, IX
                DO 620 J = JEND + 1, IY
                  Q(I,J,K,LOC) = Q(I,JEND,K,LOC)
620         CONTINUE
            ENDIF
            RETURN
            END
```

Appendix F

Output from Sample FORTRAN Program to Read and Verify the Database

Case #1-11: DFW Accident Case, Wet Microburst, Rain and Hail

For the variable = "U "
Maximum value is =   23.23900
Maximum value is at   115   81   1 (i,j,k)
Maximum value is at   1700.000   0.0000000E+00 0.0000000E+00 (x,y,z)
Minimum value is = -23.23900
Minimum value is at   47   81   1 (i,j,k)
Minimum value is at -1700.000   0.0000000E+00 0.0000000E+00 (x,y,z)

For the variable = "V "
Maximum value is =   23.23900
Maximum value is at   81   115   1 (i,j,k)
Maximum value is at   0.0000000E+00   1700.000   0.0000000E+00 (x,y,z)
Minimum value is = -23.23900
Minimum value is at   81   47   1 (i,j,k)
Minimum value is at   0.0000000E+00 -1700.000   0.0000000E+00 (x,y,z)

For the variable = "W "
Maximum value is =   7.681050
Maximum value is at   62   43   10 (i,j,k)
Maximum value is at -950.0000   -1900.000   450.0000   (x,y,z)
Minimum value is = -16.05312
Minimum value is at   78   71   21 (i,j,k)
Minimum value is at -150.0000   -500.0000   1000.000   (x,y,z)

For the variable = "TAU "
Maximum value is =   309.3200
Maximum value is at   72   33   1 (i,j,k)
Maximum value is at -450.0000   -2400.000   0.0000000E+00 (x,y,z)
Minimum value is =   289.7400
Minimum value is at   67   62   40 (i,j,k)
Minimum value is at -700.0000   -950.0000   1950.000   (x,y,z)

For the variable = "RAIN"
Maximum value is =   4.838400
Maximum value is at   79   79   1 (i,j,k)
Maximum value is at -100.0000   -100.0000   0.0000000E+00 (x,y,z)
Minimum value is =   0.0000000E+00
Minimum value is at   1   1   1 (i,j,k)
Minimum value is at -4000.000   -4000.000   0.0000000E+00 (x,y,z)

For the variable = "XIV "
Maximum value is =   17.70703
Maximum value is at   78   39   6 (i,j,k)
Maximum value is at -150.0000   -2100.000   250.0000   (x,y,z)
Minimum value is =   5.984900
Minimum value is at   81   81   40 (i,j,k)
Minimum value is at   0.0000000E+00 0.0000000E+00   1950.000   (x,y,z)

For the variable = "RRF "
Maximum value is =   64.36700
Maximum value is at   81   81   40 (i,j,k)

Maximum value is at 0.0000000E+00 0.0000000E+00 1950.000   (x,y,z)
Minimum value is = -2.161660
Minimum value is at   75   46   25 (i,j,k)
Minimum value is at -300.0000   -1750.000   1200.000   (x,y,z)
For the variable = "HAIL"
Maximum value is = 2.366000
Maximum value is at   81   81   40 (i,j,k)
Maximum value is at 0.0000000E+00 0.0000000E+00 1950.000   (x,y,z)
Minimum value is = 0.0000000E+00
Minimum value is at   1   1   1 (i,j,k)
Minimum value is at -4000.000   -4000.000   0.0000000E+00 (x,y,z)
For the variable = "EWFF"
Maximum value is = 0.2208870
Maximum value is at   81   71   13 (i,j,k)
Maximum value is at 0.0000000E+00 -500.0000   600.0000   (x,y,z)
Minimum value is = -0.1725874
Minimum value is at   32   81   3 (i,j,k)
Minimum value is at -2450.000   0.0000000E+00 100.0000   (x,y,z)
For the variable = "NSFF"
Maximum value is = 0.2208870
Maximum value is at   71   81   13 (i,j,k)
Maximum value is at -500.0000   0.0000000E+00 600.0000   (x,y,z)
Minimum value is = -0.1725874
Minimum value is at   81   32   3 (i,j,k)
Minimum value is at 0.0000000E+00 -2450.000   100.0000   (x,y,z)

Case #2-37: 6/20/91 Orlando, Florida, NASA Research Flight, Wet Microburst

For the variable = "U "
Maximum value is =   15.53889
Maximum value is at   82   75   1 (i,j,k)
Maximum value is at -734.0000   -1480.000   0.0000000E+00 (x,y,z)
Minimum value is = -17.23847
Minimum value is at   54   75   3 (i,j,k)
Minimum value is at -3534.000   -1480.000   100.0000   (x,y,z)

For the variable = "V "
Maximum value is =   11.60058
Maximum value is at   76   116   3 (i,j,k)
Maximum value is at -1334.000   2620.000   100.0000   (x,y,z)
Minimum value is = -14.93908
Minimum value is at   71   63   1 (i,j,k)
Minimum value is at -1834.000   -2680.000   0.0000000E+00 (x,y,z)

For the variable = "W "
Maximum value is =   3.975184
Maximum value is at   60   121   10 (i,j,k)
Maximum value is at -2934.000   3120.000   450.0000   (x,y,z)
Minimum value is = -13.75409
Minimum value is at   76   74   14 (i,j,k)
Minimum value is at -1334.000   -1580.000   650.0000   (x,y,z)

For the variable = "TAU "
Maximum value is =   304.4023
Maximum value is at   43   123   1 (i,j,k)
Maximum value is at -4634.000   3320.000   0.0000000E+00 (x,y,z)
Minimum value is =   287.7410
Minimum value is at   125   138   41 (i,j,k)
Minimum value is at 3566.000   4820.000   2000.000   (x,y,z)

For the variable = "XIV "
Maximum value is =   21.64085
Maximum value is at   41   94   3 (i,j,k)
Maximum value is at -4834.000   420.0000   100.0000   (x,y,z)
Minimum value is =   7.687082
Minimum value is at   71   73   41 (i,j,k)
Minimum value is at -1834.000   -1680.000   2000.000   (x,y,z)

For the variable = "RRF "
Maximum value is =   54.58204
Maximum value is at   56   94   41 (i,j,k)
Maximum value is at -3334.000   420.0000   2000.000   (x,y,z)
Minimum value is = -15.00000
Minimum value is at   1   1   1 (i,j,k)
Minimum value is at -8834.000   -8880.000   0.0000000E+00 (x,y,z)

For the variable = "RAIN"
Maximum value is =   5.819617
Maximum value is at   56   94   41 (i,j,k)

Maximum value is at -3334.000   420.0000   2000.000   (x,y,z)
Minimum value is = 0.0000000E+00
Minimum value is at   1   1   1 (i,j,k)
Minimum value is at -8834.000   -8880.000   0.0000000E+00 (x,y,z)
For the variable = "EWFF"
Maximum value is = 0.1891977
Maximum value is at   75   75   5 (i,j,k)
Maximum value is at -1434.000   -1480.000   200.0000   (x,y,z)
Minimum value is = -0.1044288
Minimum value is at   104   85   5 (i,j,k)
Minimum value is at   1466.000   -480.0000   200.0000   (x,y,z)
For the variable = "NSFF"
Maximum value is = 0.1796695
Maximum value is at   75   75   3 (i,j,k)
Maximum value is at -1434.000   -1480.000   100.0000   (x,y,z)
Minimum value is = -0.8648731E-01
Minimum value is at   76   122   3 (i,j,k)
Minimum value is at -1334.000   3220.000   100.0000   (x,y,z)

Case #3-49: 7/11/88 Denver, Colorado, Incident Case, Multiple Microburst

For the variable = "U   "
Maximum value is =   7.324199
Maximum value is at   44   62   30 (i,j,k)
Maximum value is at   5490.000   -4400.000   1450.000   (x,y,z)
Minimum value is =   -10.15697
Minimum value is at   9   55   4 (i,j,k)
Minimum value is at   1990.000   -5100.000   150.0000   (x,y,z)

For the variable = "V   "
Maximum value is =   13.33055
Maximum value is at   67   93   3 (i,j,k)
Maximum value is at   7790.000   -1300.000   100.0000   (x,y,z)
Minimum value is =   -9.167430
Minimum value is at   47   23   3 (i,j,k)
Minimum value is at   5790.000   -8300.000   100.0000   (x,y,z)

For the variable = "W   "
Maximum value is =   5.690357
Maximum value is at   46   23   38 (i,j,k)
Maximum value is at   5690.000   -8300.000   1850.000   (x,y,z)
Minimum value is =   -15.35832
Minimum value is at   138   56   24 (i,j,k)
Minimum value is at   14890.00   -5000.000   1150.000   (x,y,z)

For the variable = "TAU "
Maximum value is =   303.7999
Maximum value is at   86   65   1 (i,j,k)
Maximum value is at   9690.000   -4100.000   0.0000000E+00 (x,y,z)
Minimum value is =   282.4091
Minimum value is at   105   61   41 (i,j,k)
Minimum value is at   11590.00   -4500.000   2000.000   (x,y,z)

For the variable = "XIV "
Maximum value is =   5.352191
Maximum value is at   8   44   1 (i,j,k)
Maximum value is at   1890.000   -6200.000   0.0000000E+00 (x,y,z)
Minimum value is =   3.351608
Minimum value is at   153   58   41 (i,j,k)
Minimum value is at   16390.00   -4800.000   2000.000   (x,y,z)

For the variable = "RRF "
Maximum value is =   46.68984
Maximum value is at   108   75   41 (i,j,k)
Maximum value is at   11890.00   -3100.000   2000.000   (x,y,z)
Minimum value is =   -15.00000
Minimum value is at   1   1   1 (i,j,k)
Minimum value is at   1190.000   -10500.00   0.0000000E+00 (x,y,z)

For the variable = "RAIN"
Maximum value is =   0.3320332
Maximum value is at   107   59   38 (i,j,k)

Maximum value is at   11790.00   -4700.000   1850.000   (x,y,z)
Minimum value is = 0.0000000E+00
Minimum value is at   1   1   1 (i,j,k)
Minimum value is at   1190.000   -10500.00   0.0000000E+00 (x,y,z)
For the variable = "HAIL"
Maximum value is = 0.1497605
Maximum value is at   108   75   41 (i,j,k)
Maximum value is at   11890.00   -3100.000   2000.000   (x,y,z)
Minimum value is = 0.0000000E+00
Minimum value is at   1   1   1 (i,j,k)
Minimum value is at   1190.000   -10500.00   0.0000000E+00 (x,y,z)
For the variable = "EWFF"
Maximum value is = 0.1908372
Maximum value is at   146   57   29 (i,j,k)
Maximum value is at   15690.00   -4900.000   1400.000   (x,y,z)
Minimum value is = -0.8173751E-01
Minimum value is at   40   25   35 (i,j,k)
Minimum value is at   5090.000   -8100.000   1700.000   (x,y,z)
For the variable = "NSFF"
Maximum value is = 0.2080122
Maximum value is at   142   57   13 (i,j,k)
Maximum value is at   15290.00   -4900.000   600.0000   (x,y,z)
Minimum value is = -0.8103198E-01
Minimum value is at   68   52   2 (i,j,k)
Minimum value is at   7890.000   -5400.000   50.00000   (x,y,z)

Case #3-51: 7/11/88 Denver, Colorado, Incident Case, Multiple Microburst

For the variable = "U   "

Maximum value is =	19.27394		
Maximum value is at	150	57	1 (i,j,k)
Maximum value is at	17132.00	-4970.000	0.0000000E+00 (x,y,z)
Minimum value is =	-19.69370		
Minimum value is at	119	54	1 (i,j,k)
Minimum value is at	14032.00	-5270.000	0.0000000E+00 (x,y,z)

For the variable = "V   "

Maximum value is =	18.96012		
Maximum value is at	133	72	1 (i,j,k)
Maximum value is at	15432.00	-3470.000	0.0000000E+00 (x,y,z)
Minimum value is =	-19.14365		
Minimum value is at	128	43	1 (i,j,k)
Minimum value is at	14932.00	-6370.000	0.0000000E+00 (x,y,z)

For the variable = "W   "

Maximum value is =	6.139831		
Maximum value is at	88	73	12 (i,j,k)
Maximum value is at	10932.00	-3370.000	550.0000 (x,y,z)
Minimum value is =	-15.94755		
Minimum value is at	124	52	16 (i,j,k)
Minimum value is at	14532.00	-5470.000	750.0000 (x,y,z)

For the variable = "TAU "

Maximum value is =	303.8180		
Maximum value is at	88	62	1 (i,j,k)
Maximum value is at	10932.00	-4470.000	0.0000000E+00 (x,y,z)
Minimum value is =	282.3883		
Minimum value is at	99	64	41 (i,j,k)
Minimum value is at	12032.00	-4270.000	2000.000 (x,y,z)

For the variable = "XIV "

Maximum value is =	5.330627		
Maximum value is at	17	53	1 (i,j,k)
Maximum value is at	3832.000	-5370.000	0.0000000E+00 (x,y,z)
Minimum value is =	3.286308		
Minimum value is at	145	57	41 (i,j,k)
Minimum value is at	16632.00	-4970.000	2000.000 (x,y,z)

For the variable = "RRF "

Maximum value is =	47.41735		
Maximum value is at	105	70	41 (i,j,k)
Maximum value is at	12632.00	-3670.000	2000.000 (x,y,z)
Minimum value is =	-15.00000		
Minimum value is at	1	1	1 (i,j,k)
Minimum value is at	2232.000	-10570.00	0.0000000E+00 (x,y,z)

For the variable = "RAIN"

Maximum value is =	0.3601996		
Maximum value is at	100	62	36 (i,j,k)

```
Maximum value is at    12132.00     -4470.000      1750.000    (x,y,z)
Minimum value is =  0.0000000E+00
Minimum value is at          1            1        1 (i,j,k)
Minimum value is at    2232.000     -10570.00    0.0000000E+00 (x,y,z)
For the variable = "HAIL"
Maximum value is =  0.1641873
Maximum value is at         105           70       41 (i,j,k)
Maximum value is at    12632.00     -3670.000      2000.000    (x,y,z)
Minimum value is =  0.0000000E+00
Minimum value is at          1            1        1 (i,j,k)
Minimum value is at    2232.000     -10570.00    0.0000000E+00 (x,y,z)
For the variable = "EWFF"
Maximum value is =  0.2102184
Maximum value is at         137           58       17 (i,j,k)
Maximum value is at    15832.00     -4870.000      800.0000    (x,y,z)
Minimum value is =  -0.1665037
Minimum value is at          88           77        2 (i,j,k)
Minimum value is at    10932.00     -2970.000      50.00000    (x,y,z)
For the variable = "NSFF"
Maximum value is =  0.2412621
Maximum value is at         125           53        8 (i,j,k)
Maximum value is at    14632.00     -5370.000      350.0000    (x,y,z)
Minimum value is =  -0.1312876
Minimum value is at         130           36        4 (i,j,k)
Minimum value is at    15132.00     -7070.000      150.0000    (x,y,z)
```

Case #4-36: 7/14/82 Denver, Colorado, Stable Layer, Warm Microburst
For the variable = "U "
Maximum value is =   15.23200
Maximum value is at   111   101   1 (i,j,k)
Maximum value is at   500.0000   0.0000000E+00 0.0000000E+00 (x,y,z)
Minimum value is = -15.23200
Minimum value is at   91   101   1 (i,j,k)
Minimum value is at -500.0000   0.0000000E+00 0.0000000E+00 (x,y,z)
For the variable = "V "
Maximum value is =   15.23200
Maximum value is at   101   111   1 (i,j,k)
Maximum value is at   0.0000000E+00   500.0000   0.0000000E+00 (x,y,z)
Minimum value is = -15.23200
Minimum value is at   101   91   1 (i,j,k)
Minimum value is at   0.0000000E+00 -500.0000   0.0000000E+00 (x,y,z)
For the variable = "W "
Maximum value is =   6.074973
Maximum value is at   81   68   13 (i,j,k)
Maximum value is at -1000.000   -1650.000   600.0000   (x,y,z)
Minimum value is = -21.01300
Minimum value is at   101   101   12 (i,j,k)
Minimum value is at   0.0000000E+00 0.0000000E+00   550.0000   (x,y,z)
For the variable = "TAU "
Maximum value is =   303.8437
Maximum value is at   92   91   3 (i,j,k)
Maximum value is at -450.0000   -500.0000   100.0000   (x,y,z)
Minimum value is =   284.3200
Minimum value is at   101   101   40 (i,j,k)
Minimum value is at   0.0000000E+00 0.0000000E+00   1950.000   (x,y,z)
For the variable = "RAIN"
Maximum value is =   0.2615300
Maximum value is at   101   101   26 (i,j,k)
Maximum value is at   0.0000000E+00 0.0000000E+00   1250.000   (x,y,z)
Minimum value is =   0.0000000E+00
Minimum value is at   1   1   1 (i,j,k)
Minimum value is at -5000.000   -5000.000   0.0000000E+00 (x,y,z)
For the variable = "XIV "
Maximum value is =   7.488725
Maximum value is at   66   23   3 (i,j,k)
Maximum value is at -1750.000   -3900.000   100.0000   (x,y,z)
Minimum value is =   2.769900
Minimum value is at   101   97   40 (i,j,k)
Minimum value is at   0.0000000E+00 -200.0000   1950.000   (x,y,z)
For the variable = "RRF "
Maximum value is =   36.29500
Maximum value is at   101   101   40 (i,j,k)

Maximum value is at   0.0000000E+00 0.0000000E+00   1950.000   (x,y,z)
Minimum value is =   -15.00000
Minimum value is at   1   1   1 (i,j,k)
Minimum value is at   -5000.000   -5000.000   0.0000000E+00 (x,y,z)
For the variable = "EWFF"
Maximum value is = 0.2888719
Maximum value is at   101   101   2 (i,j,k)
Maximum value is at   0.0000000E+00 0.0000000E+00   50.00000   (x,y,z)
Minimum value is = -0.1147354
Minimum value is at   71   101   2 (i,j,k)
Minimum value is at   -1500.000   0.0000000E+00   50.00000   (x,y,z)
For the variable = "NSFF"
Maximum value is = 0.2888719
Maximum value is at   101   101   2 (i,j,k)
Maximum value is at   0.0000000E+00 0.0000000E+00   50.00000   (x,y,z)
Minimum value is = -0.1147354
Minimum value is at   101   71   2 (i,j,k)
Minimum value is at   0.0000000E+00 -1500.000   50.00000   (x,y,z)

F-11

Case #5-40: 7/8/89 Denver, Colorado, Very Dry Microburst
For the variable = "U "
Maximum value is =   19.48976
Maximum value is at   93   84   1 (i,j,k)
Maximum value is at   4990.000   10575.00   0.0000000E+00 (x,y,z)
Minimum value is =   -12.29543
Minimum value is at   63   85   1 (i,j,k)
Minimum value is at   1990.000   10675.00   0.0000000E+00 (x,y,z)
For the variable = "V "
Maximum value is =   24.91225
Maximum value is at   79   100   3 (i,j,k)
Maximum value is at   3590.000   12175.00   100.0000   (x,y,z)
Minimum value is =   -11.73100
Minimum value is at   81   70   1 (i,j,k)
Minimum value is at   3790.000   9175.000   0.0000000E+00 (x,y,z)
For the variable = "W "
Maximum value is =   4.606630
Maximum value is at   111   80   18 (i,j,k)
Maximum value is at   6790.000   10175.00   850.0000   (x,y,z)
Minimum value is =   -15.16710
Minimum value is at   79   82   24 (i,j,k)
Minimum value is at   3590.000   10375.00   1150.000   (x,y,z)
For the variable = "TAU "
Maximum value is =   307.9913
Maximum value is at   85   133   1 (i,j,k)
Maximum value is at   4190.000   15475.00   0.0000000E+00 (x,y,z)
Minimum value is =   286.7864
Minimum value is at   80   69   41 (i,j,k)
Minimum value is at   3690.000   9075.000   2000.000   (x,y,z)
For the variable = "XIV "
Maximum value is =   5.782187
Maximum value is at   128   152   14 (i,j,k)
Maximum value is at   8490.000   17375.00   650.0000   (x,y,z)
Minimum value is =   1.796745
Minimum value is at   100   109   26 (i,j,k)
Minimum value is at   5690.000   13075.00   1250.000   (x,y,z)
For the variable = "RRF "
Maximum value is =   34.20536
Maximum value is at   81   72   41 (i,j,k)
Maximum value is at   3790.000   9375.000   2000.000   (x,y,z)
Minimum value is =   -15.00000
Minimum value is at   1   1   1 (i,j,k)
Minimum value is at   -4210.000   2275.000   0.0000000E+00 (x,y,z)
For the variable = "RRFI"
Maximum value is =   34.20538
Maximum value is at   81   72   41 (i,j,k)

Maximum value is at   3790.000   9375.000   2000.000   (x,y,z)
Minimum value is = -15.00000
Minimum value is at   103   84   1 (i,j,k)
Minimum value is at   5990.000   10575.00   0.0000000E+00 (x,y,z)
For the variable = "RAIN"
Maximum value is =   0.2520440
Maximum value is at   81   73   40 (i,j,k)
Maximum value is at   3790.000   9475.000   1950.000   (x,y,z)
Minimum value is =   0.0000000E+00
Minimum value is at   1   1   1 (i,j,k)
Minimum value is at   -4210.000   2275.000   0.0000000E+00 (x,y,z)
For the variable = "EWFF"
Maximum value is =   0.2137424   ·
Maximum value is at   79   85   17 (i,j,k)
Maximum value is at   3590.000   10675.00   800.0000   (x,y,z)
Minimum value is = -0.8902939E-01
Minimum value is at   100   73   3 (i,j,k)
Minimum value is at   5690.000   9475.000   100.0000   (x,y,z)
For the variable = "NSFF"
Maximum value is =   0.2088467
Maximum value is at   80   89   7 (i,j,k)
Maximum value is at   3690.000   11075.00   300.0000   (x,y,z)
Minimum value is = -0.1144817
Minimum value is at   82   64   2 (i,j,k)
Minimum value is at   3890.000   8575.000   50.00000   (x,y,z)

Case #5-45: 7/8/89 Denver, Colorado, Very Dry Microburst
For the variable = "U   "
Maximum value is =   17.46074
Maximum value is at   103   84   3 (i,j,k)
Maximum value is at   6462.000   11993.00   100.0000   (x,y,z)
Minimum value is =   -16.05105
Minimum value is at   63   74   1 (i,j,k)
Minimum value is at   2462.000   10993.00   0.0000000E+00 (x,y,z)
For the variable = "V   "
Maximum value is =   20.70109
Maximum value is at   83   126   3 (i,j,k)
Maximum value is at   4462.000   16193.00   100.0000   (x,y,z)
Minimum value is =   -10.27237
Minimum value is at   81   63   1 (i,j,k)
Minimum value is at   4262.000   9893.000   0.0000000E+00 (x,y,z)
For the variable = "W   "
Maximum value is =   5.448867
Maximum value is at   93   128   15 (i,j,k)
Maximum value is at   5462.000   16393.00   700.0000   (x,y,z)
Minimum value is =   -12.61377
Minimum value is at   77   72   21 (i,j,k)
Minimum value is at   3862.000   10793.00   1000.000   (x,y,z)
For the variable = "TAU "
Maximum value is =   308.0083
Maximum value is at   103   130   1 (i,j,k)
Maximum value is at   6462.000   16593.00   0.0000000E+00 (x,y,z)
Minimum value is =   287.6288
Minimum value is at   78   67   41 (i,j,k)
Minimum value is at   3962.000   10293.00   2000.000   (x,y,z)
For the variable = "XIV "
Maximum value is =   5.768254
Maximum value is at   130   157   15 (i,j,k)
Maximum value is at   9162.000   19293.00   700.0000   (x,y,z)
Minimum value is =   1.846832
Minimum value is at   49   106   36 (i,j,k)
Minimum value is at   1062.000   14193.00   1750.000   (x,y,z)
For the variable = "RRF "
Maximum value is =   27.10251
Maximum value is at   83   67   41 (i,j,k)
Maximum value is at   4462.000   10293.00   2000.000   (x,y,z)
Minimum value is =   -15.00000
Minimum value is at   1   1   1 (i,j,k)
Minimum value is at   -3738.000   3693.000   0.0000000E+00 (x,y,z)
For the variable = "RRFI"
Maximum value is =   27.10250
Maximum value is at   83   67   41 (i,j,k)

```
Maximum value is at    4462.000      10293.00      2000.000    (x,y,z)
Minimum value is =  -15.00000
Minimum value is at         114           87          1 (i,j,k)
Minimum value is at    7562.000      12293.00      0.0000000E+00 (x,y,z)
For the variable = "RAIN"
Maximum value is =  0.8541232E-01
Maximum value is at          83           67         41 (i,j,k)
Maximum value is at    4462.000      10293.00      2000.000    (x,y,z)
Minimum value is =  0.0000000E+00
Minimum value is at           1            1          1 (i,j,k)
Minimum value is at   -3738.000       3693.000     0.0000000E+00 (x,y,z)
For the variable = "EWFF"
Maximum value is =  0.1965592
Maximum value is at          81           70          8 (i,j,k)
Maximum value is at    4262.000      10593.00      350.0000     (x,y,z)
Minimum value is =  -0.9361018E-01
Minimum value is at         122           86          3 (i,j,k)
Minimum value is at    8362.000      12193.00      100.0000     (x,y,z)
For the variable = "NSFF"
Maximum value is =  0.1628723
Maximum value is at          78           70         24 (i,j,k)
Maximum value is at    3962.000      10593.00      1150.000     (x,y,z)
Minimum value is =  -0.1201876
Minimum value is at          79          133          4 (i,j,k)
Minimum value is at    4062.000      16893.00      150.0000     (x,y,z)
```

Case #6-14: Derived Florida Sounding, Highly Asymmetric Microburst

For the variable = "U "
Maximum value is =   20.16742
Maximum value is at   60   43   10 (i,j,k)
Maximum value is at   13971.23   700.0000   450.0000   (x,y,z)
Minimum value is = 0.1155418
Minimum value is at   9   48   1 (i,j,k)
Minimum value is at   8871.231   1200.000   0.0000000E+00 (x,y,z)

For the variable = "V "
Maximum value is =   13.08692
Maximum value is at   63   46   1 (i,j,k)
Maximum value is at   14271.23   1000.000   0.0000000E+00 (x,y,z)
Minimum value is = -6.537601
Minimum value is at   58   34   1 (i,j,k)
Minimum value is at   13771.23   -200.0000   0.0000000E+00 (x,y,z)

For the variable = "W "
Maximum value is =   5.364121
Maximum value is at   67   53   10 (i,j,k)
Maximum value is at   14671.23   1700.000   450.0000   (x,y,z)
Minimum value is = -12.71668
Minimum value is at   65   38   11 (i,j,k)
Minimum value is at   14471.23   200.0000   500.0000   (x,y,z)

For the variable = "TAU "
Maximum value is =   304.1945
Maximum value is at   69   36   1 (i,j,k)
Maximum value is at   14871.23   0.0000000E+00 0.0000000E+00 (x,y,z)
Minimum value is =   288.4625
Minimum value is at   83   25   41 (i,j,k)
Minimum value is at   16271.23   -1100.000   2000.000   (x,y,z)

For the variable = "XIV "
Maximum value is =   19.96644
Maximum value is at   37   36   5 (i,j,k)
Maximum value is at   11671.23   0.0000000E+00 200.0000   (x,y,z)
Minimum value is =   7.623531
Minimum value is at   68   36   41 (i,j,k)
Minimum value is at   14771.23   0.0000000E+00 2000.000   (x,y,z)

For the variable = "RRF "
Maximum value is =   52.28900
Maximum value is at   65   38   3 (i,j,k)
Maximum value is at   14471.23   200.0000   100.0000   (x,y,z)
Minimum value is = -15.00000
Minimum value is at   1   1   1 (i,j,k)
Minimum value is at   8071.231   -3500.000   0.0000000E+00 (x,y,z)

For the variable = "RRFI"
Maximum value is =   52.28904
Maximum value is at   65   38   3 (i,j,k)

F-16

```
Maximum value is at    14471.23     200.0000     100.0000    (x,y,z)
Minimum value is =  -15.00000
Minimum value is at         61          43          11 (i,j,k)
Minimum value is at    14071.23     700.0000     500.0000    (x,y,z)
For the variable = "RAIN"
Maximum value is =   4.076537
Maximum value is at         65          38           3 (i,j,k)
Maximum value is at    14471.23     200.0000     100.0000    (x,y,z)
Minimum value is =  0.0000000E+00
Minimum value is at          1           1           1 (i,j,k)
Minimum value is at    8071.231    -3500.000    0.0000000E+00 (x,y,z)
For the variable = "HAIL"
Maximum value is =  0.1737424
Maximum value is at         68          36          41 (i,j,k)
Maximum value is at    14771.23    0.0000000E+00  2000.000    (x,y,z)
Minimum value is =  0.0000000E+00
Minimum value is at          1           1           1 (i,j,k)
Minimum value is at    8071.231    -3500.000    0.0000000E+00 (x,y,z)
For the variable = "EWFF"
Maximum value is =  0.1294569
Maximum value is at         62          40           3 (i,j,k)
Maximum value is at    14171.23     400.0000     100.0000    (x,y,z)
Minimum value is =  -0.8020734E-01
Minimum value is at         72          42           2 (i,j,k)
Minimum value is at    15171.23     600.0000     50.00000    (x,y,z)
For the variable = "NSFF"
Maximum value is =  0.1721279
Maximum value is at         63          41           3 (i,j,k)
Maximum value is at    14271.23     500.0000     100.0000    (x,y,z)
Minimum value is =  -0.9069768E-01
Minimum value is at         58          29           2 (i,j,k)
Minimum value is at    13771.23    -700.0000     50.00000    (x,y,z)
```

Case #7-27: 8/2/81 Adjusted Knowlton, Montana Sounding, Gust Front
For the variable = "U "
Maximum value is = 32.35432
Maximum value is at   7   16   3 (i,j,k)
Maximum value is at   19110.00   0.0000000E+00   100.0000   (x,y,z)
Minimum value is = -0.6180557
Minimum value is at   58   12   40 (i,j,k)
Minimum value is at   24210.00   -400.0000   1950.000   (x,y,z)
For the variable = "V "
Maximum value is = 10.58100
Maximum value is at   65   10   35 (i,j,k)
Maximum value is at   24910.00   -600.0000   1700.000   (x,y,z)
Minimum value is = -8.110295
Minimum value is at   1   3   1 (i,j,k)
Minimum value is at   18510.00   -1300.000   0.0000000E+00 (x,y,z)
For the variable = "W "
Maximum value is = 13.14704
Maximum value is at   95   3   21 (i,j,k)
Maximum value is at   27910.00   -1300.000   1000.000   (x,y,z)
Minimum value is = -12.30999
Minimum value is at   1   17   15 (i,j,k)
Minimum value is at   18510.00   100.0000   700.0000   (x,y,z)
For the variable = "TAU "
Maximum value is = 303.1300
Maximum value is at   107   5   1 (i,j,k)
Maximum value is at   29110.00   -1100.000   0.0000000E+00 (x,y,z)
Minimum value is = 284.0045
Minimum value is at   1   29   41 (i,j,k)
Minimum value is at   18510.00   1300.000   2000.000   (x,y,z)
For the variable = "CLD "
Maximum value is = 0.9993626
Maximum value is at   27   38   40 (i,j,k)
Maximum value is at   21110.00   2200.000   1950.000   (x,y,z)
Minimum value is = 0.0000000E+00
Minimum value is at   3   1   1 (i,j,k)
Minimum value is at   18710.00   -1500.000   0.0000000E+00 (x,y,z)
For the variable = "XIV "
Maximum value is = 16.86115
Maximum value is at   45   36   7 (i,j,k)
Maximum value is at   22910.00   2000.000   300.0000   (x,y,z)
Minimum value is = 3.033260
Minimum value is at   88   37   8 (i,j,k)
Minimum value is at   27210.00   2100.000   350.0000   (x,y,z)
For the variable = "RRF "
Maximum value is = 58.62407
Maximum value is at   1   14   41 (i,j,k)

Maximum value is at   18510.00   -200.0000   2000.000   (x,y,z)
Minimum value is = -15.00000
Minimum value is at   62   1   1 (i,j,k)
Minimum value is at   24610.00   -1500.000   0.0000000E+00 (x,y,z)
For the variable = "RRFI"
Maximum value is =   58.62407
Maximum value is at   1   14   41 (i,j,k)
Maximum value is at   18510.00   -200.0000   2000.000   (x,y,z)
Minimum value is = -15.00000
Minimum value is at   76   24   5 (i,j,k)
Minimum value is at   26010.00   800.0000   200.0000   (x,y,z)
For the variable = "RAIN"
Maximum value is =   4.505048
Maximum value is at   1   9   1 (i,j,k)
Maximum value is at   18510.00   -700.0000   0.0000000E+00 (x,y,z)
Minimum value is =   0.0000000E+00
Minimum value is at   67   1   1 (i,j,k)
Minimum value is at   25110.00   -1500.000   0.0000000E+00 (x,y,z)
For the variable = "HAIL"
Maximum value is =   1.314436
Maximum value is at   1   14   41 (i,j,k)
Maximum value is at   18510.00   -200.0000   2000.000   (x,y,z)
Minimum value is =   0.0000000E+00
Minimum value is at   1   1   1 (i,j,k)
Minimum value is at   18510.00   -1500.000   0.0000000E+00 (x,y,z)
For the variable = "EWFF"
Maximum value is =   0.1635404
Maximum value is at   38   47   6 (i,j,k)
Maximum value is at   22210.00   3100.000   250.0000   (x,y,z)
Minimum value is = -0.2435648
Minimum value is at   89   8   27 (i,j,k)
Minimum value is at   27310.00   -800.0000   1300.000   (x,y,z)
For the variable = "NSFF"
Maximum value is =   0.1911894
Maximum value is at   1   17   13 (i,j,k)
Maximum value is at   18510.00   100.0000   600.0000   (x,y,z)
Minimum value is = -0.1559161
Minimum value is at   24   40   16 (i,j,k)
Minimum value is at   20810.00   2400.000   750.0000   (x,y,z)

REPORT DOCUMENTATION PAGE

Public reporting burden for this collection of information is estimated to average 1 hour per response, including the time for reviewing instructions, searching existing data sources, gathering and maintaining the data needed, and completing and reviewing the collection of information. Send comments regarding this burden estimate or any other aspect of this collection of Information, including suggestions for reducing this burden, to Washington Headquarters Services, Directorate for Information Operations and Reports, 1215 Jefferson Davis Highway, Suite 1204, Arlington, VA 22202-4302, and to the Office of Management and Budget, Paperwork Reduction Project (0704-0188), Washington, DC 20503.

1. AGENCY USE ONLY (Leave blank)	2. REPORT DATE	3. REPORT TYPE AND DATES COVERED
	November 1993	Technical Memorandum

4. TITLE AND SUBTITLE

Windshear Database for Forward-Looking Systems Certification

5. FUNDING NUMBERS

505-64-12-01

6. AUTHOR(S)

G. F. Switzer; F. H. Proctor; D. A. Hinton; and J. V. Aanstoos

7. PERFORMING ORGANIZATION NAME(S) AND ADDRESS(ES)

NASA Langley Research Center
Hampton, Virginia 23681-0001

8. PERFORMING ORGANIZATION REPORT NUMBER

9. SPONSORING / MONITORING AGENCY NAME(S) AND ADDRESS(ES)

National Aeronautics and Space Administration
Washington, DC 20546

10. SPONSORING / MONITORING AGENCY REPORT NUMBER

NASA TM-109012

11. SUPPLEMENTARY NOTES

G. F. Switzer and J. V. Aanstoos - Research Triangle Institute
F. H. Proctor and D. A. Hinton - NASA Langley Research Center

12a. DISTRIBUTION / AVAILABILITY STATEMENT

Unclassified - Unlimited

Subject Category 47

12b. DISTRIBUTION CODE

13. ABSTRACT (Maximum 200 words)

This document contains a description of a comprehensive database that is to be used for certification testing of airborne forward-look windshear detection systems. The database was developed by NASA Langley Research Center, at the request of the Federal Aviation Administration (FAA), to support the industry initiative to certify and produce forward-look windshear detection equipment. The database contains high-resolution, three-dimensional fields for meteorological variables that may be sensed by forward-looking systems. The database is made up of seven case studies, which have been generated by the Terminal Area Simulation System, a state-of-the-art numerical system for the realistic modeling of windshear phenomena. The selected cases represent a wide spectrum of windshear events. General descriptions and figures from each of the case studies are included, as well as equations for F-factor, radar-reflectivity factor, and rainfall rate. The document also describes scenarios and paths through the data sets, jointly developed by NASA and the FAA, to meet FAA certification testing objectives. Instructions for reading and verifying the data from tape are included.

14. SUBJECT TERMS

Windshear; Microburst; Sensors; Certification; Modeling

15. NUMBER OF PAGES

133

16. PRICE CODE

A07

17. SECURITY CLASSIFICATION OF REPORT	18. SECURITY CLASSIFICATION OF THIS PAGE	19. SECURITY CLASSIFICATION OF ABSTRACT	20. LIMITATION OF ABSTRACT
Unclassified	Unclassified		